Title

THE ROLE OF HYPERMODIFIED BASES IN TRANSFER RNA-SOLUTION PROPERTIES OF DINUCLEOSIDE MONOPHOSPHATES

Author

Watts, Mark Terrill.

Publication Date

1977-05-01

THE ROLE OF HYPERMODIFIED BASES IN TRANSFER RNA-SOLUTION PROPERTIES OF DINUCLEOSIDE MONOPHOSPHATES

Mark Terrill Watts
(Ph. D. thesis)

May 1977

Prepared for the U. S. Energy Research and Development Administration under Contract W-7405-ENG-48

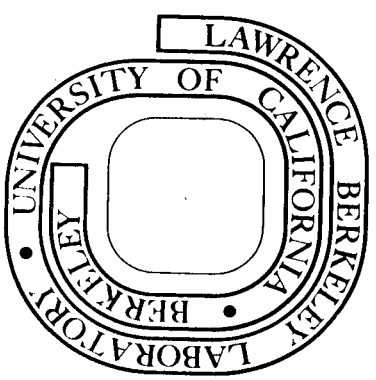

DISCLAIMER

The Role of Hypermodified Bases in Transfer RNA - Solution Properties of Dinucleoside Monophosphates

by

Mark Terrill Watts

ABSTRACT

The hypermodified dinucleoside monophosphates, uridylyl-(3'-5')N-[9(β-*D*-ribofuranosyl)-purin-6-ylcarbamoyl]threonine (Upt^{6}A), adenylyl(3'-5')N^6-(Δ^2-isopentenyl)adenosine (Api^{6}A), adenylyl(3'-5')N^6-(Δ^2-isopentenyl)-2-methylthio-adenosine (Apms^{2}i^{6}A), and adenylyl(3'-5')1-N^6-ethenoadenosine (ApεA - a synthetic model for adenylyl(3'-5')wybutosine, ApyW), which represent the most common sequences found as the third letter of the anticodon triplet and its adjacent 3'-neighbor, have been isolated. Upt^{6}A was purified after an enzymatic degradation of yeast tRNA, and Api^{6}A, Apms^{2}i^{6}A, and ApεA were isolated subsequent to their chemical syntheses from their component nucleosides. Their solution properties have been investigated using UV absorption, circular dichroism (CD), and high resolution proton magnetic resonance. The properties of these molecules have been compared to those of their unmodified counterparts, uridylyl-(3'-5')adenosine (UpA) and adenylyl(3'-5')adenosine (ApA), in order to learn of the function(s) of the hypermodified bases in transfer RNA.

The properties measured as a function of temperature have been analyzed employing a two-state intramolecular

stacking model. The results from all of the techniques used indicate that hypermodification of the unmodified dinucleoside phosphates changes their stacking abilities. Static measurements of the properties suggest that the stacking differences are caused by conformational changes induced by the hypermodifications of the A residue.

All of the properties show that the stacking of Upt^{6}A is stabilized relative to UpA, while Api^{6}A, Apms^{2}i^{6}A, and ApεA are destabilized relative to ApA. Thus, Upt^{6}A, Api^{6}A, Apms^{2}i^{6}A and ApεA have comparable stacking equilibria, indicating that the modifications remove the large difference in stacking between UpA and ApA. Furthermore, cytidylyl-(3'-5')adenosine (ĊpA), which is the most common unmodified sequence in this particular anticodon region, exhibits a stability similar to those of the hypermodified dinucleoside phosphates.

Hypermodification therefore seems to keep the flexibility of this crucial part of the tRNA constant. It is proposed that this may result in a more smoothly regulated translation step. Also, it is proposed that the enhanced stacking of Upt^{6}A relative to UpA prevents the incorrect wobble base-pairing of this U residue in the tRNA during translation.

to my best friend, Sue,

and my families -

including future additions

Acknowledgments

It has been my extreme pleasure and good fortune to be associated in work and play with Nacho Tinoco. I will be forever grateful to Nacho for teaching me his approach to science, which requires the constant questioning of the motives for one's research. I have hopefully acquired through my fellowship with Nacho, some of his ability to pose the proper questions in solving a problem. Mostly though, I thank Nacho for being my friend, for that relationship has allowed freedom in the discussion of science and in the constructive criticism which is so much a part of learning.

Alan Levin deserves special thanks here. His impeccable tastes gave the Texan another view of the world, and in his absence this thesis was somberly completed. I profited most from observing his constant efforts in doing his best in all that he does - in science or in play.

Of course, David Koh provided invaluable harassment. This jack-of-all-trades introduced me to innumerable facets of daily life that I previously had been unaware of. Our companionship during my stay in the window seat served to pleasurably waste many priceless moments. David's greatest contribution to my work and to the Tinoco lab though, is that he instills confidence to those around him.

There is no exaggeration in saying that this thesis could not have been completed without the help and advice of

the hard-working Robert (Che-Hung) Lee. I also learned from his constant and uncompromising attention to detail, for he is certainly an embodiment of perfection in experimental work.

It is also a pleasure for me to thank the one who got me started in the lab, and who has served to maintain the high moral in the lab. Barbara Dengler's efforts in beautifying this place with her green thumb and general good cheer have been a joy to behold.

Ken Breslauer and Doug Turner aided a great deal with my approach to science (and plunging in the case of K.B.) during my formulative first year here. Dexter Moore I thank especially for pointing out and helping with career options which I had previously not considered. My discussions of science with Soo Freier and Kyong Yoon were often the most enlightening, for they generally told me what they thought. I'm appreciative to both for their friendship under the constant tormenting they received from me. I also thank Adrienne Drobnies for putting up with (or enjoying) the feminist harassment.

It has been enjoyable and helpful to be associated with our token organic chemist, Kentuckian Stephen Winkle. My south-of-the-border amigo Carlos Bustamante has provided fruitful and necessary distraction, gusto, and a warm hearty laugh. In addition, I thank Bruce Johnson for taking a lot more than he ever deserved or dealt out himself. As it has always been a help to my work, I thank Dave Kehres for many

pleasurable rounds on the links.

I would like to also acknowledge Dr. Roy Morris (Oregon State University) and Dr. Michael Gray (Dalhousie University) for supplying molecules and advice. Also I thank Dr. Woody Conover, Dr. Steven Patt, and the Stanford Magnetic Resonance Laboratory for their help in obtaining the NMR spectra.

Finally, I have received incessant support for this work from my wife Sue, and both of our families. Their encouragements have certainly been the very most meaningful. I thank especially my parents for teaching me by example always to do my best.

Work performed under the auspices of the U. S. Energy Research and Development Administration.

TABLE OF CONTENTS

Chapter 1 INTRODUCTION

I. Purpose

II. Background

(A) Hypermodification - Definition and Description

(B) Occurrence

(C) Biological Significance of Hypermodification - Experiments with tRNAs and Protein Synthesis

III. A Need for Modification?

(A) An Anticodon 'Quartet'

(B) Wobble

(C) Regulation

IV. Summary

Chapter 1

INTRODUCTION

I. Purpose

We begin the study of biological phenomena with the premise that the attainment of an understanding of the workings of a process will lead us to the solutions of the inevitable malfunctions, and eventually to the control of the system. We will set our sights on the level of understanding the chemistry of certain biomolecules and their interactions with one another, with the expectation that this knowledge will guide us to the more general comprehension of the biological processes.

All of a living organism's hereditary information is contained in its DNA. This information is transcribed onto RNA molecules, and from there is translated into protein molecules, which perform or control most of the functions of the organism. While a great deal is known about these transcription and translation steps of protein synthesis, they are deceptively complex, and many of the quantitative and even qualitative aspects remain a mystery. How is it that the transcription and translation can be so incredibly accurate, as we know they must if the synthesis of faulty proteins is to be prevented? What are the rates of these steps, and how are the rates controlled, and controlled they must be to repress unbridled growth? In order to answer these kinds of questions, we are obliged first

to compromise by limiting ourselves to manageable tasks, and then to carefully define these tasks, so that their solutions necessarily will form a basis for an understanding on a grander scale.

We turn to a consideration of the translation step, and the molecular species involved. Transfer RNA molecules act as crucial middlemen in this process by deciphering the code written from the DNA into the messenger RNA. The mRNA consists of a series of codes, each called a codon, and each tRNA possesses a corresponding anticodon. The tRNA 'reads' the message on the mRNA and performs the translation by adding successive amino acids onto a growing protein. The accuracy, rate and regulation of these codon-anticodon interactions must follow the same restrictions as the whole of protein synthesis. We look for insight into these features of the reaction by narrowing our vision to the tRNA molecule itself, and more appropriately to the region of the molecule containing the anticodon.

In many species of tRNA, large naturally occurring modifications of the common structural features of the tRNA are found in the region near the anticodon. These modifications have been implicated in controlling the accuracy and rate of the codon-anticodon interaction, but their ability to carry out these functions is not understood. By following the precept that the structures and energies of biomolecules often dictate their functions, this dissertation addresses itself to the function of these modifica-

tions, through a study of the physical properties of portions of the anticodon region.

II. Background

(A) Hypermodification - Definition and Description

The term hypermodified refers to structural modifications of certain nucleosides in tRNA which are rather elaborate alterations of the major nucleosides, as opposed to the modified nucleosides found in RNA and DNA, which only contain relatively simple changes in the structure. These large modifications generally result from the attachment of a complex side chain or in some cases, an adduct ring, to the base portion of the nucleoside.

The additions create more bulk for the nucleoside, and by providing organic functional groups not commonly found in the major nucleosides, they confer on these bases different and often new chemical reactivities, as well as different possibilities for physical interactions. For reasons that will become clear later, we will be more interested in the physical interactions, and hence the reader is referred to references 1 - 3 for a detailed discussion of the chemical reactivities of these bases and nucleosides.

Figure 1 illustrates the four predominant hypermodified nucleosides. From inspection it can be seen that i^6A, ms^2i^6A, and t^6A all appear to be derived from adenosine, whereas yW (designated previously as the Y base - see refe-

Figure 1: The predominant hypermodified nucleosides.

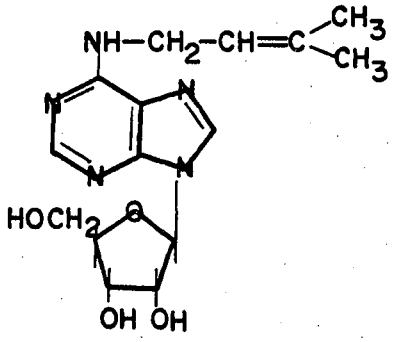

i^6A

N^6-(Δ^2-isopentenyl)adenosine

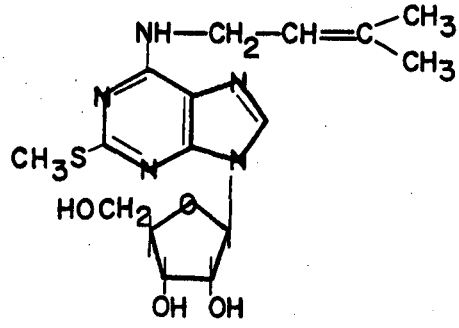

ms^2i^6A

N^6-(Δ^2-isopentenyl)-2-methylthioadenosine

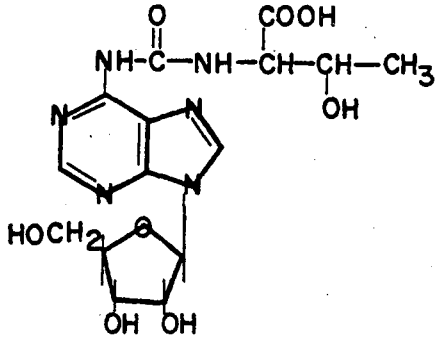

t^6A

N-[9-(β-*D*-ribofuranosyl)purin -6-ylcarbamoyl]-*L*-threonine

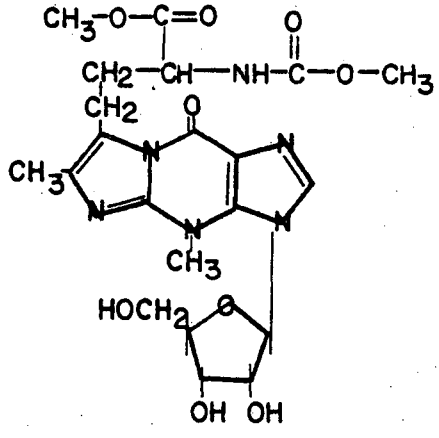

yW

Wybutosine[4]

rence 4 for new ACS approved nomenclature) is probably derived from guanosine (see discussion of biosynthesis in the next section).

Other hypermodified bases which occur naturally to a lesser degree include N^6-(cis-4-hydroxy-3-methylbut-2-enyl) adenosine[5] and N^6-(cis-4-hydroxy-3-methylbut-2-enyl)-2-methylthioadenosine[6], derivatives of i^6A and ms^2i^6A respectively, N-[N-methyl-N-(9-β-D-ribofuranosyl)purin-6-ylcarbamoyl]threonine (mt^6A)[7], a methylated derivative of t^6A, and Wyosine (W) and Wybutoxosine (O_2yW), both derivatives of yW[4]. Recently, analogues of t^6A, N-[9-(β-D-ribofuranosyl)purin-6-ylcarbamoyl]glycine (g^6A)[8], and a corresponding derivative containing aspartic acid[9] in place of threonine, have been found. Also known are some derivatives of cytidine and uridine which will be briefly discussed in the following section.

(B) Occurrence

The isolation and characterization of hypermodified bases has only been realized in the past decade. i^6A was first characterized in 1966[10,11], ms^2i^6A and t^6A were identified in 1968[12,13,14], and the structure of yW was solved finally in 1970[15]. Various combinations of these have been found in all organisms investigated, except for the Mycoplasma[16], which are the smallest free-living cells that have been examined. As for the individual nucleosides, t^6A has been detected in all but Mycoplasma[50], and i^6A is found

in most organisms aside from Mycoplasma and E. coli. The presence of yW type nucleosides has only been discerned in eucaryotic organisms, while ms^2i^6A has been discovered only in E. coli.

A closer look at the occurrence of these nucleosides quickly reveals that they are found only in the tRNA (or in the pool of metabolic products of the tRNA) of the organisms. Sequencing studies to date of approximately thirty tRNAs containing hypermodified bases, further disclose their appearance only in the position immediately adjacent to the 3' side of the anticodon triplet (see Figure 2 and Table I, which lists the anticodon loop sequences that contain hypermodified bases next to the anticodon.). (Not included in this category are those hypermodifications of uridine and cytidine, which are located in the anticodon itself. Because of this difference in location, we feel that their function, though unknown, will be different and perhaps even unrelated to the before-mentioned bases, and thus we will henceforth be concerned only with the hypermodified nucleosides located adjacent to the anticodon.)

Even more striking than this regularity of position is the almost uncanny presence of a uridine or an adenosine residue in the anticodon next to the hypermodification. Notice in Table I, that without exception, a t^6A is always preceeded by a U, and all other hypermodifications are invariably preceeded by an A. With only a few exceptions, the converse is also found to hold - a U in the first position

Figure 2: $tRNA^{Phe}$ from Baker's Yeast, exhibiting the locations of the anticodon triplet and hypermodified nucleoside in the anticodon loop.

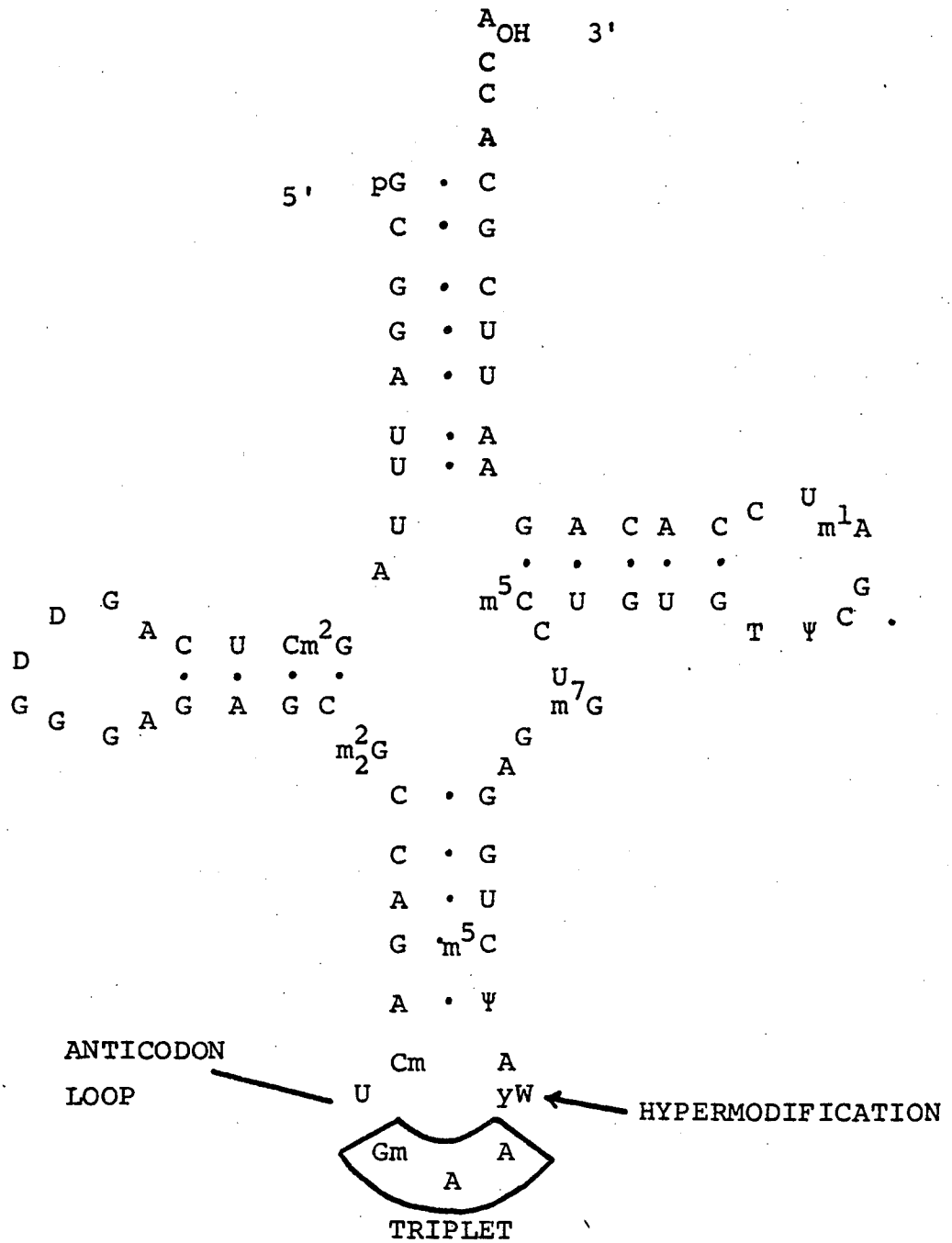

Table I. Anticodon loop sequences of tRNAs containing hypermodified nucleosides. 5'-3', left to right.

Amino Acid	Organism	Anticodon Loop triplet						
Arg 3	Br. Yeast	C	U	U*	C	U	t^6A	A
Ile	T. Utilis	C	U	I	A	U	t^6A	A
Ile 1	E. coli	C	U	G	A	U	t^6A	A
Lys 1	E. coli	C	U	mam^5s^2U	U	U	t^6A	A
Lys 2	Bk. Yeast	C	U	mam^5s^2U	U	U	t^6A	A
Met_f	Bk. Yeast	C	U	C	A	U	t^6A	A
Met_f	Rabbit liver	C	C	C	A	U	t^6A	A
Met_f	Sheep liver	C	C	C	A	U	t^6A	A
Met_f	Mouse myeloma	C	C	C	A	U	t^6A	A
Met_m	E. coli	C	U	ac^4C	A	U	t^6A	A
Ser 2	Rat liver	m^3C	U	G	C	U	t^6A	A
Ser 3	E. coli	s^2C	U	G	C	U	t^6A	A
Ser 3	Rat liver	m^3C	U	G	C	U	t^6A	A
Phe	Bk. Yeast	Cm	U	Gm	A	A	yW	A
Phe	T. Utilis	Cm	U	Gm	A	A	W	A
Phe	Wheat germ	Cm	U	Gm	A	A	o_2yW	A
Phe	Rabbit liver	Cm	U	Gm	A	A	o_2yW	A
Leu	E. coli(T4)	C	U	U*	A	A	ms^2i^6A	A
Phe	E. coli	Ψ	U	G	A	A	ms^2i^6A	A
Ser 1	E. coli	N	U	o^5ac^4U	G	A	ms^2i^6A	A
Trp	E. coli	C	U	C	C	A	ms^2i^6A	A

Table I. (Continued)

Amino Acid	Organism	Anticodon Loop triplet						
Tyr 1,2	E. coli	C	U	Q	U	A	ms^2i^6A	A
Tyr(mut)	E. coli	C	U	C	U	A	ms^2i^6A	A
Ser 1	Br. Yeast	Ψ	U	I	G	A	i^6A	A
Ser 1	Rat liver	m^3C	U	I	G	A	i^6A	A
Ser 2	Br. Yeast	Ψ	U	I	G	A	i^6A	A
Tyr	Bk. Yeast	C	U	G	Ψ	A	i^6A	A
Tyr	T. Utilis	C	U	G	Ψ	A	i^6A	A
Tyr	Sacc. C.	C	U	G	Ψ	A	i^6A	A
Lys 1	Sacc. C.	C	U	C	U	U	A*	A
Ser	E. coli(T4)	Cm	U	N	G	A	A*	A

* - unidentified modification

N - unknown base

See abbreviations in references for definitions of all other letters.

References:

All sequences are in

Barrell, B.G. and Clark, B.F. Handbook of Nucleic Acid Sequences, Joynson-Bruvvers Ltd., Oxford (1974).

except Lys 1 E. coli (Nucl. Acids Res. 2(11), 2069(1975));
Phe T. Utilis (J. Biochem. 75(5), 1169(1974));
Tyr Sacc. C. (J. Biochem. 72, 1185(1972)).

of the anticodon always has t^6A as its 3' neighbor, and an A will have one of the other hypermodified nucleosides as its 3' neighbor (see Table II for a listing of the present known anticodon loop sequences which do not contain hypermodified bases next to the anticodon.). Furthermore, hypermodified bases have been established as present in certain unsequenced tRNAs which code for specific amino acids. The first letter of the codon for each of these amino acids is unambiguous, and is listed in Table III with the appropriate tRNA, and the corresponding hypermodified nucleoside detected in that tRNA. Obviously, since the code is unambiquous in this position, the first letter in the anticodon must be the Watson-Crick counterpart of that codon letter. And, on the other hand, it would be surprising considering the trends present in the sequences amassed, if the hypermodified bases occupied positions other than that next to the anticodon. If this is indeed a general rule, we see again that with few exceptions, a U in the first position of the anticodon has as its 3' neighbor a t^6A residue, and an A will have as its neighbor one of the other hypermodified nucleosides. We will discuss the implications of these interesting facts as well as those of the exceptions in following sections.

Biosynthetically, these hypermodifications are believed to result from enzymatic transformations of the normal nucleosides in intact tRNAs[17]. In some cases, enzymes have been isolated which will fully transform the

Table II. . Anticodon loop sequences of tRNAs that do not contain hypermodified bases. 5'-3', left to right.

Amino Acid	Organism	Anticodon Loop triplet						
Arg 2	Br. Yeast	C	U	I	C	G	A	A
Gly 1	Yeast	Ψ	U	G	C	C	A	Ψ
Gly 3	E. coli	U	U	G	C	G	A	A
Gly 1	S. Typh.	U	U	C	C	C	A	A
Gly 1	E. coli	U	U	C	C	C	A	A
Gly_{ins}	E. coli	U	U	U	C	C	A	A
Gly	E. coli(T4)	C	U	U*	C	C	A	A
Val 1,2	Bk. Yeast	Ψ	U	I	A	C	A	C
Val 1,2	T. Utilis	Ψ	U	I	A	C	A	C
Val 2A,B	E. coli	U	U	G	A	C	A	U
Arg 2	E. coli	C	U	G	C	G	G	A
Gly 1	Staph.	C	U	U	C	C	C	G
Gly 1	Staph.	C	U	U	C	C	U	G
Arg 1	E. coli	s^2C	U	I	C	G	m^2A	A
Asp 1	E. coli	C	U	Q	U	C	m^2A	C
Gln 1	E. coli	Um	U	N	U	G	m^2A	Ψ
Gln 2	E. coli	Um	U	C	U	G	m^2A	Ψ
Glu 2	E. coli	C	U	mam^5s^2U	U	C	m^2A	C
His 1	E. coli	U	U	Q	U	G	m^2A	Ψ
His 1	S. Typh.	U	U	Q	U	G	m^2A	Ψ
Val 1	E. coli	C	U	o^5ac^4U	A	C	m^6A	A
Asp 1	Br. Yeast	Ψ	U	G	U	C	m^1G	C
Leu 1	E. coli	U	U	C	A	G	m^1G	A

Table II. (Continued)

Amino Acid	Organism	Anticodon Loop triplet							
Leu 3	Bk. Yeast	Ψ	U		G	C	C	m^1G	C
Phe	Mycoplasma	C	U		G	A	A	m^1G	C
Pro	E. coli(T4)	Um	U		N	G	G	m^1G	A
Leu 1	S. Typh.	U	U		C	A	G	G*	Ψ
Leu 2	E. coli	U	U		G	A	G	G*	Ψ
Ala 1	Bk. Yeast	U	U		I	G	C	m^1I	Ψ
Ala 1	T. Utilis	U	U		I	G	C	m^1I	Ψ
Met_f	E. coli	Cm	U		C	A	U	A	A
Trp 1,2	Br. Yeast	Cm	U		Cm	C	A	A	A

* - unidentified modification

N - unknown base

See abbreviations in references for definitions of all other letters.

References:

All sequences are in

Barrell, B.G. and Clark, B.F. Handbook of Nucleic Acid Sequences, Joynson-Bruvvers Ltd., Oxford (1974).

except Arg 2 Br. Yeast (Nucl. Acids Res. 2(10), 1787(1975));
Phe Mycoplasma (Nucl. Acids Res. 1(12), 1713(1974)).

Table III. Hypermodification content of unsequenced tRNAs.

Amino Acid	Organism	First Codon Letter	Modification Present
Cys^{i}	Yeast	U	i^6A
Cys^{ii}	E. coli	U	ms^2i^6A
Leu 1A,2[iii]	E. coli	U	ms^2i^6A
Asn^{iv}	E. coli	A	t^6A
Arg^{v}	E. coli	A	t^6A
Met_m^{vi}	Rabbit liver	A	t^6A
Thr^{iv}	E. coli	A	t^6A
Tyr^{vi}	Rat liver	U	t^6A
Tyr^{vi}	Silk worm	U	t^6A

References:

[i] FEBS Let. 46(1), 268(1974).

[ii] Biochem. Biophys. Acta 247, 170(1971).

[iii] Proc. Nat. Acad. Sci. 67, 1448(1970).

[iv] Prog. Nucl. Acid Res. Mol. Biol. 12, 49(1972).

[v] J. Biol. Chem. 247(20), 6394(1972).

[vi] Biochimie 56(5), 787(1974).

[vii] Nature 263, 167(1976).

appropriate nucleosides in hypermodified-deficient tRNAs[18,19]. i^6A and ms^2i^6A are known to be derived from adenosine (with ms^2i^6A being synthesized from i^6A)[20,21,22], and t^6A is thought to be derived from adenosine[23,24]. yW on the other hand, is believed to originate from a guanosine residue[15,48,49]. (In this regard, notice in Table I, that yW-type nucleosides are found only in tRNAs specfic for phenylalanine.) Later it will be seen, that it is important that we keep in mind these origins of the hypermodified nucleosides, as one approach in gaining further insight into the functions of these bases, will be to ask ourselves the question, - why were the original nucleosides adjacent to the anticodon not sufficient for the tRNAs' functions?

(C) Biological Significance of Hypermodification - Experiments with tRNAs and Protein Synthesis

As in all scientific endeavors, it is essential that we familiarize ourselves with the past work of others, and in the case of hypermodification, it is peculiarly important that we do so. The striking occurrence in tRNAs seen above, reflects only a small portion of the literature of these bases; the more important segment comprises those experiments which demonstrate a biological function of the hypermodifications. Acquaintance with these findings clearly indicates the need for further investigations, and oftentimes sets the directions for these studies. This section briefly describes the experiments that plainly

show a biological significance of the hypermodified bases, and that, in doing so, set the basis for the studies described in this dissertation.

It has been observed by several authors, that tRNAs deficient in their proper content of i^6A or ms^2i^6A, are less efficient than the normal tRNAs in in vitro protein synthesis, or polymer directed polypeptide synthesis. Fleissner, in 1967[25], found that an undermethylated E. coli $tRNA^{Phe}$ performed the transfer of phenylalanine into polyphenylalanine more slowly than normal $tRNA^{Phe}$. He also found this submethylated tRNA to bind less efficiently to ribosomes and synthetic mRNAs. Presumably i^6A was in place of ms^2i^6A (see biosynthesis references). Faulkner and Uziel in 1971[26] determined that E. coli $tRNA^{Phe}$, containing an ms^2i^6A residue which was modified by treatment with triiodide, did not function in polyphenylalanine synthesis. Thiosulfate treatment reversed the I_3^- modification, and the tRNA's activity was thereby restored. Kitchingman et al. in 1976[27], showed an undermodified $tRNA^{Phe}$ from relazed control E. coli to be only 60% as efficient in poly U directed polyphenylalanine synthesis. Here also, i^6A had replaced ms^2i^6A.

Binding assays using ribosomes and synthetic polymer messages have also been found to depend upon the content of ms^2i^6A and i^6A. Fittler and Hall in 1966[28] modified the i^6A residue in yeast $tRNA^{Ser}$ with I_3^-, and found the change to interfere with the binding of this tRNA to the ribosome-

mRNA complex. Similarly, Furuichi et al. in 1970[29], found that when the i^6A in yeast $tRNA^{Tyr}$ was modified by bisulfite, there resulted a decrease of the ability of the tRNA to bind in ribosomal binding assays. Stern et al. (1970)[30] established that methyldeficient E. coli $tRNA^{Phe}$ exhibited a marked reduction in ribosomal binding to poly U.

The most convincing and perhaps the most ideal experiments however, were performed by Gefter and Russell in 1969[31], when they were able to isolate three forms of a suppressor $tRNA^{Tyr}$ from E. coli. The forms differed only in their content of hypermodification, and contained the residues A, i^6A, and ms^2i^6A, respectively. The tRNAs were found to differ markedly in their abilities to support protein synthesis in vitro, with the abilities ranking with the extent of modification, as $ms^2i^6A > i^6A > A$. Likewise, the same trend was found in their ability to bind to ribosomes. These results are undeniable, for the authors possessed excellent experimental controls. The tRNAs were modified in only one residue, as opposed to the methyl-deficient tRNA experiments, and the change in the hypermodification was to a biologically relevant lower level of modification, and not, as was described above, a chemical treatment that produces derivatives not normally found in the tRNA. Furthermore, the authors demonstrated large differences in both in vitro protein synthesis, and ribosomal binding assays.

If this listing seems lengthy and overwhelming, then

the reader hasafeeling for the breadth of facts which suggest a biological function of ms^2i^6A and i^6A. Moreover, there exists a corresponding number of reports which associate a similar biological significance with yW and t^6A. While a discussion of these in the manner of those above is unnecessary, it behooves us to briefly summarize the results, and reference those who have laid the groundwork for this present study.

The base portion of the yW nucleoside can be selectively cleaved off of the yeast $tRNA^{Phe}$ by a mild treatment with acid. After this treatment, the yW can be replaced with other analogues such as proflavin. Several workers have found the resulting various types of yW deficient tRNAs to be less efficient in polypeptide synthesis and/or show reduced binding in ribosomal assays (Thiebe and Zachau (1968)[32], Ghosh and Ghosh (1970)[33], Wintermeyer (1971)[34], and Odom et al. (1974)[35]). Yoshikami and Keller made a minor change in the o_2yW of $tRNA^{Phe}$ in wheat germ, and found a reduction in polyphenylalanine synthesis[36]. Grunberger found a o_2yW deficient $tRNA^{Phe}$ from a rat liver hepatoma to be less efficient in ribosomal binding assays[37].

Experiments delving into the significance of t^6A have been slower in coming, but recently, Miller and Schweizer[38], and Miller et al.[39] isolated $tRNA^{Ile}$ from E. coli which was deficient in t^6A. Here again the polymer directed ribosomal binding was significantly less than with the normal tRNA.

In addition, it is important to mention, that in all

of these studies, with tRNAs deficient or changed in their content of hypermodification, the aminoacylation of the tRNAs were affected little if at all by the changes, as opposed to the large changes observed in the binding or transfer reaction. (See also references 40-43).

It would be more than just a little biased if we were not to include the conflicting evidence uncovered by some workers. Litwack and Peterkofsky[44] engineered a mixture of Lactobacillus acidophilus tRNAs that was 50% deficient in i^6A. They found no effect upon in vitro protein synthesis caused by this reduction. Kimball and Söll[45] found $tRNA^{Phe}$ from Mycoplasma, which has m^1G instead of a yW type base, to be completely functional in polyphenylalanine synthesis. These reports are few in number. However, we can not simply discount them, as they inform us that the picture perhaps is not as clear as we suspect. Nevertheless, we choose to ride the crest of the observations in favor of a biological significance of the hypermodified nucleosides, and forge on.

Having seen that polypeptide synthesis and ribosomal binding were impaired by a loss of hypermodification, some workers turned to less complicated systems involving tRNAs, in order to probe the effects of these bases. Högenauer et al. in 1972[46], found that yeast $tRNA^{Met}_f$ bound the trinucleotide complementary to its anticodon significantly stronger than did E. coli $tRNA^{Met}_f$. Both tRNAs have identical anticodons, but the E. coli tRNA has only an A residue adjacent to the anticodon, whereas the yeast tRNA has a t^6A. In a

different light, Grosjean et al.[47] studied complexes between tRNAs with complementary anticodons. They report a special stabilization of the complex due to the yW base of up to a factor of seven over the stability of a similar complex of trinucleotides. Thus, as with the ribosomal binding assays, these binding experiments also showed an effect, due to hypermodification, upon the 'codon'-anticodon interaction.

We close this section with very definite impressions of the importance of these hypermodified nucleosides. It is almost beyond a doubt now, that they indeed perform some function which alters the characteristics of the translation step in protein synthesis. With few exceptions, the presence of these bases has been demonstrated to affect in vitro polypeptide synthesis. This effect, at least in part, is due to a more efficient binding of the tRNA to the ribosome-mRNA complex.

III. A Need for Modification?

Aside from the observed effects of the presence of the hypermodifications as seen in the last section, we may gainfully speculate about possible roles of the bases in tRNA. A brief look at some of the aspects of the anticodon-codon interaction suggests that there may exist the necessity for hypermodification, in order for protein synthesis to be accurate and well regulated. In this section we will discuss three rather obvious possibilities for a hypermodification's role in aiding the necessary progress and outcome of the

codon-anticodon interaction.

(A) An Anticodon 'Quartet'

One of the simplest roles that hypermodifications may play is to prevent the formation of a fourth base-pair between the tRNA and mRNA (which would result in a kind of a 'frame shift' error). This has been suggested by many[51-53], and stems from the fact the hypermodification replaces one of the possible hydrogen bonding protons of adenine in the case of t^6A, i^6A, and ms^2i^6A (see Figure 1). Although there remains a hydrogen on the N^6 which could conceivably pair with a U, x-ray studies of crystals of the bases and nucleosides rule this out[51-56]. They indicate that in t^6A, i^6A and ms^2i^6A, the side chain(s) invariably is in a position relative to the ring that would prevent base-pairing. Likewise, the structure of a yW type base has been determined[57], and it is not too difficult to visualize the interference with normal base-pairing.

However, then we must entertain questions of the sort: i) why are there several tRNAs with no hypermodifications?, ii) why would such an elaborate modification be necessary just to eliminate base-pairing?, and iii) why are there not hypermodifications on the other side of the anticodon triplet? These questions make it seem unlikely that a hypermodified base's only role is to prevent base-pairing in that position. Let us also consider two other possibilities.

(B) Wobble

An interesting body of literature deals with the suggestion that the role of t^6A is to prevent wobble on the 3' side of the tRNA (references 58-60 and those about to be discussed). E. coli $tRNA^{fMet}$ and yeast $tRNA^{fMet}$ possess identical anticodon triplets, however the E. coli tRNA lacks t^6A whereas the yeast tRNA contains t^6A (see Tables I and II). Dube et al.[61] showed that both AUG and GUG are read by E. coli $tRNA^{fMet}$, whereas Stewart et al.[62] found that the yeast $tRNA^{fMet}$ read only AUG. Ribosome binding assays by Takeishi et al.[63] exhibited similar trends. The E. coli tRNA bound AUG and GUG to the same extent, whereas the yeast tRNA preferred AUG. A comparison between the E. coli $tRNA^{fMet}$ and E. coli $tRNA^{Met}$ (which contains t^6A) supported the same idea[64]. $tRNA^{fMet}$ could initiate with poly rUG, however the $tRNA^{Met}$ could not read this and thus no methionine was incorporated. Unfortunately, the trimer binding both with and without ribosomes generally produced conflicting results[46,63,65-67]. Because of this, and of the fact that these experiments are really observations and not explanations, it is useful to view the wobble story in the following way.

Figure 3 illustrates the tRNA-mRNA interactions which are allowed by the genetic code and the concept of wobble[68]. As is indicated, wobble is only allowed on the 5' side of the anticodon triplet (the third letter of the anticodon or codon). The lower portion of the figure demonstrates

Figure 3: tRNA-mRNA interactions which are allowed by the genetic code and wobble. Pictured are the anticodon arm and triplet, and the codon triplet in a strand of mRNA. Solid lines indicate Watson-Crick base-pairs; dashed lines indicate wobble base pairs. X and Y are two complementary bases. Wobble is only allowed on the 5'-side of the anticodon triplet.

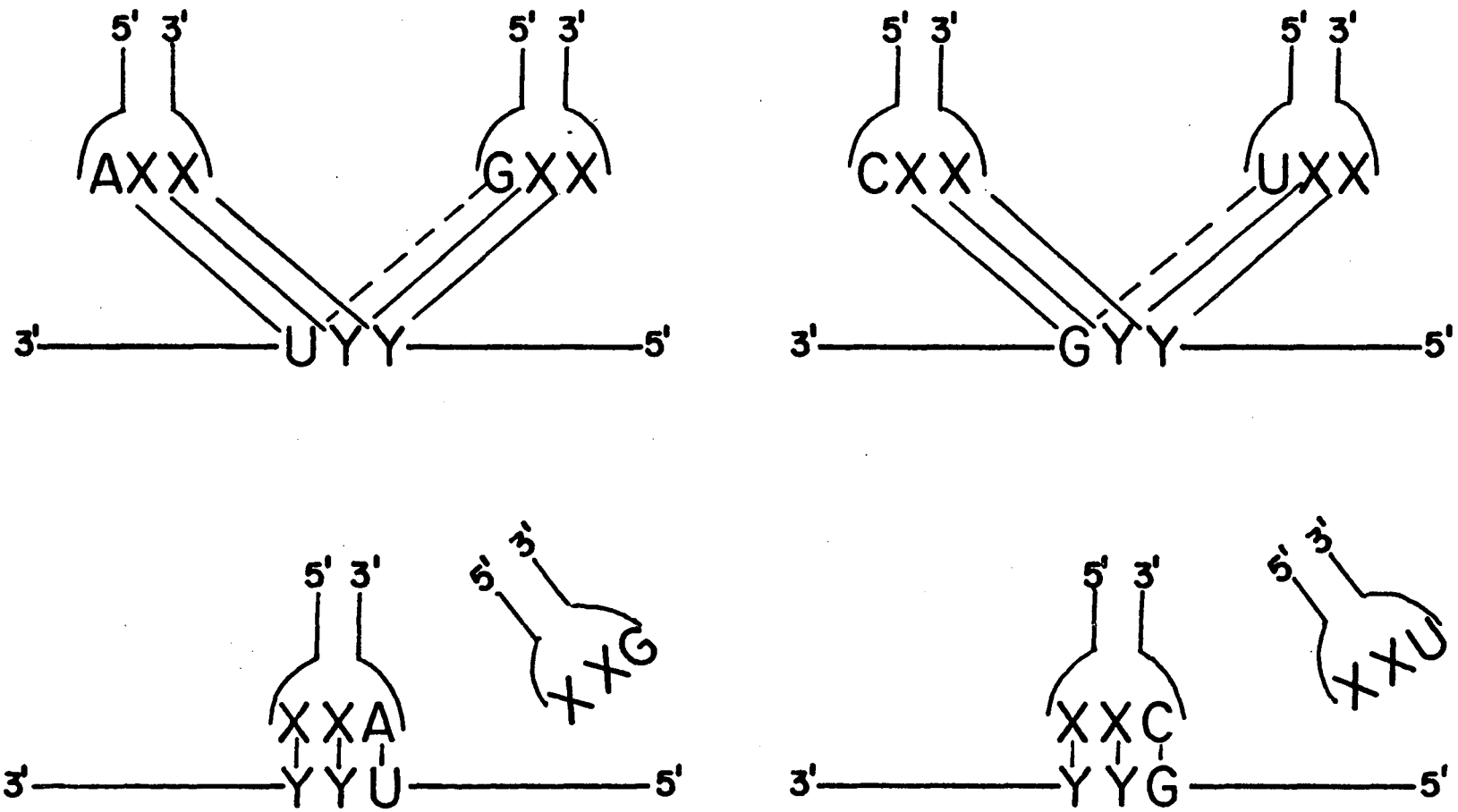

that only Watson-Crick pairing is allowed in the first letter (3' side of the tRNA) of the codon and anticodon. Therefore, the anticodons 5'-XXG-3' and 5'-XXU-3', pictured at a slant, cannot interact with the lower codons.

The wobble hypothesis states i) that the anticodons, 5'-AXX-3' and 5'-GXX-3', must belong to tRNAs which transfer the same amino acid, and ii) that 5'-CXX-3' and 5'-UXX-3' must belong to tRNAs which transfer the same amino acid. The available data bears ii) out (see Lys tRNAs and Gly tRNAs in Tables I and II); however, no 5'-AXX-3' anticodons have been found, and hence i) has not been as yet verified.

On the other hand, the anticodons 5'-XXA-3' and 5'-XXG-3' are found <u>not</u> to belong to tRNAs which transfer the same amino acid (e.g. see Phe and Leu tRNAs in Tables I and II). Likewise, the anticodons 5'-XXC-3' and 5'-XXU-3' do not belong to cognate tRNAs (see Arg and Gly; Ile and Val; and others in Tables I and II). Thus, the 5'-XXG-3' and 5'-XXU-3' anticodons pictured cannot interact with the mRNAs in the lower portion of Figure 3.

The important point to notice is this: for some reason(s), simply a change in the order of the codon letters, e.g. 5'-UYY-3' to 5'-YYU-3', results in the inability of a wobble base-pair to form. If we assume for the moment that this change in letters does not change the properties of the mRNA, then we must look to the tRNA for the asymmetry of structure and properties which produces this position selective wobble. (This seems like a reasonable assumption, un-

less one invokes the ribosomes to produce an asymmetric codon reading triplet. However we must remember that sequence isomers of even dinucleotides - e.g. UpA and ApU - often have very different physical properties[69-72].)

We cannot attribute this asymmetry to a special ordering of the sequences in tRNAs, for we can find examples of mirror image anticodon triplets (5'-XYZ-3' and 5'-ZYX-3') for tRNAs (compare E. coli Val 1 and Met tRNAs; E. coli Glu 2 and Sacc. C. Lys 1 tRNAs) - one of which will wobble and the other that cannot. For any asymmetry then, we must look to the bases on either side of the anticodon triplet.

Following this notion, the wobble allowed on the 5' side of the anticodon may perhaps be explained by the constant occurrence of a pyrimidine (almost exclusively a U residue) immediately adjacent to the 3rd letter of the anticodon (see Tables I and II). It is well documented that the pyrimidines, and in particular U, show the least tendency of the four regular bases to stack[69-72], and thus a flexible linkage at this point in the tRNA may allow the 'mispairing' of wobble[73].

On the other hand, in almost no case do we find a U or C adjacent to the first letter of the anticodon. This alone, without invoking hypermodification, accounts for a significant asymmetry. We do not always observe a hypermodified base in this position. However what we do find, as was mentioned in section II B, is the occurrence of t^6A adjacent to almost every first letter - when that letter is a

U. It is now important to remember as above, that a UpX linkage is relatively flexible; and hence that the t^6 modification of A may be necessary to prevent this flexibility and the resultant probable mismatching.

This speculation is useful, and that will be readily apparent in the next chapter. While it is a possible explanation for the observed facts, it says nothing about the role of the other hypermodifications. It is also conceivable that the other hypermodified bases play a role in preventing wobble[59], although devising such a simple picture as that above is not as obvious. For now then, we will close this discussion simply with the thought that hypermodification may very well be needed to prevent incorrect wobble. Let us turn to one further possibility for the necessity of hypermodification.

(C) Regulation

One might suspect that it would be desirable for translation to be regulated as is the whole of protein synthesis. More specifically, this thinking could be extended naively to the codon-anticodon interaction. If the different amino acids are to be incorporated at a uniform rate into the growing peptide chain, this would require the codon-anticodon interaction to proceed with the same efficiency from one codon to the next, and from one tRNA to the next.

Without at this time delving into the dynamics of double helix formation, we can say that the equilibrium

Chapter 2 THE DESIGNED APPROACH

Chapter 2

THE DESIGNED APPROACH

I. Preface

The foregoing chapter contains the observations. Aside from some very brief speculations in section III of that chapter, it contains only the observations, and not the explanations. At this time there are no molecular explanations for the functions of the hypermodifications. Indeed, some of the functions themselves are quite possibly unknown. Nor will this present chapter offer explanations. What will be put forth here are the hypotheses adopted to encompass the observations. More importantly, these hypotheses will guide us in the investigation of new observations. Hopefully thus, the careful choice of hypotheses will suggest manageable experiments which will test these hypotheses, and ideally confirm them.

We would like to define and explain in molecular terms the function(s) of hypermodifications. It should be obvious that only observations made on a molecular scale can lead to this understanding. Thus for instance, until we comprehend the dynamics of protein synthesis on the scale of molecular interactions, the in vitro protein synthesis assays of the 'function' of hypermodifications (discussed in Chapter 1) will not yield molecular explanations. Of course, one can argue that we understand little even of the mononucleotides (or of the atom for that matter). But, it will be my con-

tention that we must study the smallest scaled system in which the effects of the hypermodifications are still evident. The experiments on the grander scales (e.g. in this case protein synthesis experiments) will then serve to test the hypotheses formed by the findings of these studies.

II. The Hypotheses

The hypotheses we formulate must reflect these ideas. We must attempt to choose the most precise postulate which is consistent with the observed facts, so that only the very specific of new observations can test it. Otherwise, the new experiments may not in reality test the hypothesis; they may again only be consistent with a vague all-encompassing postulate.

The attainment of this type of ideal hypothesis, in which the suggested experiments essentially yield a yes or no answer concerning the validity of the postulate, may in practice be very difficult. However, we can avoid hypotheses such as: i) the hypermodification is "essential for the conformation of the anticodon loop and the formation of an anticodon-messenger-ribosome complex"[56], and ii) the hypermodification "promotes a single stranded conformation for the anticodon loop"[51]. While these statements may in fact be correct, they are too ambiguous and do not lend themselves well to experimental testing. With all of these things in mind then, let us now design the approach to the problem.

In the case of the possibility of several functions of

the hypermodifications, the desirability of a precise hypothesis compels us to limit our vision at first to a single function. Thus, for a first approximation for these basic studies I will ignore the possible effects of the ribosomes, although some believe a function(s) of the hypermodification is linked to them[39,76]. I will ignore the possibility of a function brought about by the chemical reactivities of the hypermodifications[76]. Finally, in this thesis I will not attempt to deal with the anticodon quartet hypothesis (see Chapter 1, section III A). That there even exist functions aside from these that I am bypassing seems evident from the trimer binding studies in the absence of the ribosomes (see again Chapter 1, section II C). In these studies, in spite of the absence of ribosomes, detected chemical reactions, or a fourth base-pair, an effect due to the presence of the hypermodifications was found[46,47]. We then set our directions on the study of the effect of the hypermodifications upon the isolated phenomenon of the mRNA trimer-tRNA interaction.

Just a glance at the literature however quickly reveals the true complexity of this interaction, and the difficulty in the measurement of its characteristics[46,65-67]. An attempt to understand the differences (brought on by the hypermodifications) in these characteristics therefore appears unlikely by the direct study of tRNA-trimer binding. Here arises the second reason for working on the smallest scaled system which exhibits observable differences (see the

preface of this chapter for the first reason). By studying smaller systems in which an effect is still evident, the measurements become much easier and more interpretable.

The smaller system in this case will be the isolated tRNA molecule. The structure of the anticodon loop and mRNA trimer, and the stability of these structures, will determine the outcome of the interaction between them. We will begin by assuming that the hypermodification on the tRNA does not alter the structure of the mRNA trimer during this interaction. Thereby, we can focus our attention on the structure and energy of the anticodon loop.

X-ray studies on crystals of yeast $tRNA^{Phe}$ have given us information about the anticodon loop[77-79]. The important points to mention are the following. The various studies were not performed at a resolution sufficient to give reproducible details around the hypermodification (the yW base). Furthermore, the loop is thought to be flexible in solution and perhaps in a different conformation than in the crystal[80]. Finally, x-ray tells us nothing about the relative stabilities or energies of the various linkages in the loop. In short, the x-ray data has yielded little information concerning the hypermodification's function. Aside from some success in the case of the fluorescent yW base[80], solution studies of intact tRNA molecules have also been unable to yield good information concerning the structure around the modifications, or of their effect upon the properties of the anticodon loop (see for instance reference 81).

It is clear that one must look to even smaller systems for the molecular information. In following with this realization, I have chosen to study the properties of the smallest unit of the tRNA containing the hypermodification which still exhibits the characteristics of a polynucleotide - the dinucleoside monophosphate. There is of course no guarantee that the dimers containing the hypermodifications will show different physical characteristics than their unmodified counterparts. More importantly, in looking at such small molecules I have sacrificed the assay of biological function (e.g. - the trimer binding assay). But I will continue with the thinking that the structure and energies of biomolecules dictate their function, and thus that knowledge of the former informs us of the latter.

This now brings us to the working hypothesis which I chose in the beginning of this study: *Through their stacking interactions with the first letter of the anticodon triplet, hypermodifications function to lock the terminal A·U base-pair into a correct reading frame, thus promoting mRNA binding, eliminating wobble, and perhaps regulating translation.* This kind of idea is not new[39,58,59]. What this particular formulation offers however (although it is still rather unfortunately vague), is the suggestion of experiments to perform which will test it. Since dinucleotides exhibit polymer-like characteristics with regard to intramolecular stacking, the dimers containing hypermodifications should exhibit different and in fact stronger stacking interactions

than those without. If not, then we must revise our hypothesis; but in so doing, we will have learned something about the function. The real supposition here is that knowledge of the structures and energies of the dinucleotides will yield information as to the function(s) of hypermodifications.

III. The Dinucleoside Monophosphates

The specific nature of my hypothesis requires that the dinucleotides we choose be those which contain the first letter of the anticodon triplet and the hypermodified base. I will not in this thesis delve into the properties of the other possible dinucleotides containing hypermodifications. Thus the molecules XpH, where H is the hypermodified base and X is either an A or a U, will be studied. The dimers HpZ, where Z has so far been found to be only an A residue in the tRNAs (see Tables I and II), will not be investigated here.

I desire then to examine the properties of the following dinucleoside monophosphates: Upt^{6}A, Api^{6}A, Apms^{2}i^{6}A, and ApyW. Unfortunately, because of the complexity of protecting the side chain of yW, the synthesis of the ApyW dimer through chemical means is not practical by present day methods (see Chapter 3, Section I E). Even the nucleoside yW is difficult to obtain[4]. And since it occurs in only one of the many species of tRNA (Phe), it seemed unreasonable to attempt to obtain the dimer by means of a degradation of that tRNA (e.g. see in Chapter 3, Table I which

gives the amount of bulk tRNA required for the obtainment of Upt^{6}A, which occurs in several of the species of tRNA present). Because of these reasons, the properties of ApyW were not investigated. However, the properties of the dinucleoside phosphate Apε A have been examined, where εA (1-N^6-ethenoadenosine)[82] is pictured in Figure 1. εA is a synthetic compound not found in tRNA. It is however perhaps the closest synthetically obtainable model of yW (compare with yW in Figure 1 of Chapter 1 - Actually, it is a closer model to W, a derivative of yW which lacks the large side chain[4]). Hence, we may through this model compound learn something about the properties of dinucleotides containing yW or its derivatives.

In addition to Upt^{6}A, Api^{6}A, Apms^{2}i^{6}A, and Apε A, the unmodified counterparts UpA and ApA have been studied. Also, in order to characterize the dinucleotides, the pertinent properties of all of the component monomers have been examined.

IV. The Experiments to Perform

Again, the nature of the hypothesis suggests very definite experiments to perform. If we desire to learn of the 'stacking' interaction we must choose those techniques which will monitor this interaction. Since stacking is indeed a dynamic equilibrium, we must look not only at the static properties, but also at the properties as a function of the position of the equilibrium.

We further desire to study the stacking interaction as

Figure 1: The synthetic nucleoside εA.

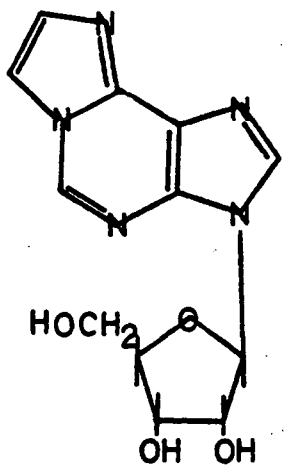

εA

1, N^6-ethenoadenosine

an isolated event, and will therefore work at concentrations low enough to avoid intermolecular effects. These more or less 'physiological' concentrations demand the sensitivity of spectroscopic techniques. Consequently, the optical absorption, circular dichroism (CD), and high resolution NMR properties of the dimers in solution have been studied. (Due to a lack of crystals of the dinucleotides, no x-ray data were obtained. Even if the crystals and expertise were available for an x-ray analysis, it is not clear how the packing and intermolecular forces would affect the observed structure.) Since the equilibrium of the stacking is very temperature dependent, the spectral characteristics of the dimers have been obtained as a function of temperature. Thus, we can begin to talk about the structures and relative energies of the dinucleotides.

V. Summary

In this, the most important of chapters, we have progressed from the observations to the hypothesis and finally to the approach chosen to test the hypothesis. I have emphasized the desire for a molecular understanding of the function of the hypermodifications, and in so doing have scaled the system down to the point of very basic molecular interactions. I have also emphasized the advantages of a precise hypothesis, and as a result have chosen very precise experiments to perform on a well-defined series of molecules. This approach has in a large part derived from

the belief that the physical chemistry of small biomolecules can lead to an understanding of the biological functioning of larger systems. Thus as the title of this dissertation states, we will now attempt to learn about the role of hypermodified bases in tRNA by studying the solution physical properties of dinucleoside monophosphates.

Chapter 3 PREPARATION AND PURIFICATION OF MONO- AND DINUCLEOTIDES

I. Techniques

(A) Glassware

(B) Chromatography

(i) Column Chromatography

(ii) Paper Chromatography

(C) Evaporations

(D) Degradative Assays

(E) Chemical Synthesis of Dinucleotides

II. t^6A Compounds

(A) Preface

(B) Snake Venom Phosphodiesterase Digest

(C) Isolation and Purification

III. i^6A Compounds

(A) Preface

(B) pi^6A - Synthesis and Purification

(C) Api^6A - Synthesis and Purification

IV. εA Compounds

(A) Preface

(B) $Ap\varepsilon A$ - Synthesis and Purification

V. ms^2i^6A Compounds

(A) Preface

(B) $Apms^2i^6A$ - Synthesis and Purification

(C) pms^2i^6A - Source and Purification

VI. Unmodified Compounds

Chapter 3

PREPARATION AND PURIFICATION OF MONO- AND DINUCLEOTIDES

I. Techniques

(A) Glassware

Glassware was routinely cleaned in L.O.C. detergent and in ordinary cleaning solutions when necessary (sodium-dichromate-sulfuric acid or aqueous ethanol-sodium hydroxide). This was followed by drying in Precision Co. ovens at approximately 200°C. Sterile polypropylene tubes and vials (Falcon) were used and then discarded or cleaned in a similar manner as the glassware above. Polypropylene fraction collector tubes (Gilson) and Teflonware were cleaned as the glassware, and dried in lower temperature ovens.

(B) Chromatography

(i) Column Chromatography

Columns were, in general, buret-style cylinders with teflon stopcocks and fittings for teflon needles. They were packed with sterile glass wool (∿1 cm high), followed by acid-washed glass beads (Schwarz/Mann 900806, ∿1 cm high), and then followed by the resin, under flow.

Resins included both ion-exchangers and gels. DEAE A-25 Sephadex (Pharmacia) was the only ion-exchange resin used. This resin separates mostly on the basis of charge, but also shows differential affinities for the various bases (e.g. see Figure 1). Chelex-100 (Bio-Rad), a chelating resin,

was used for removing divalent cations. Bio-Gel P-2 (Bio-Rad, 50 - 100 mesh), a sizing gel, was used for desalting. (The desalting is very efficient with dimers, but much less so with monomers.) Sephadex LH-20 (Pharmacia) is an affinity gel for lipophilic groups. Thus, it proved to be very effective for the separation of modified and unmodified molecules having the same ionic charge. All were equilibrated, packed, and cleaned according to the manufacturers' instructions. Degassing, in a Precision Co. vacuum oven, of equilibrated resins was performed prior to packing of columns to be run at low temperatures (cold room at 4°C).

Eluents varied of course, depending upon the resin used. Distilled water was used alone with Bio-Gel P-2 and Chelex-100. A mixture of ethanol and water was used for elution with Sephadex LH-20 (33% v/v of 95% EtOH/H_2O). By far the most common column run was the ion-exchange DEAE A-25 Sephadex resin, using a salt solution as the eluent. In all these cases, the salt chosen was triethylammonium bicarbonate (TEAB). This is a volatile salt, which under reduced pressure forms triethylamine (TEA) and carbon dioxide (this is enhanced in the presence of methanol), and hence simplifies greatly the desalting of column fractions.

In order to prepare the TEAB solutions, TEA (Aldrich, 13, 206-3) was glass distilled with a Vigreux column over Molecular Sieve (Linde, 13X) at atmospheric pressure (heat controlled by a Glas-Col mentel in conjunction with a Powerstat regulator). In the case of a column run as a final

step in a purification, this distillation was repeated up to five times. 1 M solutions of TEAB were prepared by dissolving 139 ml of TEA (ρ=0.7255 g/ml, MW=101.2 g/mole) in cold water by extensive bubbling of CO_2 from dry ice. Bubbling was continued until the pH was $\sim$7.5, at which point the TEA was essentially all in the form of the aqueous salt. Molar solutions were generally prepared shortly before a column run, but were stored cold if not used immediately. TEAB columns requiring long times were run in a cold room, as the volatile salt will evaporate, forming bubbles in columns, and changing the salt concentration and often the pH as well. Solutions left cold for later use, and all those made by dilution of stock solutions, were purged with CO_2 again before elution, until a pH of at least 7.5 was obtained. Thus, all DEAE A-25 columns were run at pH$\sim$7.

All eluents were applied to the top of the column, utilizing closed system siphoning from a reservoir with 1/8" flexible plastic tubing (Tygon). Reservoirs included both single bottle reservoirs and gradient reservoirs. Salt gradients were used only with DEAE A-25 Sephadex columns, and were simply comprised of two beakers or two flasks (of the same dimensions - all gradients were linear), containing the extremes of the salt concentrations desired, and connected via a glass U tube. Drainage to the column was always from the vessel with a lower salt content, and the two salt concentrations were mixed by magnetic stirring (Thermolyne). A few columns were run under higher pressures

than could be obtained by raising the reservoirs. In these cases, a peristaltic pump was used (Gilson Minipuls II).

The eluate from all column types was fractionated by automatic fraction collectors (Gilson VFC, or Micro Fractionator FC 80L). Fractions were collected either in polypropylene tubes in the case of the VFC (15 ml capacity, 200 - 400/spool), or in glass tubes when using the micro collector (10 ml capacity, 80/rack). Monitoring of fractions was performed by measurement of UV absorption on a Cary 15.

(ii) Paper Chromatography

While column chromatography was the most often used separation technique for preparative purposes, paper was also occasionally used for large scale separations. More frequently however, paper was used for analytical separations of degradation and identification assays. Chromatography paper (Whatman 3^{M}_{M}) was cut into 20 x 57 cm strips and attached to glass racks made to order (glass shop). Concentrated samples and markers of a few µl were applied to a region near the top of the paper, in either spots or streaks, depending upon the size of the sample[83] (using Drummond disposable Microcaps). For a descending elution, the tops of the racks were placed in glass or metal trays containing the eluent (100 - 200 mls), and these were set in chromatography tanks (either made by the glass shop or Dohrmann) preequilibrated with the vapor of the eluent.

Eluents were most often mixtures of 95% ethanol and

1 M ammonium acetate (pH 7)[83]. After elution, the papers were removed from the tanks, air dried in a hood, and then monitored with a UV lamp (Mineralight UVS·12). When collection of the samples was desired, the resulting spots were cut out, and a preliminary desalting step was performed by repeatedly washing the papers in a tray of 100% ethanol, followed by a rinse of ethyl ether to facilitate drying. The papers were then rolled and placed into plastic spin thimbles (Reeve Angel), and these were placed in 12 or 15 ml centrifuge tubes. They were successively washed with ∿1/2 ml of H_2O, and the sample was spun down into the centrifuge tube (International Equipment Co. clinical centrifuge), until no UV absorbing material remained on the paper (∿5 - 10 times).

(C) Evaporations

Pooled column fractions and paper washes were evaporated with either a rotary vacuum evaporator (Büchi/Rinco), for larger sample volumes, or a shaker vacuum evaporator (Buchler 3-2100), for small samples. Both were used in conjunction with a Vac$_T$orr 20 pump, and a dry ice-methanol trap. The rotary evaporator also utilized a preliminary ice water trap. After evaporation of TEAB containing pools, methanol was repeatedly added and evaporated until no salt crystals remained, or until the odor of TEA was undetectable. Careful heating was sometimes used to ease the evaporations, and was effected by the built in heat bath in the shaker, or by a water bath (Corning hot plate) with the

rotary evaporator.

Frozen samples of various volumes could be evaporated with a freeze dryer (Thermovac). A Duo Seal vacuum pump (Welsh Scientific) was used with an additional trap of absolute ethanol cooled by a CryoCool cold finger (Neslab).

(D) Degradative Assays

Enzymatic and chemical cleavage of phosphoester bonds in nucleotides and dinucleotides were performed as an aid in identifying their sizes and compositions. These degradations were also carried out for preparative and quantitative reasons, but those procedures will not be covered in this section.

Phosphomonoester bonds of nucleotides were cleaved by the action of bacterial alkaline phosphatase (BAP) (Worthington 3.1.3.1 (E. coli)). The enzyme solution was prepared by dialyzing the Worthington solution against 10 mM $MgCl_2$, 0.1 M NaCl (both Mallinckrodt), and 10 mM tris-HCl (Sigma/Allied) (pH 8)[83]. The sample was shaken down or lyopholized to dryness in a conical tube, whereupon for a sample of 2 - 3 mg, 50 µl of Q' buffer (25 mM $MgCl_2$, 1 M NaCl, and 0.5 M tris-HCl (pH 8.2)) and 15 µl of BAP were added (smaller samples were scaled accordingly), the tube sealed with Parafilm, and the mixture incubated at 37°C for 3 hours (Precision Scientific Co. incubator 66648). The sample was then shaken down and spotted on paper with markers.

The phosphodiester bonds of dinucleoside monophosphates could be cleaved with several agents. Snake venom phosphodiesterase (SVP) (Worthington 3.1.4.1 Phosphodiesterase I) was used when the desired products were the nucleoside on the 5' side of the dimer plus the 5' nucleotide (X + pY from XpY). Bovine spleen phosphodiesterase (BSP) (Worthington 3.1.4.1 Phosphodiesterase II) was used to obtain the products Xp + Y from XpY. Degradation using simply NaOH also yielded the products X>p + Y (X>p here being the 2' - 3' cyclic phosphate).

The SVP assay was run with a 1 mg/ml enzyme solution, 0.5 M ammonium formate (Eastman) (pH 9.2), plus a sample of 5 mg/ml in water, with a ratio of volumes of 5:5:1[84]. The mixture was sealed and incubated at 37°C for 24 hours.

The entire contents of the BSP vial (∿10 - 15 Worthington units) were added to 1 ml of H_2O. For the assay, this solution was mixed with 0.25 M sodium succinate (Eastman)-HCl (pH 6.3), substrate at 5 mg/ml, and water, with a ratio of volumes of 1:2:2:4. This was incubated at 37°C for 24 hours.

The OH^- degradation was performed by adding 5 M NaOH (Allied) to a 5 mg/ml solution of sample in the ratio of 1:10. Again, this was sealed and uncubated at 37°C for 24 hours.

(E) Chemical Synthesis of Dinucleotides

The synthesis of dinucleoside monophosphates contain-

ing hypermodified bases was performed according to a procedure by Follman[85]. This procedure entails the condensation of a protected 3' nucleotide with an unprotected nucleoside using dicyclohexylcarbodiimide (DCC). As a result of using an unprotected nucleoside, a mixture of phosphodiester isomers is obtained. Fortunately, the 3'-3' and 3'-2' isomers are formed in smaller amounts than the desired 3'-5' compound; and more importantly, the former isomers are preferentially hydrolyzed upon treatment with methanolic ammonia. A short synopsis of this procedure will be presented here, as the experimental details differ slightly from those of Follman's.

Dry pyridine was prepared by careful distillation of reagent grade pyridine (Mallinkrodt, 7180) with practical grade chlorosulfonic acid (Eastman, P669) (set up as with the TEA distillation), followed by distillation over special reagent grade KOH pellets (MCB, 11170) with a calcium hydride (Alfa Products, 19111, -4+40 meth) drying tube. It was then tightly sealed and stored over molecular sieve (linde, 4X).

In order to ensure that little if any H_2O was present in the reaction mixture, the appropriate amounts (see following sections) of protected nucleotide and the hypermodified nucleoside were rendered anhydrous by repeated evaporation with dry pyridine. This was performed in a hood, utilizing the rotary vacuum evaporator with a 50 ml round bottom flask (₹14/20). The usual preliminary ice trap

was by-passed, and the dry ice-methanol trap was replaced with a liquid N_2 trap to prevent excessive contamination of the pump oil with pyridine. Hot water was pumped through the evaporator's cooling coils, such that the pyridine was coll ected only in the LN_2 trap.

After four or five evaporations (∿10 - 15 ml pyridine each time), the preweighed DCC (Aldrich, D8000-2) was added to the flask. Enough pyridine was added to dissolve the bulk of the reagents (∿5 - 10 ml), a flea stir bar (Tekpro, S8304-3) was added, and the vessel was sealed with a ₹14/20 stopper, teflon tape, and parafilm. The flask was placed in a beaker, which was then covered entirely with aluminum foil, and this arrangement was placed on a magnetic stirrer (Lab-Line, 1250) insulated with two layers of asbestos sheets (to minimize heating caused by long hours of stirring). The beaker was further covered with a black box, and the mixture was stirred at room temperature for 12 - 14 days.

At the completion of this time, the reaction was stopped by the addition of ∿5 - 10 ml of H_2O, thus forming insoluble dicyclohexyl urea from unreacted DCC. This was filtered through paper on a sintered glass crucible with suction, and rinsed with more water. The combined filtrate was then extracted at least three times with petroleum ether (Mallinkrodt, 4980), the pet ether fraction being discarded. The aqueous mixture was placed in a 100 ml rb flask (₹14/20), and evaporated to dryness using the same

assembly in the hood as described above. To the resultant film was added ∿35 ml of cold methanolic ammonia (MeOH saturated with NH_3 gas at 0°C), and the flask was tightly sealed and left to stand overnight at room temperature. The NH_3 was consequently removed by aspiration, and the MeOH removed using the rotovap assembly used for TEAB evaporations. The final film was dissolved in H_2O and chromatographically purified.

II. t^6A Compounds

(A) Preface

pt^6A and $pUpt^6A$ were two of the numerous products formed from SVP digests of crude tRNA, carried out according to a procedure outlined by Cunningham and Gray[84]. A short summary of the digest procedure will be given here, as some slight modifications have been made, and this will be followed by a more detailed discussion of the isolations, because they differ markedly from those of the above authors'. Also described with the isolations, is the formation of Upt^6A, which was isolated after BAP treatment of $pUpt^6A$.

(B) Snake Venom Phosphodiesterase Digest

For this digest, we utilized mixed bakers' yeast tRNA (Plenum) which was deficient in $tRNA^{Phe}$ and $tRNA^{fMet}$. (S. Freier[86,87] passed the mixed tRNA through BD Cellulose in order to isolate $tRNA^{fMet}$. That tRNA passes through first, and the remainder of the tRNAs, with the exception of

$tRNA^{Phe}$, are readily eluted with NaCl. We used this NaCl eluate.)

The enzyme used was the SVP described in section I D of this chapter. The enzyme:tRNA ratio, and their concentrations, were similar to those used by Cunningham[84]. The activity of the enzyme (Cunningham's unit of activity is not equal to Worthington's unit) was determined using the yeast tRNA instead of rRNA.

To minimize the size of the chromatography column used, the tRNA was divided, and two separate degradations were carried out. Table I describes the conditions used. At the ends of the reaction times, the preparations were titrated to a pH of ∿7 with formic acid (MCB, 5044). They were then, as is described in the next section, chromatographically purified.

(C) Isolation and Purification

The isolation and purification of pt^6A and Upt^6A can be most easily described by the Tables II and III. Figures 1 - 5 illustrate some of the representative steps formulated in these tables. (Volumes of the columns refer to the lowest salt conditions. After the columns had been loaded with the samples, they were routinely washed (2 - 3 column volumes) with the solution they were initially packed in - i.e. the lowest salt concentration. This removes uncharged molecules, e.g. nucleosides, from the column.) We will discuss here only those details of the steps which have not

Table I. Conditions for the SVP digestions of yeast tRNA.

	Preparation A	Preparation B
tRNA	53,000 A_{260} units in 250 ml H_2O	60,8000 A_{260} units in 250 ml H_2O
Enzyme	15 bottles* in 130 ml H_2O	15 bottles* in 125 ml H_2O
Buffer	125 ml of 0.5 M Ammonium Formate** pH 9.2	same as prep. A

All the ingredients were simultaneously mixed, and the preparations carried out in sealed 500 ml polypropylene vessels at 37°C for 21 hr.

* - 100 Worthington units/bottle or ∿4 mg enzyme/bottle

** - B&A, #1292 - titrated with NaOH

Table II. Steps in the purification of Upt^{6}A. * marks the steps which are pictured in subsequent Figures. See text for further details of certain steps.

* 1. Large DEAE A-25 Sephadex column of Preparation A (see Figure 1)

2. Large DEAE A-25 Sephadex column of Preparation B.

3. Small DEAE A-25 Sephadex column of pUpt^{6}A from Preparation A.

* 4. Small DEAE A-25 Sephadex column of pUpt^{6}A from Preparation B. (see Figure 2)

5. Pool pUpt^{6}A from Preparations A and B.

6. Paper chromatography in system A^{84}.

7. Paper chromatography in system B^{84}.

8. Remove terminal phosphate with BAP treatment.

9. Small DEAE A-25 Sephadex column.

10. Chelex-100 column.

*11. Final DEAE A-25 Sephadex column. (see Figure 3)

12. Change cation from $TEAB^+$ to Na^+.

13. Bio-Gel P-2 column.

14. Sephadex LH-20 column.

Table III. Steps in the purification of pt^6A. * marks the steps which are pictured in subsequent Figures. See text for further details of certain steps.

* 1. Large DEAE A-25 Sephadex column of Preparation A. (see Figure 1)

2. Large DEAE A-25 Sephadex column of Preparation B.

3. Small DEAE A-25 Sephadex column of pt^6A from Preparation A.

* 4. Small DEAE A-25 Sephadex column of pt^6A from Preparation B. (see Figure 4)

5. Pool pt^6A from Preparations A and B.

6. Paper chromatography in system A^{84}.

7. Paper chromatography in system B^{84}.

8. Chelex-100 column.

9. Final DEAE A-25 Sephadex column.

10. Change cation from $TEAB^+$ to Na^+.

11. Bio-Gel P-2 column.

*12. Sephadex LH-20 column. (see Figure 5)

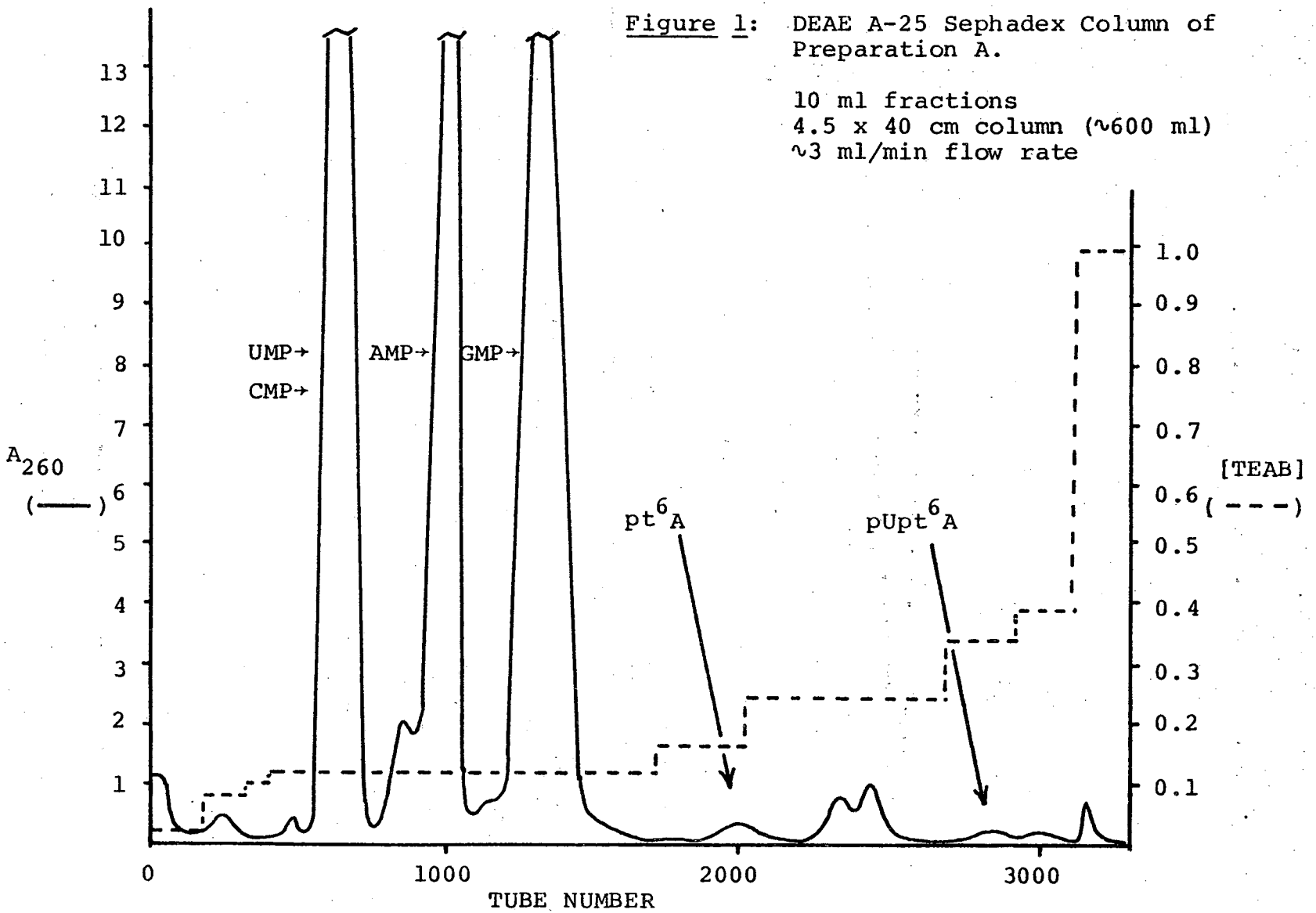

Figure 1: DEAE A-25 Sephadex Column of Preparation A.

10 ml fractions
4.5 x 40 cm column (∿600 ml)
∿3 ml/min flow rate

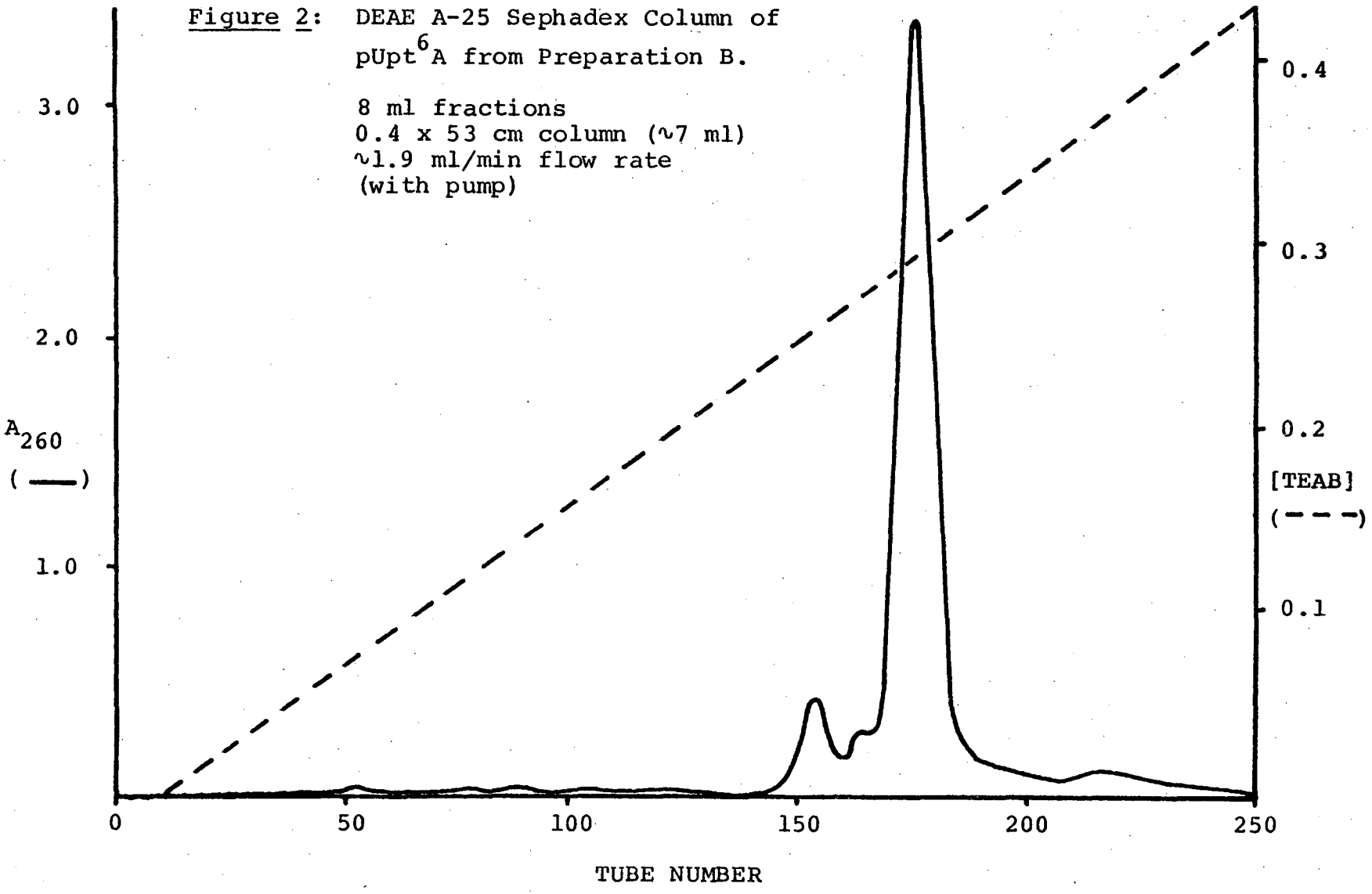

Figure 2: DEAE A-25 Sephadex Column of pUpt^{6}A from Preparation B.

8 ml fractions
0.4 x 53 cm column (∿7 ml)
∿1.9 ml/min flow rate
(with pump)

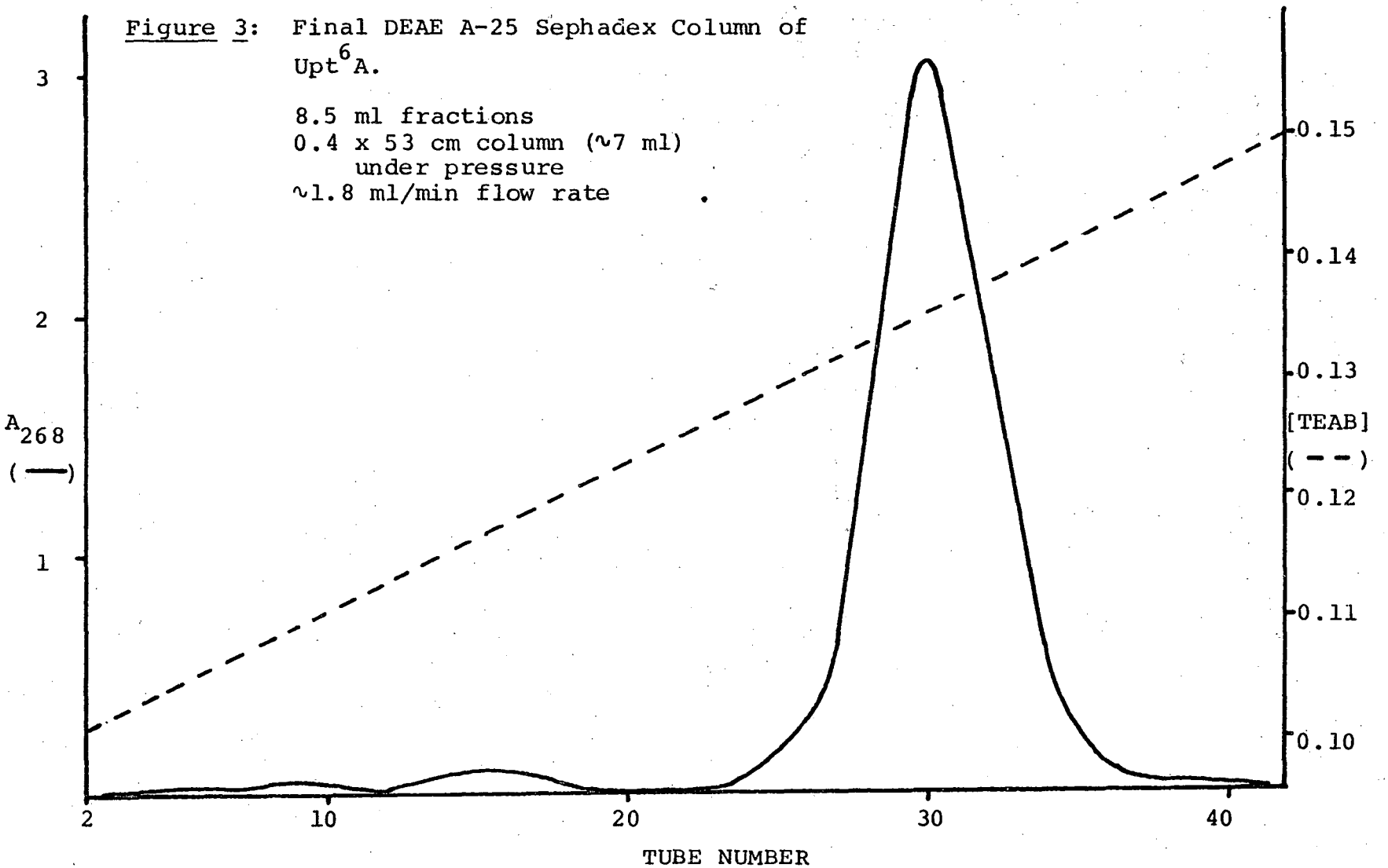

Figure 3: Final DEAE A-25 Sephadex Column of Upt^6A.

8.5 ml fractions
0.4 x 53 cm column (∿7 ml)
under pressure
∿1.8 ml/min flow rate

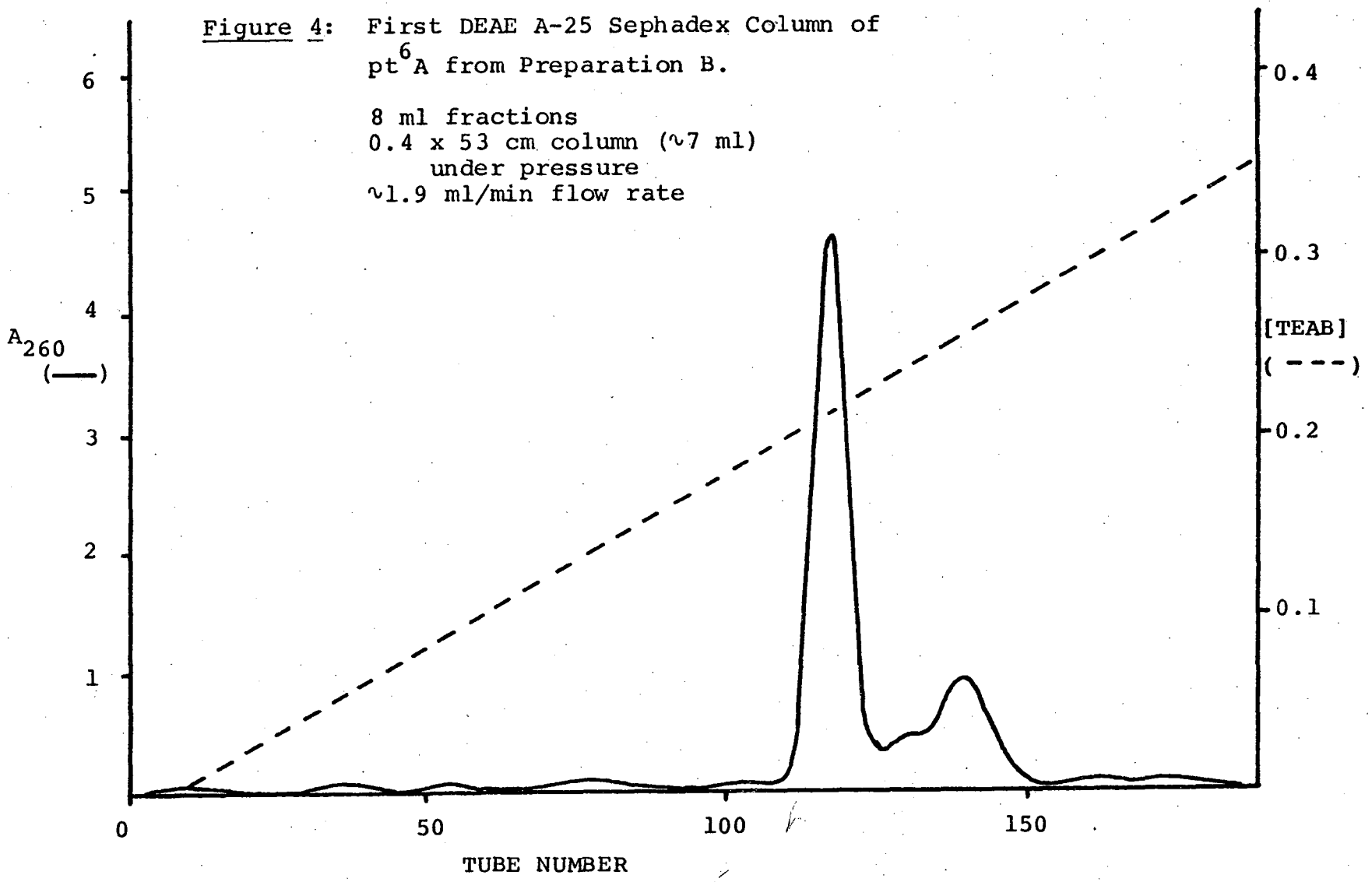

Figure 4: First DEAE A-25 Sephadex Column of pt^6A from Preparation B.

8 ml fractions
0.4 x 53 cm column (∿7 ml)
under pressure
∿1.9 ml/min flow rate

Figure 5: Sephadex LH-20 Column of pt^6A.

1 ml fractions
50 ml buret column
∿0.08 ml/min flow rate
95% EtOH/H_2O (33% v/v)

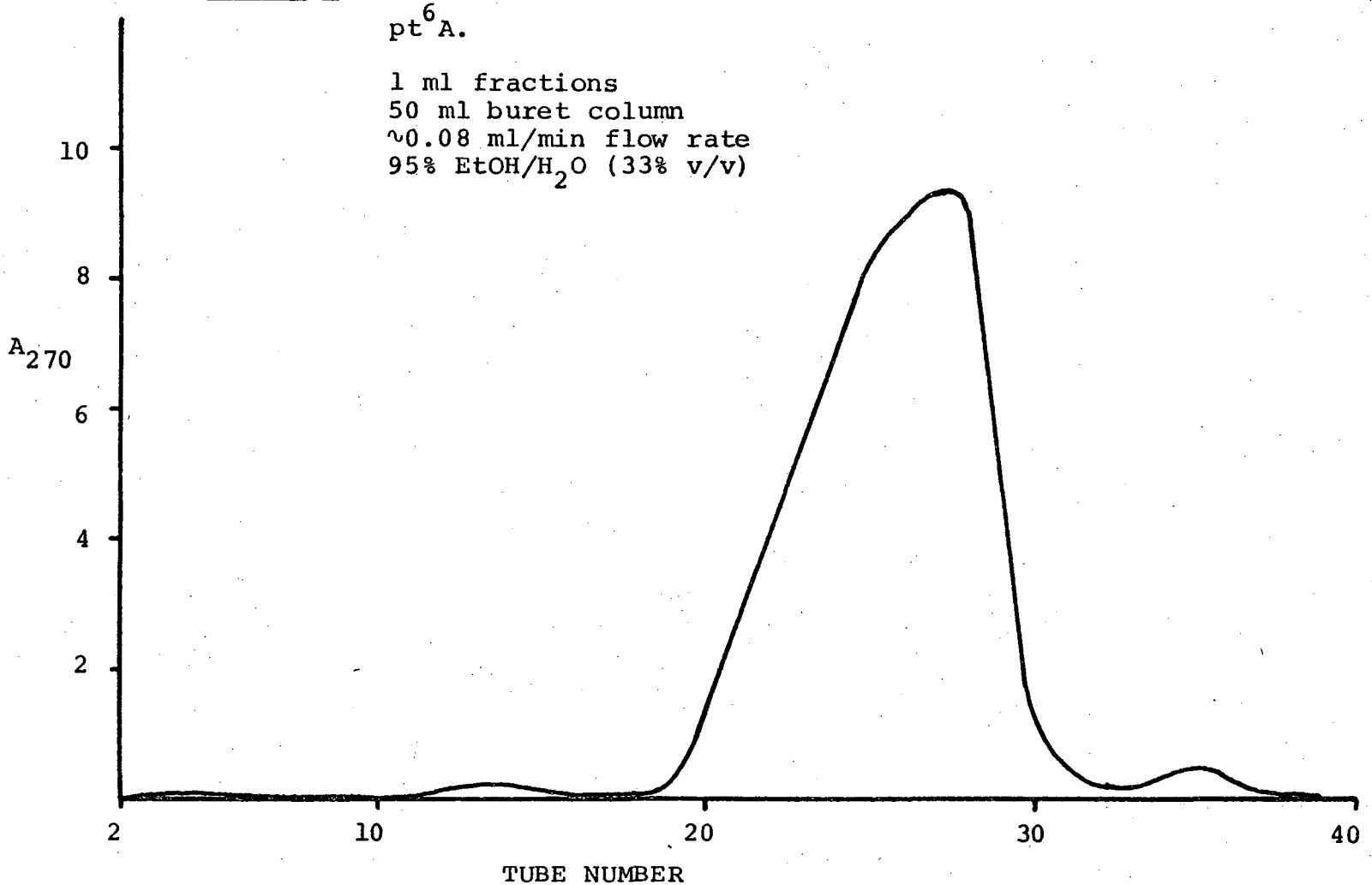

been covered in the Techniques section of this chapter.

Note in Figure 1 the tiny amounts of pt^6A and $pUpt^6A$ relative to the four major nucleotides. Also note the relatively good separation of the complex mixture with only a single column (which can further be seen by the small impurity peaks in subsequent columns, e.g. see Figures 2 and 4). The identities of pt^6A and $pUpt^6A$ were initially determined by their characteristic UV spectra, as well as with paper chromatography with markers kindly supplied by Gray[84]. (Gray supplied us with ∿40 A_{260} units of partially purified $pUpt^6A$. A portion of this was used for markers, and the remainder was pooled with our $pUpt^6A$.) Both pt^6A and $pUpt^6A$ were subjected to the same preparative paper chromatography used by Cunningham[84].

For ease of comparison to unmodified dimers, of which most have been previously studied and characterized, we chose to remove the terminal phosphate from $pUpt^6A$. The $pUpt^6A$ was run through a very small (∿5 ml) DEAE A-25 Sephadex column after the paper chromatography, in order to remove the large amounts of ammonium sulfate (which precipitates proteins). Then, to the $pUpt^6A$ in ∿0.4 ml of H_2O, was added 600 µl of Q' buffer, 100 µl of BAP, and the mixture incubated at 37°C for 3 hours (see Section I D of this chapter). This was then followed by a 5 ml DEAE A-25 Sephadex column and a ∿40 ml Chelex-100 column (sample applied in a few µl - elution with H_2O only), followed by a final DEAE A-25 Sephadex column. For reasons that will become

clear when we discuss the properties of Upt^{6}A, TEA^+ was replaced by Na^+ as the counterion for the dimer. This was accomplished by the addition of $NaHCO_3$ (Fischer, S-233) in a five fold excess of the dimer itself. Repeated evaporation with methanol liberated the TEA^+ as TEA and CO_2 (the CO_2 coming from the $NaHCO_3$). The excess $NaHCO_3$ was then to a large degree removed by a Bio-Gel P-2 column. The effluent from this column was monitored conductometrically with the aid of a conductivity electrode (Radiometer, CDC 114) and a Wheatstone bridge arragnement. The conductance of the dimer fraction was approximately equivalent to that of a 5×10^{-4} M solution of KCl; and the dimer concentration of the pool was also $\sim 5 \times 10^{-4}$ M, indicating that the desalting was very successful. The relative absorbances at 268 nm and 213 nm also show that the salt elutes in later fractions than the dinucleotide (salt absorbs much greater at lower wavelengths than at higher wavelengths). NMR spectra show that the exchange of cations was also complete (there were no TEA peaks).

pt^{6}A was subjected to similar steps as was Upt^{6}A. The exchange of cations and desalting were not as complete as with Upt^{6}A however, and the consequences of this will be discussed in later sections.

One can calculate, from the several DEAE A-25 Sephadex columns run with pUpt^{6}A, Upt^{6}A, and pt^{6}A, the average salt concentrations at which they elute from the columns. These numbers are 0.29 M, 0.14 M, and 0.20 M TEAB, respectively

(see Figures 2 - 4).

III. i^6A Compounds

(A) Preface

The i^6A nucleoside can be obtained in a pure form from Sigma (D-7257). pi^6A had to be synthesized from pA, in a manner analogous to that described by Walker and Uhlenbeck[88] and Grimm and Leonard[89]. pi^6A was also obtained from a SVP degradation of Api^6A. Api^6A was synthesized as described in section I E of this chapter, and as is also described by Schweizer et al.[90]. Again, the pertinent details of the syntheses, when they differ from those of the literature, will be briefly discussed; while the purifications will be covered in slightly more detail, because they tend to deviate from those described in the references.

(B) pi^6A - Synthesis and Purification

The procedure of Walker[88] was followed almost verbatim, except that pA (Sigma, A-2002) was used in place of ppA. The reagents used were 1-bromo-3-methyl-2-butene (Chemical Procurement Labs, B6147), DMSO (Aldrich, 15 493-8), acetone (Mallinckrodt, 2440), and dilute NH_4OH (FSN, 6810; a 1:100 dilution of the concentrated reagent). The monitoring steps described[88] were omitted.

In this instance, the purification was very similar to that of Walker's[88]. A DEAE A-25 Sephadex column (see Figure 6) was followed by a Sephadex LH-20 column identical to

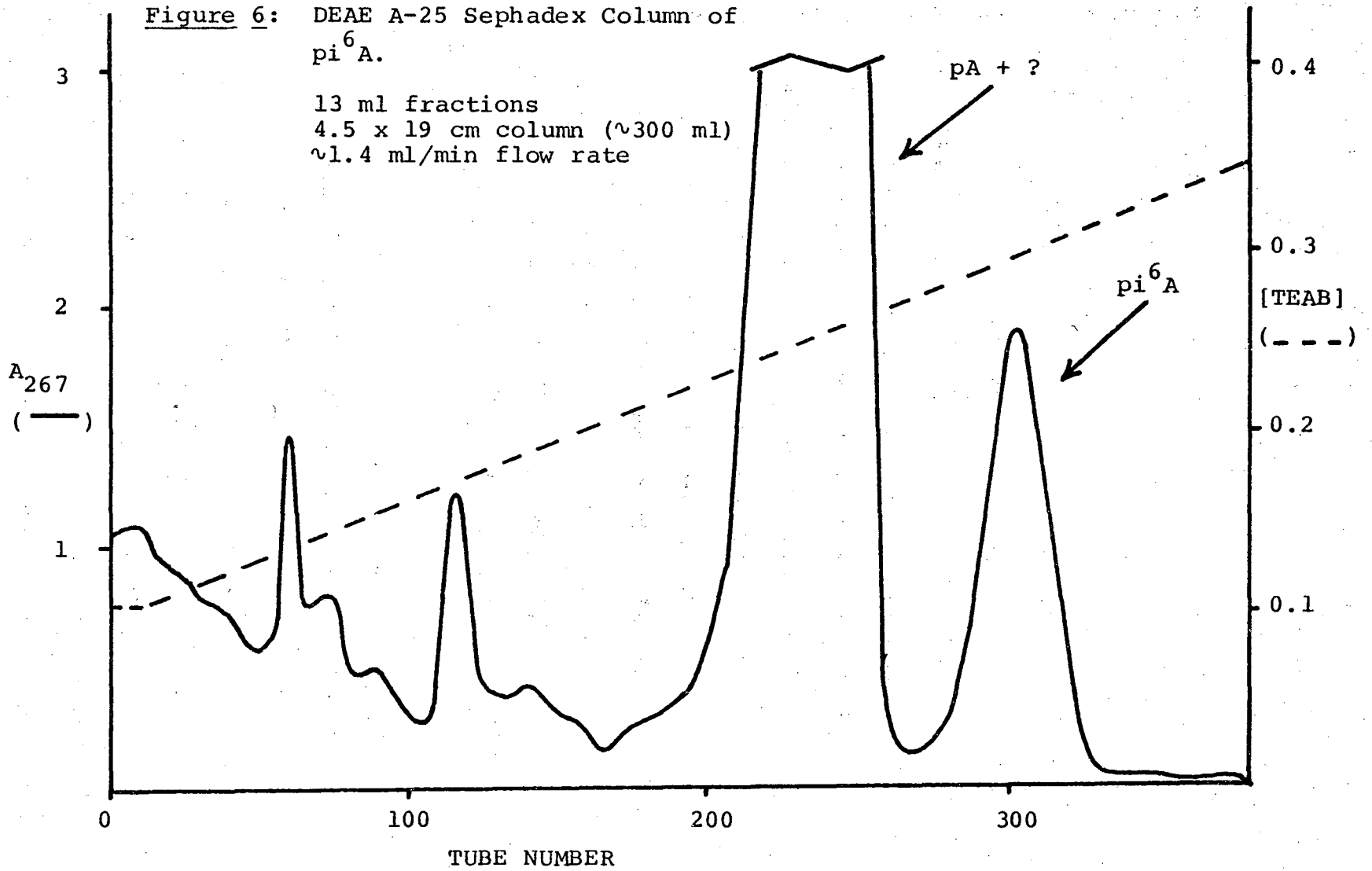

that used for Upt^{6}A and pt^{6}A. An equivalent amount of $NaHCO_3$ was added to the pi^{6}A, and repeated MeOH evaporations carried out. No Bio-Gel P-2 column was therefore run, as no excess $NaHCO_3$ was expected to be present. (The exchange of cations was performed in this fashion after noting the less than ideal desalting results with pt^{6}A.) The exchange here also was not complete. The identity of pi^{6}A was initially determined by its characteristic UV spectrum.

However, as we will discuss later, the NMR of this pi^{6}A preparation posed questions as to its authenticity. Thus, pi^{6}A was also isolated from an SVP degradation of Api^{6}A in the following way. 150 A_{263} units of Api^{6}A were dissolved in 0.5 ml H_2O. To this was added 0.25 ml of the ammonium formate buffer (see Section I D of this chapter) and 0.25 ml of 1% (w/w) SVP. This was incubated for 48 hr. in a 37°C bath. It was purified by passage through a large DEAE A-25 Sephadex column similar to that in Figure 6. Again, its identity was determined initially by its absorption spectrum.

(C) Api^{6}A - Synthesis and Purification

Api^{6}A was synthesized according to the procedure in section I E of this chapter. The amounts of the reagents used were as follows: 0.5 mmole of $N^6,O^{2'},O^{5'}$-triacetyl-adenosine 3'-phosphoric acid (Sigma, T-1630), 0.75 mmole of i^{6}A, and 3.0 mmole of DCC. The reaction was allowed to proceed for 12 days.

The purification of Api^{6}A was accomplished by a large

DEAE A-25 Sephadex column (see Figure 7), followed by a Sephadex LH-20 column similar to that used for all of the above compounds. An exchange of cations was attempted in a manner like that for pi^6A, but for unclear reasons, it again was not complete. Thus, the final product was the pure TEA^+ salt. The identity was initially determined by its characteristic UV spectrum and by the degradation to the component monomers, using NaOH, SVP and BSP assays.

IV. εA Compounds

(A) Preface

εA can be obtained in a pure form from Sigma (E 2378), but for the bulk synthesis of ApεA, it was synthesized by Dr. Che-Hung Lee of this laboratory, according to a procedure given by Secrist et al.[82]. pεA also can be obtained in a pure form (Sigma, E 9127). ApεA was synthesized according to section I E of this chapter.

(B) ApεA - Synthesis and Purification

The amounts of the reagents used were as follows: 0.42 mmole of $N^6,O^{2'},O^{5'}$-triacetyl adenosine 3'-phosphoric acid, 0.75 mmole of εA, and 3.0 mmole of DCC. The reaction was allowed to proceed for 12 days.

ApεA was purified by first passing it through a large DEAE A-25 Sephadex column (see Figure 8). This was followed by preparative paper chromatography (see Section I B ii of this chapter) using 95% EtOH/1 M ammonium acetate (70% v/v).

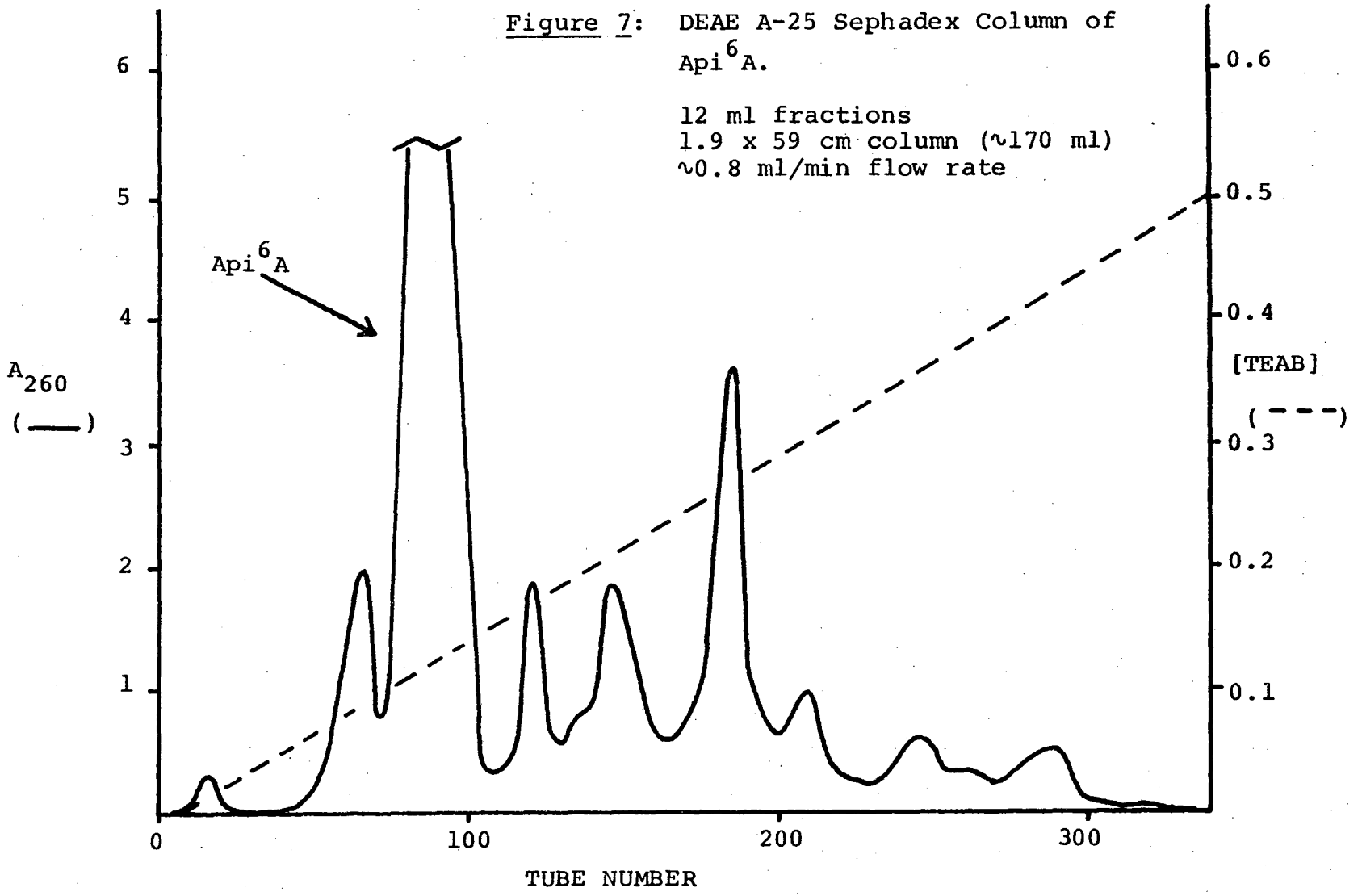

Figure 7: DEAE A-25 Sephadex Column of Api^{6}A.

12 ml fractions
1.9 x 59 cm column (∿170 ml)
∿0.8 ml/min flow rate

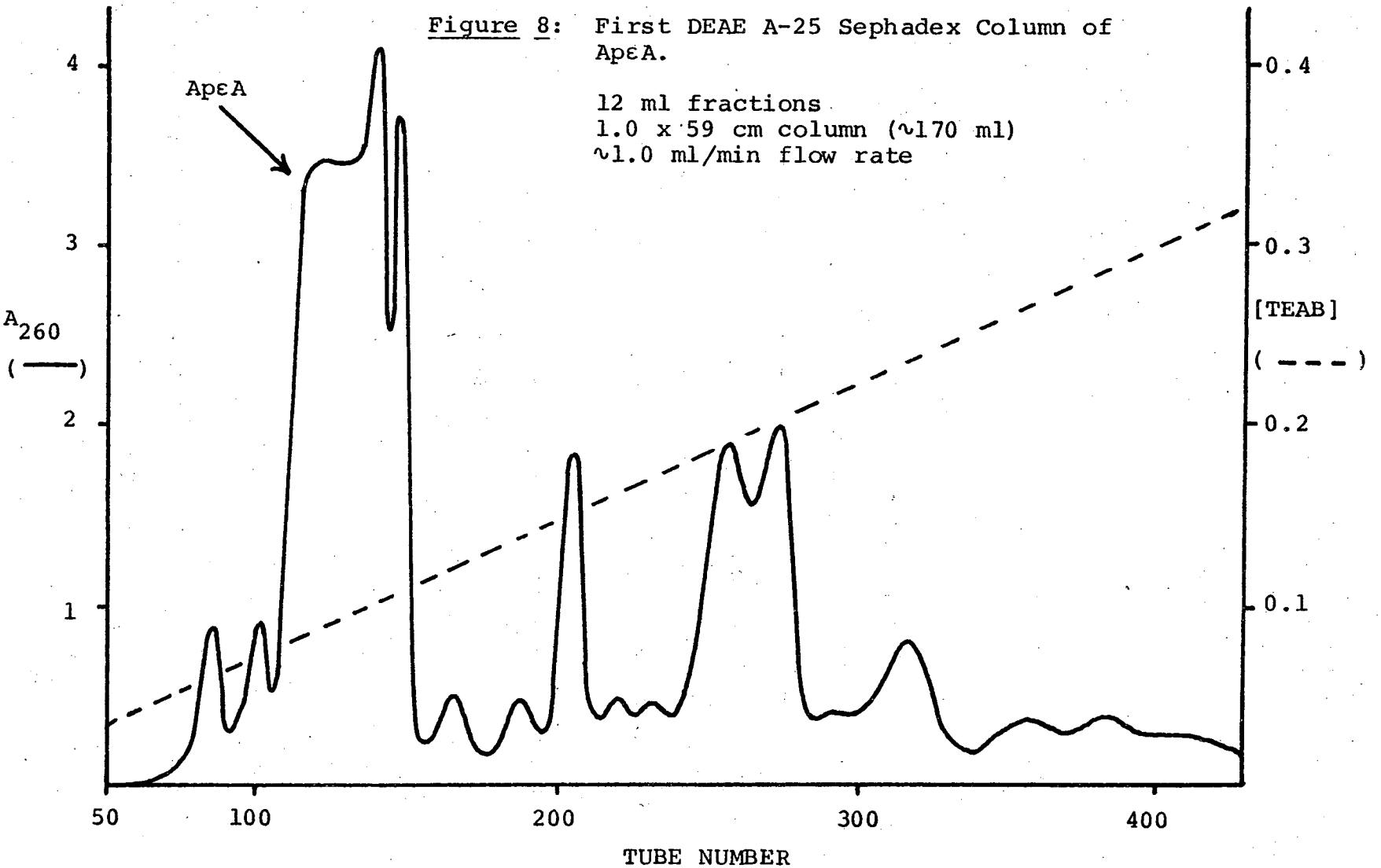

Figure 8: First DEAE A-25 Sephadex Column of ApεA.

12 ml fractions
1.0 x 59 cm column (∿170 ml)
∿1.0 ml/min flow rate

This was followed finally by another DEAE A-25 Sephadex column. The final product was a very pure TEA^+ salt. The identity of the dimer was verified by its degradation to the component monomers with NaOH, SVP and BSP, as well as by its very characteristic UV spectrum.

V. ms^2i^6A Compounds

(A) Preface

A very gracious gift of ∿200 mg of ms^2i^6A was made by Dr. Roy O. Morris (Dept. of Agric. Chem., Oregon State Univ.). $Apms^2i^6A$ was synthesized according to the procedure in section I E of this chapter. pms^2i^6A was obtained from an SVP degradation of $Apms^2i^6A$. Only a few of the important details of these syntheses and the purifications will be discussed here.

(B) $Apms^2i^6A$ - Synthesis and Purification

The amounts of the reagents used were as follows: 0.33 mmole of $N^6,O^{2'},O^{5'}$-triacetyl adenosine 3'-phosphoric acid, 0.49 mmole of ms^2i^6A, and 2.0 mmole of DCC. The reaction was allowed to proceed for 14 days.

It was purified by passage through a large DEAE A-25 Sephadex column (see Figure 9). This was followed by a Sephadex LH-20 column run in water alone. The $Apms^2i^6A$ fractions yielded the TEA^+ salt as a fluffy white compound. Its identity, aside from its characteristic absorption and NMR spectra (see later sections), was demonstrated by its

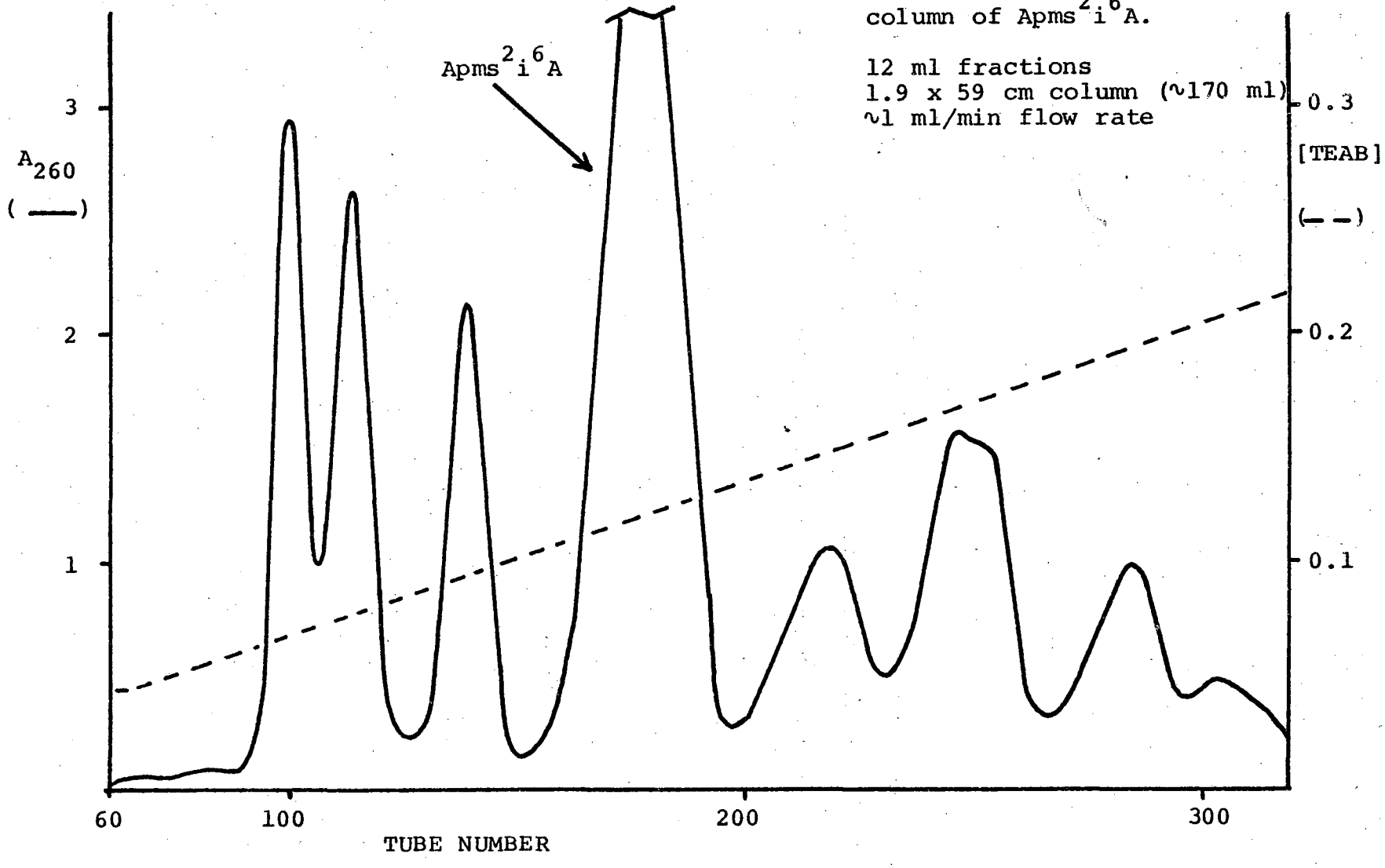

Figure 9: DEAE A-25 Sephadex column of $Apms^2i^6A$.

12 ml fractions
1.9 x 59 cm column (∿170 ml)
∿1 ml/min flow rate

degradation with OH^- yielding the essentially insoluble ms^2i^6A, and by the SVP degradation used to obtain pms^2i^6A (see the next section).

(C) pms^2i^6A - Source and Purification

pms^2i^6A was obtained in a fashion similar to the second procedure used to obtain pi^6A. It was isolated after the SVP degradation of $Apms^2i^6A$. 200 A_{260} units of $Apms^2i^6A$ were suspended in 0.5 ml of H_2O. To this was added 0.4 ml of the ammonium formate buffer and 1 ml of 1% SVP. This was sealed and incubated at 37°C for 48 hours.

It was then diluted to 2 liters and loaded onto a DEAE A-25 Sephadex column similar to that used for $Apms^2i^6A$. Elution was carried out with 0.13 M TEAB followed by 0.5 M TEAB. This column was followed by a Sephadex LH-20 column using 95% EtOH/H_2O (33% v/v). The resulting nucleotide was left as the pure TEA^+ salt.

VI. Unmodified Compounds

All unmodified nucleosides, nucleotides and dinucleoside monophosphates were purchased in very pure forms from Sigma.

Chapter 4 EXPERIMENTAL PROCEDURES - THE ACQUISITION OF PRIMARY DATA

I. Absorption

(A) General Techniques

(B) Absorption Characteristics

(i) Monomers

(ii) Dinucleoside Monophosphates

(C) Determination of ε and %h for the Dimers

(D) Determination of %h vs. Temperature

(i) The Experimental Arrangement

(ii) The Analysis to Obtain %h vs. Temperature

(E) ε and %h Dependence Upon Salt, pH and Solvent

(i) Salt Dependence

(ii) pH Dependence

(iii) Ethanol Dependence

II. Circular Dichroism (CD)

(A) Techniques

(B) CD Characteristics

(i) Monomers

(ii) Dimers

(C) Δε Temperature Dependence

(D) Δε Dependence Upon Salt

III. Nuclear Magnetic Resonance (NMR)

(A) Techniques

(i) Instrumentation

(ii) Sample Preparation

(B) Characteristic NMR Information

(i) Monomers

(ii) Dinucleoside Monophosphates

(C) Temperature Dependence of the Dimerization Changes in the Chemical Shifts

(D) Temperature Dependence of the Dimerization Changes in the H1' Coupling Constants

Chapter 4

EXPERIMENTAL PROCEDURES - THE ACQUISITION OF PRIMARY DATA

I. Absorption

(A) General Techniques

Absorption spectra were obtained on Cary spectrophotometers (Models 14, 15, and 118c). Pyrocel quartz cells were washed first in dichromate cleaning solution (see Chapter 3, Section I A) and rinsed extensively with water. They were then washed with L.O.C. detergent, rinsed, and dried using a Precision Ceels, Inc. cell washer. In using the double beam spectrophotometers, samples were often run against a blank containing the solvent. Alternatively, the sample was run against air followed by the solvent vs. air. This was performed regularly since the air vs. air baselines themselves were not flat, and thus a subtraction by hand was necessary regardless of the method chosen.

Unless otherwise designated, solvents were generally merely water (pH$\sim$5.5 - 7), or more frequently 2 m$\underline{M}$ sodium phosphate buffer (pH$\sim$7; 1.22×10^{-3} $\underline{M}$ Na_2HPO_4, 0.78×10^{-3} $\underline{M}$ NaH_2PO_4). This low concentration buffer was used since it eliminated changes due to CO_2 absorption, but allowed easy titration to other desired pHs.

The temperature of the spectra obtained, unless otherwise specified; was $\sim$23 - 25 degrees Celsius (the measured room temperature). Samples were generally kept frozen, then allowed to equilibrate to room temperature before their

spectra were measured.

(B) Absorption Characteristics

(i) Monomers

Hypermodification of the adenine moiety generally produces characteristic changes in its absorption spectrum. Figures 1 and 2 illustrate the very characteristic absorption spectra of the hypermodifications studied in this dissertation. The spectra were obtained as described above. They were then scaled to the extinction coefficients at the wavelengths of the maxima, which are reported in the literature (A,U,C^{91}; i^6A^{89}; $ms^2i^6A^6$; εA^{82}; t^6A^1). These spectra are essentially unchanged from the nucleoside to the nucleoside monophosphate, or to the triphosphosphate. Of course they are affected (sometimes to a great extent) by the protonation of the base moiety itself, and thus these spectra were obtained near neutral pH (unprotonated bases).

(ii) Dinucleoside Monophosphates

Figures 3 - 6 illustrate the absorption spectra of the hypermodified dinucleoside monophosphates used in this study. Their extinction coefficients (ε) were determined as described in the following section. With them are the spectra of the component nucleotides. It is easily seen that the dimers' spectra are approximately the sums of the spectra of the component monomers. Thus they are useful in initially determining the identity of the dinucleoside mono-

Figure 1: UV Absorption Spectra of A, i^6A, and ms^2i^6A. pH = 7.

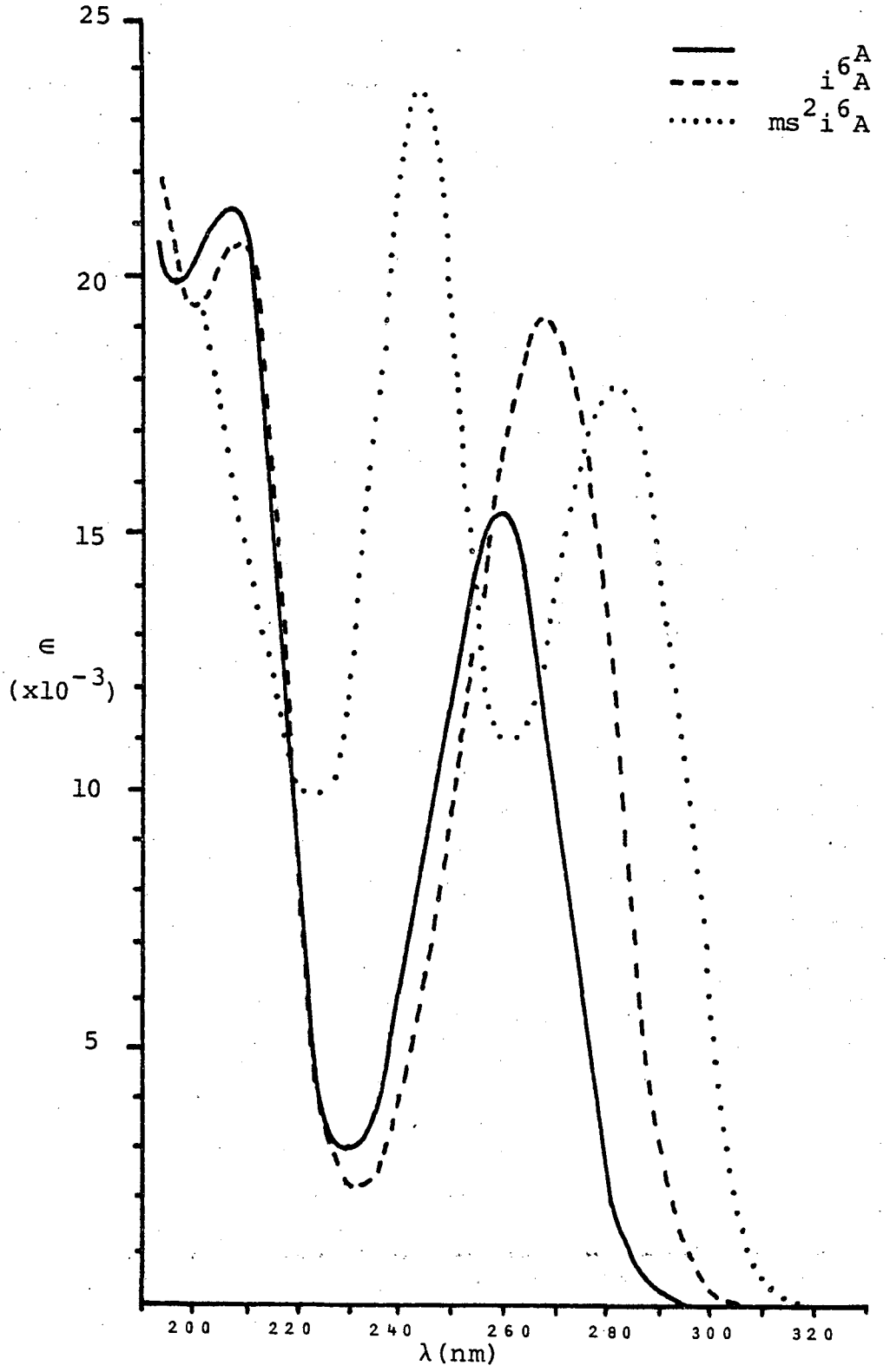

Figure 2: UV Absorption Spectra of A, t^6A, and εA. pH = 7.

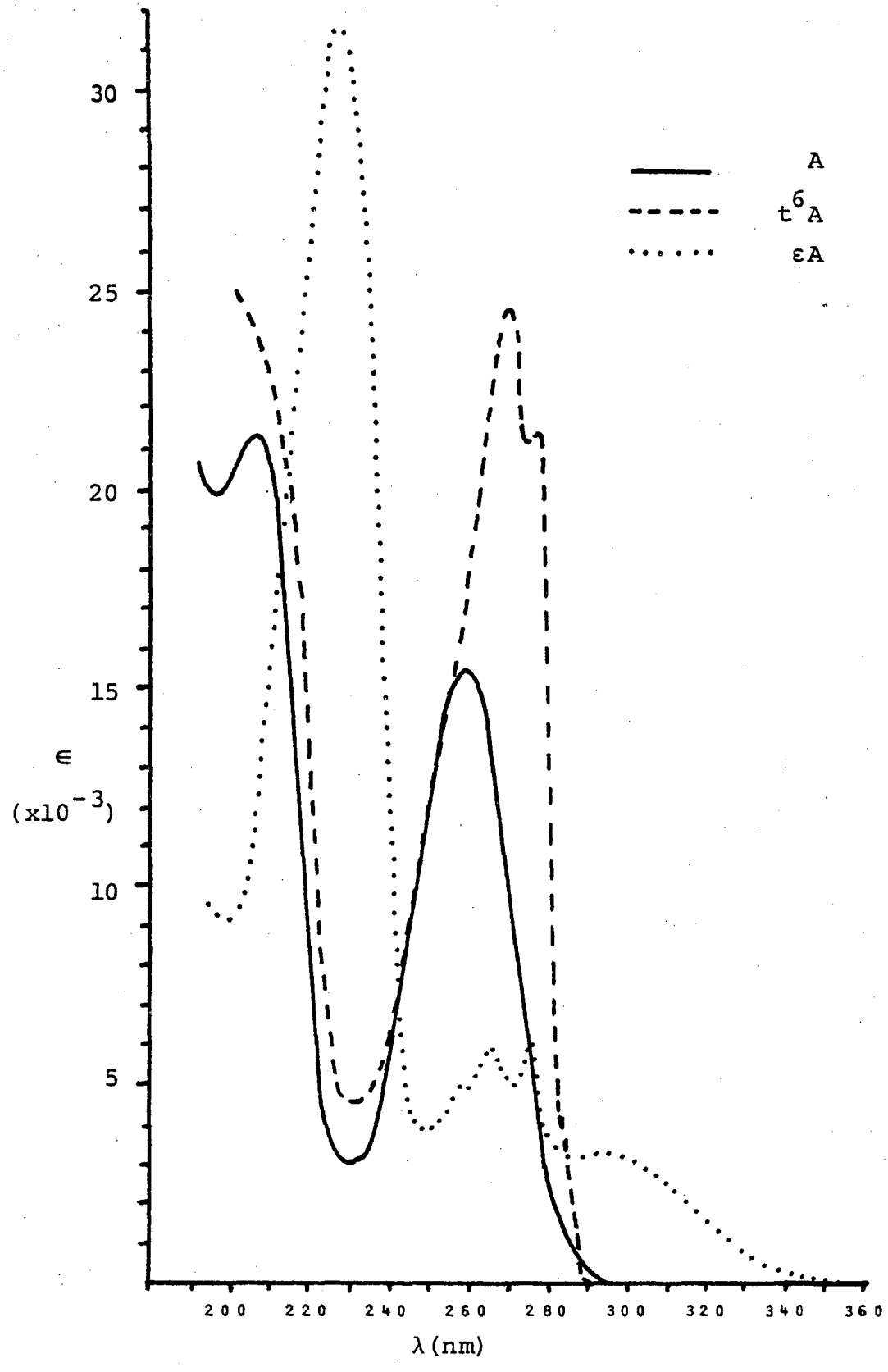

Figure 3: UV Absorption of Api^6A and its component monomers.

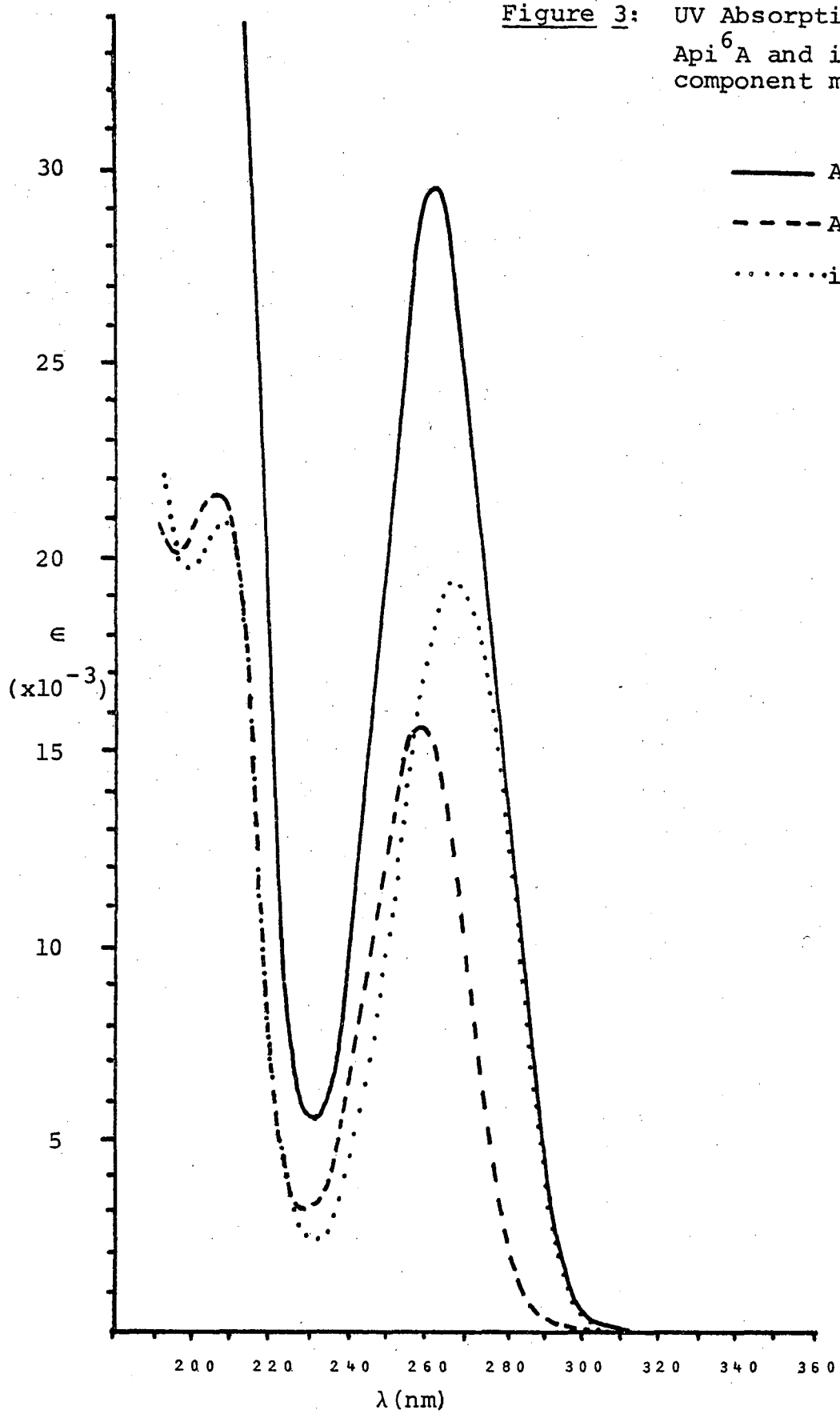

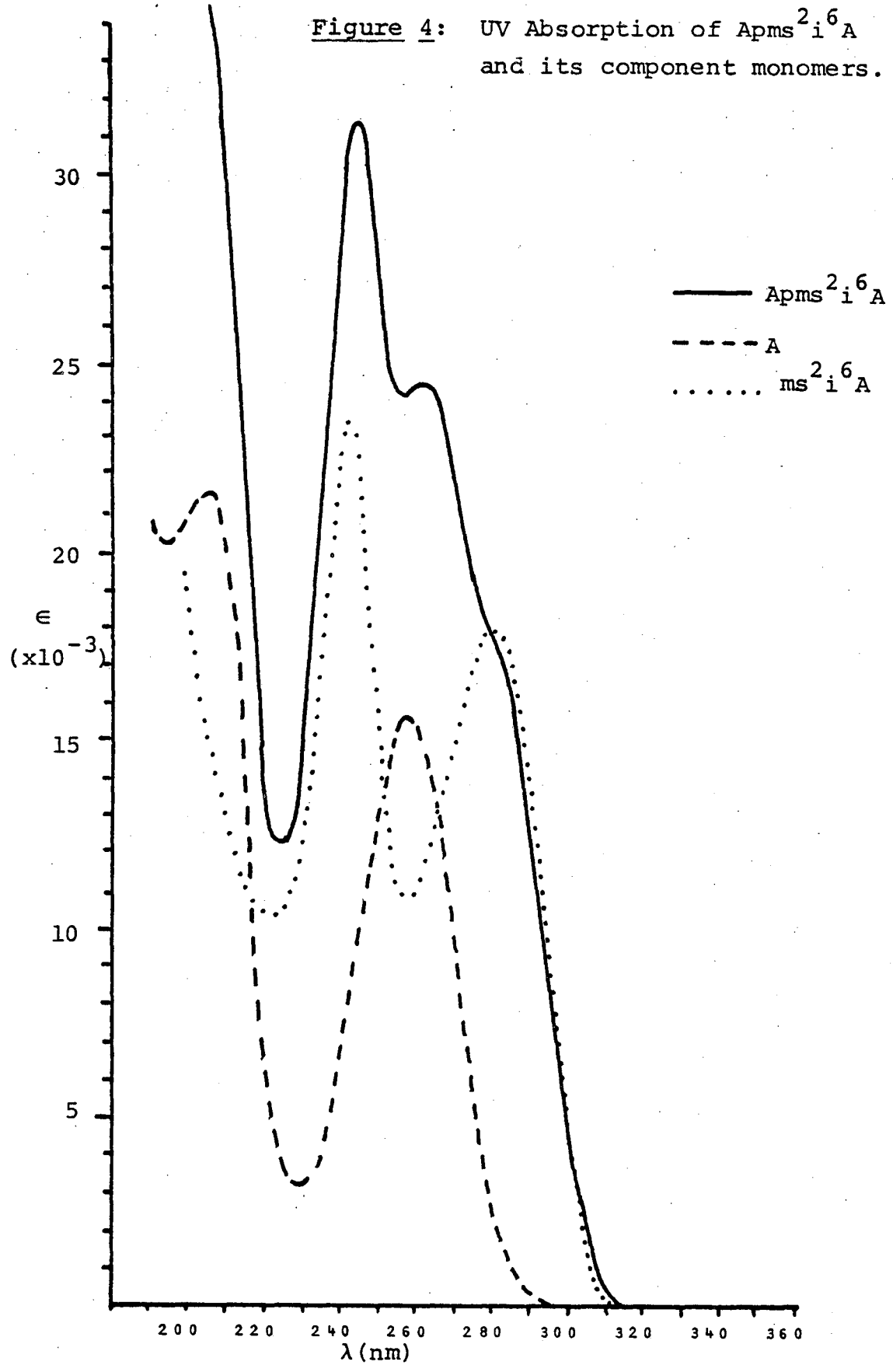

Figure 4: UV Absorption of Apms^{2}i^{6}A and its component monomers.

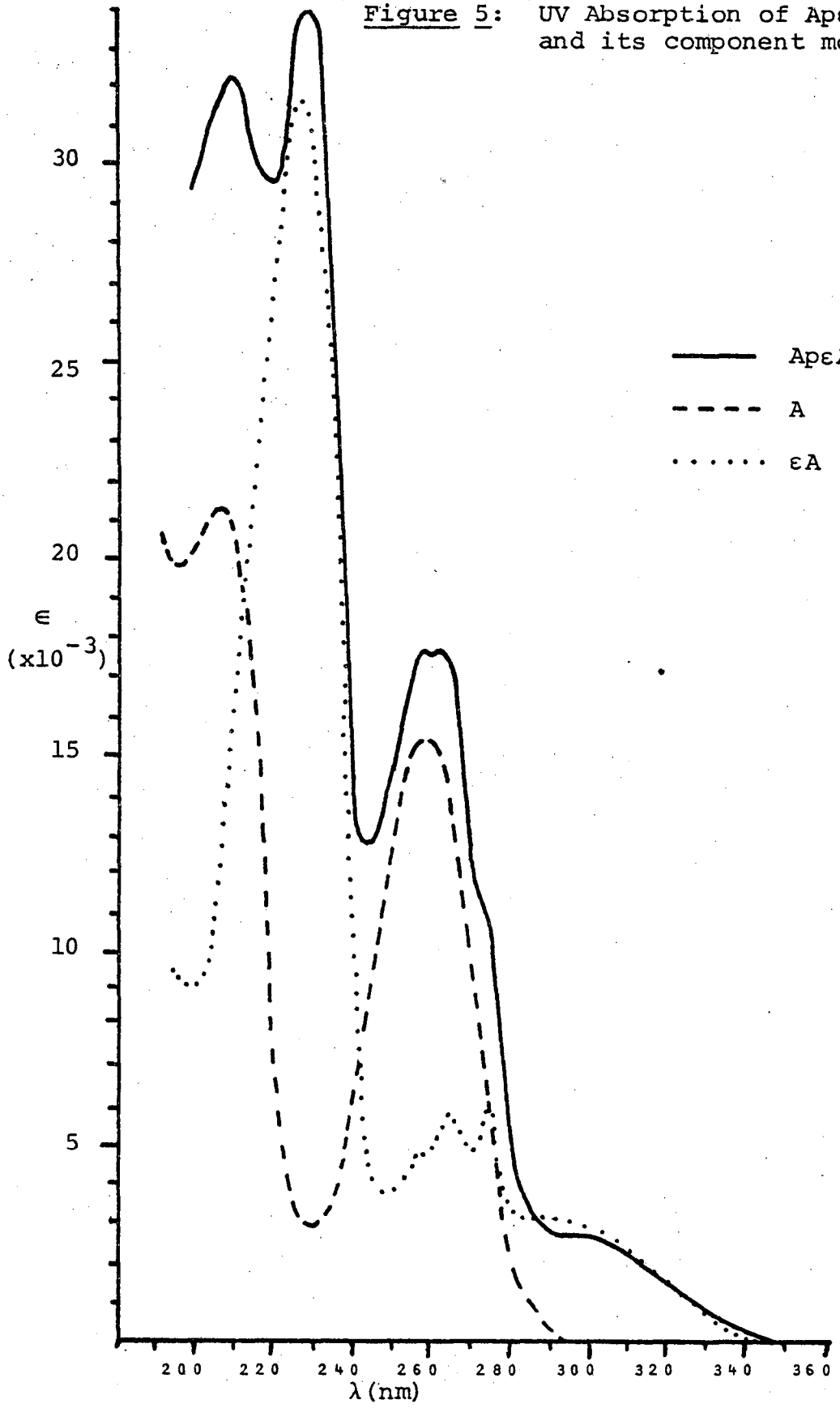

Figure 5: UV Absorption of ApεA and its component monomers.

Figure 6: UV Absorption of Upt^{6}A and its component monomers.

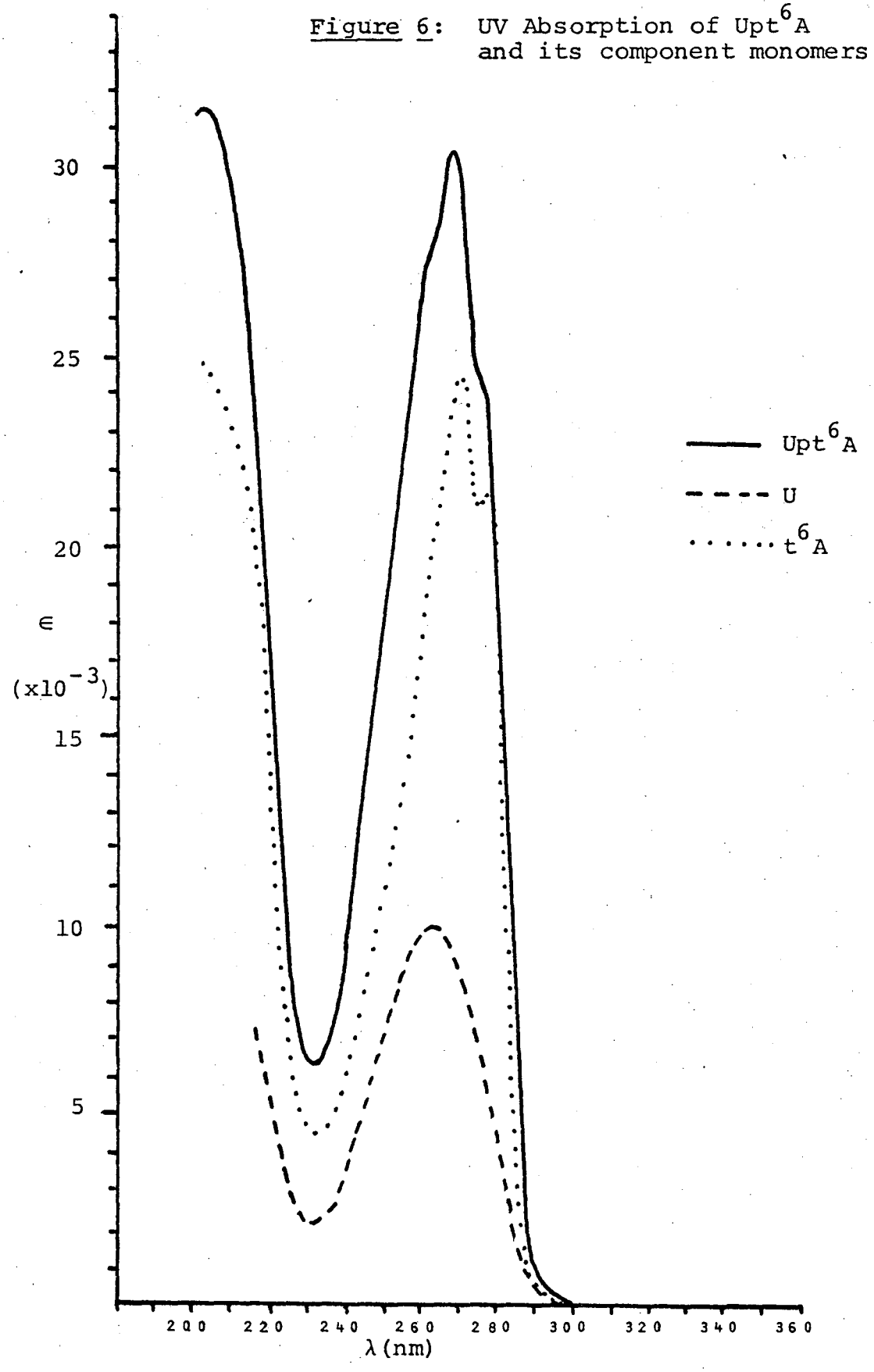

phosphates. However, if one makes careful measurements, one finds that a dimer's spectrum is not exactly the sum of its monomer spectra. Figure 7 demonstrates this phenomenon with the simple case of ApA, in which both monomers are identical. ApA's spectrum has been divided by 2 in order to allow for the fact that there are 2 adenosines/mole of ApA. This well-known and often-studied change in absorption upon polymerization of monomers is known as hypochromism (H)[72]. Specifically, as is diagrammed in the figure, hypochromism is the difference between monomer and dimer in the integrated intensity of a given band. A more easily measured difference which is closely related in origin to the hypochromism, is the percent hypochromicity (%h - also defined in the figure) - the difference in the extinction at a given wavelength. For reasons to be discussed in the next chapter, the percent hypochromicity will be used as a measure of the interaction of the bases in dimers.

(C) Determination of ε and %h for the Dimers

Since the %h of a dinucleotide is generally in the neighborhood of only 10%, accurate measurements of the ε's for the dimers were imperative. The general procedure for this determination was very similar to that used by Borer[83], with some important changes adopted to increase the accuracy. Also, some variations on this procedure were necessary in the cases of Upt^{6}A and ApεA. Thus the detailed steps of the determinations will be described here.

Figure 7: Hypochromism of the Absorption Bands of ApA.

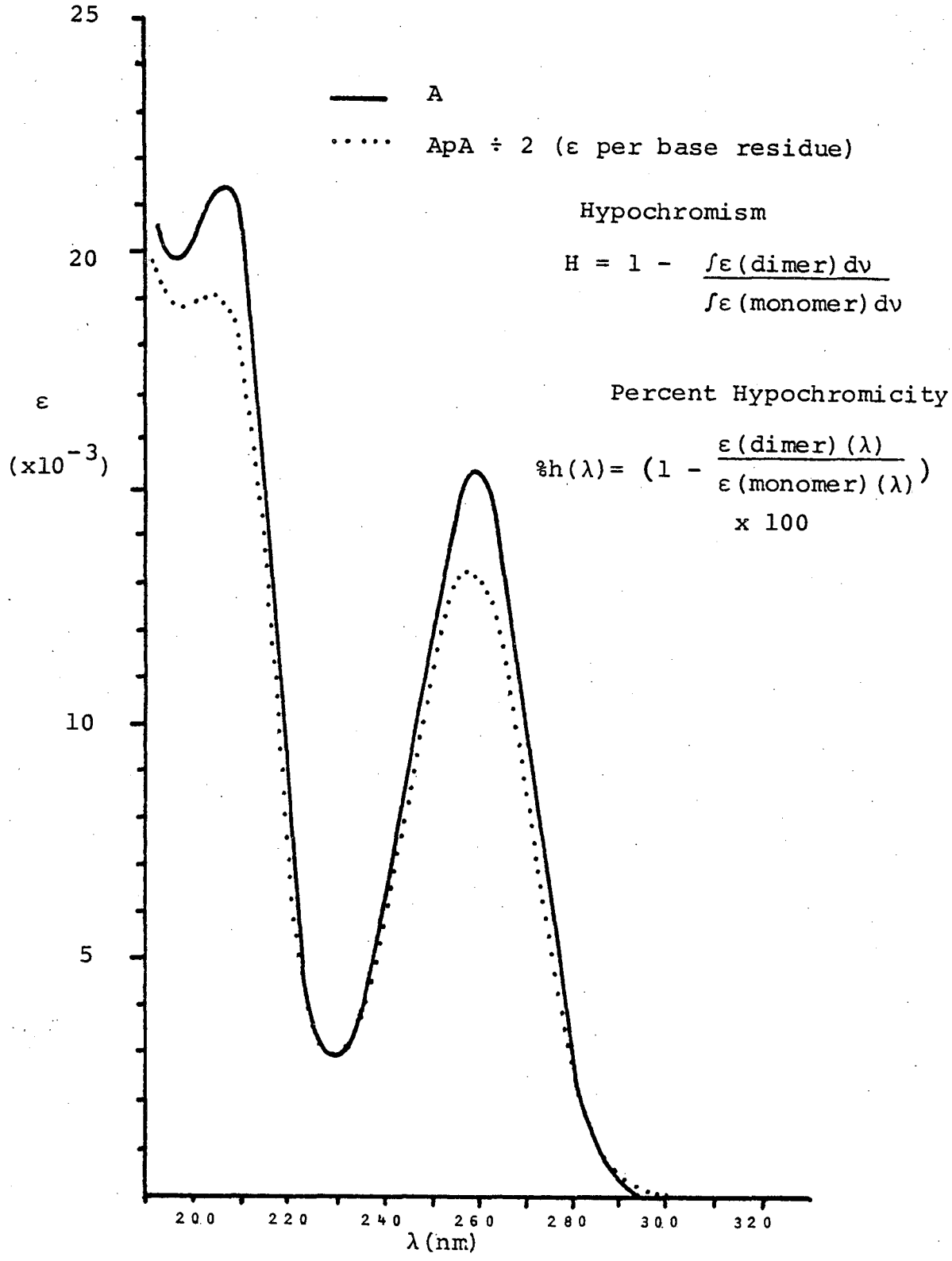

A sample of dinucleoside monophosphate was prepared in which the absorption (optical density - OD) at the wavelength (λ) of the maxima was close to 1.0 in a small volume 0.5 cm path length cell. This was chosen because of the small volume used for the determinations ($\sim$0.5 ml), and to minimize the baseline corrections to the final spectra (corrections for the absorption of the resulting salt and buffer solvent - a 1.0 OD in 0.5 cm cell corresponds to an increase in the ratio of sample:salt of a factor of 2 over the usual 1.0 OD in a 1.0 cm cell). The sample was dissolved in H_2O only; the pH was never found to be below $\sim$5.5, nor did the absorption vary with pH over this neutral range ($\sim$5.5 - 7).

From 4 - 8 aliquots of 0.50 ml each of the sample were pipetted (Gilson Pipetman) into preweighed glass screw cap vials (SP B7805-1X) and weighed. 30 µl (also designated as λ) of 5 N NaOH was pipetted into each vial (30λ Drummond Microcaps) and the vial weighed again. The vials were then further sealed with Parafilm and placed in a 37°C incubator. At the end of 48 hours, the vials were removed, dried with tissue, and the Parafilm removed. The vials were then weighed.

Then 30λ of 5 N HCl was added to each and the vials weighed. Finally, 30λ of 1 M sodium phosphate buffer (pH 7; 0.61 M Na_2HPO_4, 0.39 M NaH_2PO_4) was added and the final weighing of the vials performed.

The spectra of the contents of each vial were then

measured. The pH was routinely checked and always found to be very near neutrality. A correction to the spectra was performed in allowance for the absorption of the various additives in the water (NaCl and buffer). On a few occasions a small correction had to be made for scattering by the final solution. The essentially linear artifact in the absorption was corrected by noting the absorption at long wavelengths and extrapolating to the wavelength of the maxima. Thus a correct value was obtained for the OD at the wavelength of the maximum of the resultant monomer mixture. (This wavelength was usually close but not necessarily equal to the dimers' maxima - particularly in the case of Upt^6A and ApεA as we will discuss below.)

The initial volume of the sample added was determined from its weight and the density of H_2O at 25°C (the dimer was at a concentration low enough not to significantly affect the density of water - $\sim 10^{-4}$ M). The volume of the sample after the addition of NaOH, HCl and buffer (after the incubation) was determined by summing the initial weight of sample plus the weight gained upon the various additions. There was often ∿5 mg gained just upon incubation and reweighing. Testswere run however with vials containing sample only (no NaOH) and samples insensitive to NaOH which contained NaOH. In all cases this ∿5 mg was gained, but no change in absorption was noted - therefore no evaporation or dilution occurred. Thus the weight gained upon incubation was not included in the total final weight (it is suspected that the

plastic screw caps can retain moisture). The volume of the final solution determined by its weight and its density which I determined as 1.020 g/ml.

From the OD of the final solution and the extinction coefficients of the monomers at the wavelength chosen, a concentration of the monomer mixture was calculated:

$$\text{Conc. of monomer mixture} = \frac{OD_{final}}{0.5 \times (\varepsilon_{monomer\ 1} + \varepsilon_{monomer\ 2})}$$

From the final volume, a number of mmoles of mixture was obtained:

mmoles of mixture = (Conc. of mix) x (final volume)

This mmoles of mixture equals the mmoles of dimer in the beginning, and we can thereby calculate the original concentration of the sample:

$$\text{Conc. of dimer} = \frac{\text{mmoles dimer}}{\text{original volume}}$$

Lastly, the ε can be determined from the initial OD measurement:

$$\varepsilon_{dimer} = \frac{OD_{initial}}{0.5 \times (\text{Conc. of dimer})}$$

Table I lists the ε's of the dimers studied, and the %h's calculated from them. They are insignificantly affected by variations in salt conditions (see Section I E of this chapter).

t^6A and εA are degraded by the NaOH treatment and require a slightly different analysis. t^6A is converted smoothly and completely to A^{13} (as was also observed in the

Table I. The extinction coefficients (ε) of the dinucleoside monophosphates at 25°C. Shown also are the sum of extinctions of the monomers used in obtaining the ε's and %h's. The derivation of the ± values is discussed in Appendix 2.

Dimer	λ_{max} of Monomer Mixture	$\varepsilon(x10^{-3})$ Monomer Mixture at λ_{max}	λ_{max} of Dimer	$\varepsilon(x10^{-3})$ Dimer at λ_{max}	$\varepsilon(x10^{-3})$ Monomer Mix at Dimer λ_{max}	%h
ApA	259	30.8	258	27.1±.1	30.7	11.7 ±0.7
Api^{6}A	264	33.4	262.5	29.5±.2	33.1	10.8 ±0.8
Apms^{2}i^{6}A	263	26.4	263	24.4±.2	26.4	7.7 ±1.0
Apε A	260.5	19.2	260	17.6±.1	20.1	13.1 ±1.0
UpA	260	25.3	258	24.4±.1	25.3	3.4 ±0.9
Upt^{6}A	260	23.1	268	30.4±.4	34.3	11.2 ±1.3
CpA	260.5	22.7	261.0	21.2±.1	22.8	7.1 ±0.9

degradation of Upt^{6}A, yielding a spectrum characteristic of U + A only). Thus, the extinction of A was used for t^{6}A after treatment with NaOH. εA was unfortunately degraded to a mixture of products with different spectral characteristics. However, after ∿36 hours of treatment with NaOH an isosbestic point with time at 260.5 nm was observed. An extinction coefficient equal to $(3.84\pm.06)\times10^3$ was determined for the resulting mixture of two products at that time. From ∿36 hours and longer this is the value of the extinction for the unknown mixture of products formed from εA at 260.5 nm. As with the other dimers, ApεA was treated with NaOH for 48 hours.

Enzymatic digests to obtain ε's were of little use with dimers containing hypermodifications. They are in this regard unfortunately very resistant to the action of phosphodiesterases.

%H (percent hypochromism) values were obtained for the dimers ApA and Api^{6}A. The %H was determined by integrating (weighing) the first absorption band (230 nm and up) of the monomers and dimers. ApA gave 12.9 %H, and Api^{6}A yielded 9.98 %H at 25°C. As expected, they are approximately the same but not equal to the corresponding %h's at the λ_{max}[72,92].

(D) Determination of %h vs. Temperature

As was mentioned in Chapter 2, the stacking equilibrium is temperature dependent. This is well-known, and has often

been studied in an attempt to obtain the thermodynamic parameters describing the equilibrium ($\Delta H°$, $\Delta S°$)[72]. Thus I have monitored the %h vs. temperature as a measure of the change in the stacking equilibrium. Since the changes observed are small over the temperature range studied (0 - 80°C), careful attention to detail in the 'melting' experiment is required. A short description of the procedure will be given, followed by the processing of the raw data into %h vs. temperature.

(i) The Experimental Arrangement

The experimental setup consisted of a hodgepodge of components. The optics arrangement (lamp, monochromator, slits) was that of a Beckman DU. The sample compartment, detection system and recording system was a Gilford Multiple Sample Absorption Unit. This also consisted of auto slit, thermosensor, and high absorption offset controls. The temperature of the circulating ethylene glycol was controlled with a Neslab bath and bath cooler, in conjuction with a Bodine fractional horsepower gearmotor and Minarik speed regulator (which continuously changed the thermostat on the bath). Thus, the absorption at one λ of 3 samples and blank could be monitored smoothly from 0 - 80°C.

Cells had 1 cm path lengths and ground glass stoppered tops. Samples with OD's of $\sim$1 (in H_2O, dilute buffer, or salt) were sealed in the cells by wrapping Teflon tape around the stoppers and <u>firmly</u> seating them. Checks for evaporation after the heating of the experiment were always

made after the cell had reequilibrated to room temperature. Those few runs which gave different absorptions before and after the melt were simply discarded.

The melts were always run from low to high temperatures after a steady reading of the absorption was obtained at the lowest temperature. The temperature was generally increased at a rate of ∿10°C/hour - with absorption and temperature monitoring taking place every 1 minute. The λ chosen was that tabulated in Table I as the λ_{max} of the dimer. Each of the component monomers and the dimers were melted at these λ's.

(ii) The Analysis to Obtain %h vs. Temperature

It was found that the simplest method was to calculate the % change in the absorption from the lowest temperature to any given temperature. From this quantity the %h was determined:

R_T = Chart reading at Temp. T (not the OD - because of the arbitrary offset control)

OD_L = Absorption at the lowest temperature

$Y = \rho_L/\rho_T$ (ρ_L = density of H_2) at lowest temp.; ρ_T = density of H_2O at temperature = T)

X = Chart reading at lowest temperature

FS = Full scale of the chart expansion - usually 0.100 absorption units

Then,

$$(R_T - X)FS + OD_L = OD_T$$

$(OD_T)Y = OD_T^C$ (corrected to volume at lowest temp.)

$= (R_T - X)(FS)Y + (OD_L)Y$

The % change in absorption from temp. L to T is

$$\%_{L-T} = [(OD_T^C - OD_L)/OD_L]100$$

$$= [\frac{(R_T - X)(FS)Y}{OD_L} + (Y - 1)]100$$

$$= [(\varepsilon_T C_L - \varepsilon_L C_L)/\varepsilon_L C_L]100$$

$$= [\frac{\varepsilon_T}{\varepsilon_L} - 1]100$$

We know $\varepsilon_{25°C}$ of all the monomers and dimers, and hence by rearrangement we can obtain ε at all temperatures:

$$\varepsilon_T = [\frac{\varepsilon_{25}}{(1 + \%_{L-25}/100)}] [1 + \%_{L-T}/100]$$

From measurements of this sort on each of the component monomers and dimers, I arrived at the %h vs. temperature values tabulated in Table II. The melts did not change upon variations in the salt conditions as will be described in the next section.

In certain cases (especially UpA, in which the changes were so small) the melt had to be repeated several times. The results were averaged in order to arrive at a meaningful mean value for the $\%_{L-T}$ at every T. The implications of the errors inherent in these measurements will be discussed later when we attempt to derive conclusions from the melt data. For now, the reader may choose to refer to Appendix 2 for a discussion of the errors - particularly in order to understand the tabulation of three significant figures in

Table II. The %h vs. temperature for the dinucleoside monophosphates studied. See Appendix 2 for a discussion of the errors.

T(°C)	ApA	Api^{6}A	Apms^{2}i^{6}A	ApεA	UpA	Upt^{6}A	CpA
2	14.8	13.3	8.69	16.8	4.20	13.0	
4							9.30
5	14.4	12.8	8.58	16.2	4.13	12.7	9.22
10	13.7	12.2	8.44	15.4	3.93	12.3	8.73
15	13.3	11.7	8.19	14.6	3.75	11.9	8.14
20	12.4	11.2	7.97	13.8	3.60	11.6	7.64
25	11.7	10.8	7.72	13.3	3.44	11.2	7.14
30	11.1	10.4	7.46	12.4	3.37	10.9	6.63
35	10.4	9.93	7.20	11.7	3.21	10.6	6.21
40	9.67	9.43	6.91	11.0	3.14	10.4	5.79
45	9.03	9.08	6.61	10.6	3.06	10.1	5.41
50	8.33	8.64	6.35	9.80	2.95	9.82	5.02
55	7.62	8.26	6.06	9.17	2.79	9.56	4.59
60	6.94	7.85	5.65	8.48	2.71	9.23	4.25
65	6.30	7.62	5.23	7.94	2.56	9.06	3.72
70	5.75	7.18	4.93	7.55	2.52	8.73	3.28
75	5.26	6.82	4.59	6.91	2.48	8.37	2.93
78	4.87	6.70					
80			4.33			7.95	2.63
85						7.80	

Table II.

(E) ε and %h Dependence Upon Salt, pH and Solvent

A limited number of studies were performed to determine the effects upon the ε and %h of parameters other than temperature. These included the effect of the addition of NaCl, $MgCl_2$, HCl, and ethanol to solutions containing some of the dinucleotides.

(i) Salt Dependence

The absorption was monitored for ApA, Api^6A, and Upt^6A as Mg^{++} was added (10 m$\underline{M}$), and then as EDTA was added (15 m$\underline{M}$). There were unfortunately rather large baseline corrections necessary after the addition of the EDTA. Hence, if actual small changes due to Mg^{++} binding were occurring, they were lost in experimental error (∿±1%). Api^6A showed a very small (∿1%) decrease at the λ_{max} upon the addition of Mg^{++}. ApA and Upt^6A showed even smaller changes if any at all. The absorption melts of each of these dimers (and UpA) were determined in 2 m$\underline{M}$ Na phosphate buffer with and without 10 m$\underline{M}$ $MgCl_2$ or 100 m$\underline{M}$ NaCl. No changes in the melts could be detected. Thus, it is believed that salt variations (up to the limits studied) or Mg^{++} binding (if any) do not significantly alter the absorption, nor in fact the stacking of these dimers. In particular, there were no changes between the dimers containing hypermodifications and the ones that did not (ApA, UpA).

(ii) pH Dependence

It is known that the stacking equilibrium is drastically affected by protonation of the bases[72]. For ApA and Api^{6}A and their monomers, an experiment was performed to determine the change in %h upon a change at room temperature from pH 7 to pH 1 (in which both bases of the dinucleotide will be essentially completely protonated). This required obtaining the ε's of the monomers in their protonated states. For ApA a change of 9.7% in the percent of hypochromicity was observed. For Api^{6}A, a change of 8.9% was observed. Thus, in both cases protonation of the 2 bases does not cause complete destacking of the dimers. In fact, using the values of the %h's in Table I, these changes correspond to an 83% change in the base-base interaction present at 25°C for both ApA and Api^{6}A. Therefore, an analysis of the sort described in reference 72, in which thermodynamic parameters of the stacking equilibrium are obtained from titrations, was not feasible.

(iii) Ethanol Dependence

Also known to affect the equilibria of stacking is the addition of ethanol[72]. This was performed with ApA and Api^{6}A in an attempt to note differences in their ethanol 'melt denaturation' behavior.

Changes in the absorption were monitored for the dimers and their monomers as the concentration of ethanol was varied from 0 to 11 M (60% by weight EtOH). The concentra-

tion of EtOH and the resultant volume changes were determined by direct weighing and the use of published density values for EtOH-H_2O solutions (CRC Handbook). The % change in the % hypochromicity between these 2 concentration limits was found to be ∿11.3 % for ApA and ∿9.9 % for Api^{6}A. This corresponds to a ∿97 % loss of the stacking present at 25°C for ApA, and a ∿93 % loss for Api^{6}A. Furthermore, the shapes of the % change in the percent hypochromicity curves calculated in this way were virtually identical (see Figure 8). Thus, no significant difference in the ethanol melts were observed between ApA and Api^{6}A.

II. Circular Dichroism (CD)

(A) Techniques

CD spectra were measured with a Cary Spectropolarimeter (Model 60) equipped with a circular dichroism assembly. The data were directly encoded to a PDP8/e minicomputer, where it was smoothed and corrected for baseline deviations. Variable temperatures were obtained with the help of a frigistor heating and cooling system which was controlled by a Hallikainen Thermotrol.

Cells used were ∿1 ml capacity 1 cm path length cylinders (Pyrocel). These were fitted into a holder specially made by the shop, and then placed in a reproducible position in the instrument's cell holder. For variable temperature measurements, the cell's ground glass stoppers were wrapped with Teflon tape and firmly seated.

Figure 8: Ethanol denaturation of ApA and Api^{6}A. Plotted is the % change in the %h at the λ_{max} at 25°C.

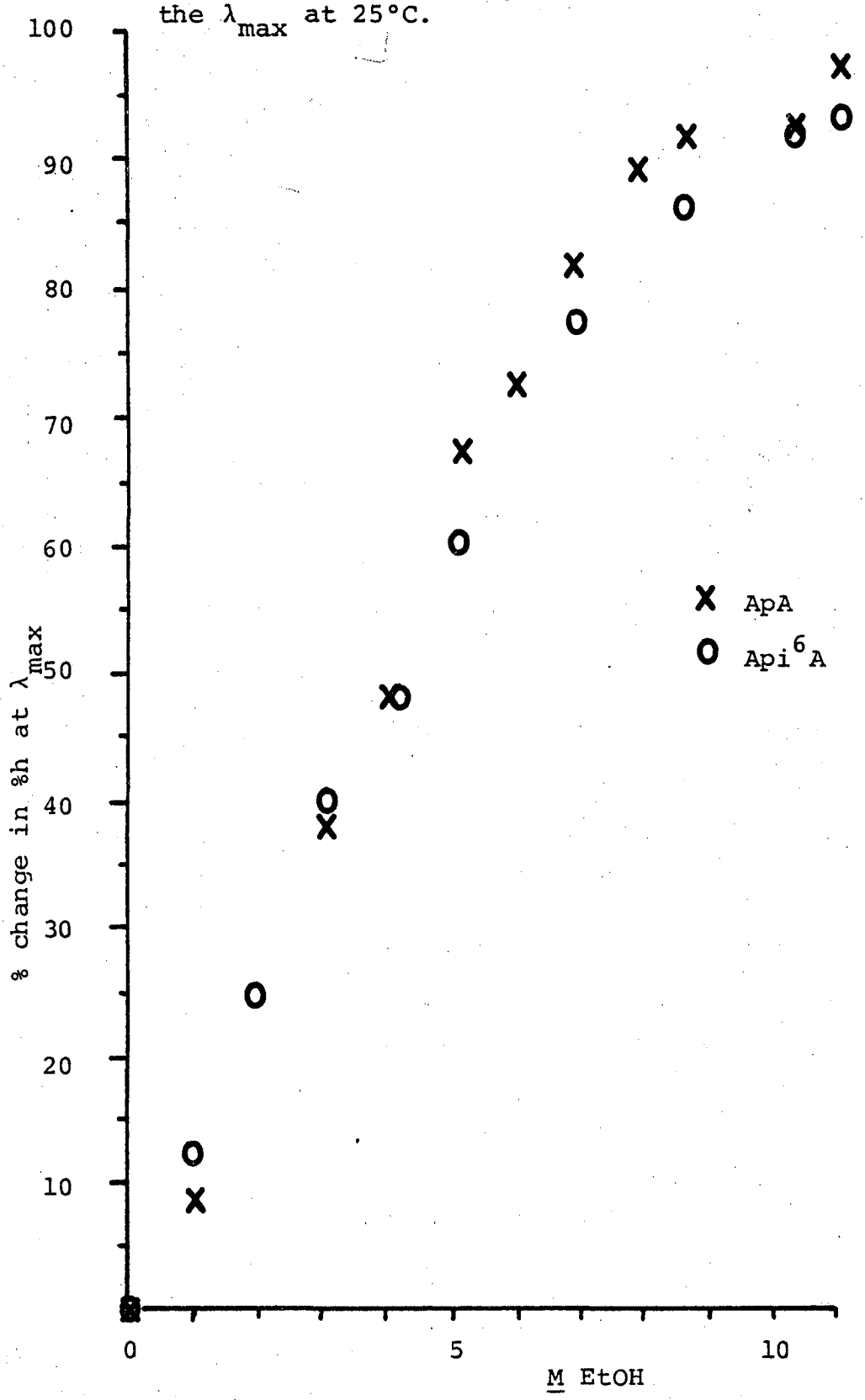

The cell containing solvent (blank) was first inserted and a baseline recorded. Subsequently, the sample of OD ∿1 was placed in the cell and spectra recorded with the baseline automatically subtracted by the PDP8/e. As with the absorption variable temperature experiments, the CD samples were checked for evaporation and the data discarded if necessary.

(B) CD Characteristics

(i) Monomers

The CD of adenosine and the hypermodifications of it arise from the asymmetry of the sugar portion and the restricted rotation about the glycosidic bond[72]. The CD characteristics of the nucleosides essentially do not change as the phosphate is added. All of the monomers CDs are small, and will not be studied in any detail more than that required to interpret the spectra of the dimers containing them.

Figures 9,10 and 11 illustrate the CD of the hypermodified monomers studied. They of course will differ from that of adenosine's because of their different absorption characteristics. Aside from this, the only thing to note is that the magnitudes of the bands are not significantly larger (except for t^6A) or smaller than those of adenosine's, and thus that the rotation about the glycosidic bond is not greatly affected by the addition of the hypermodification. The CD of t^6A could contain some contributions from the

Figure 9: CD of the Hypermodified Monomers. pH = 7. $(\varepsilon_L - \varepsilon_R)$

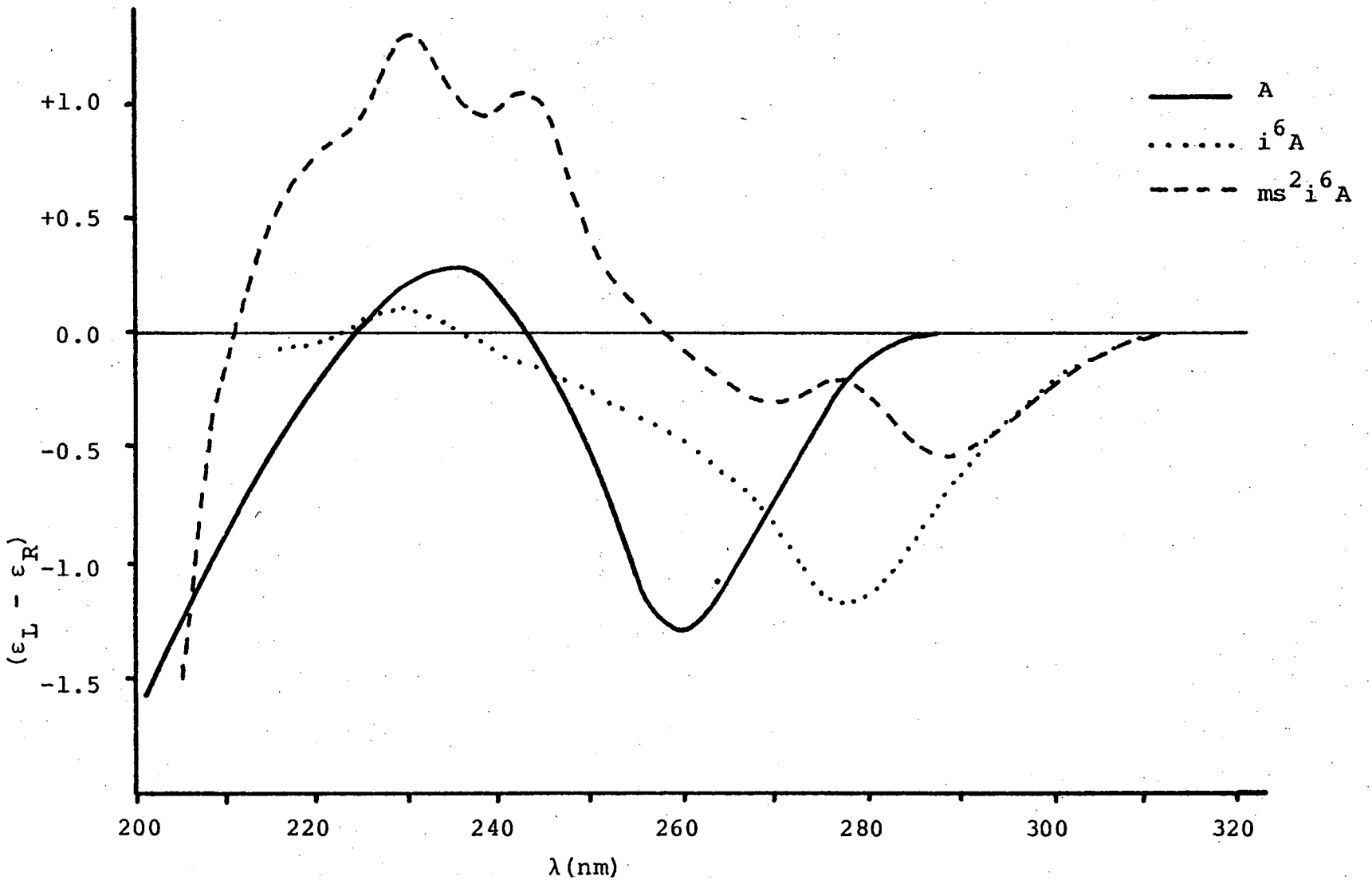

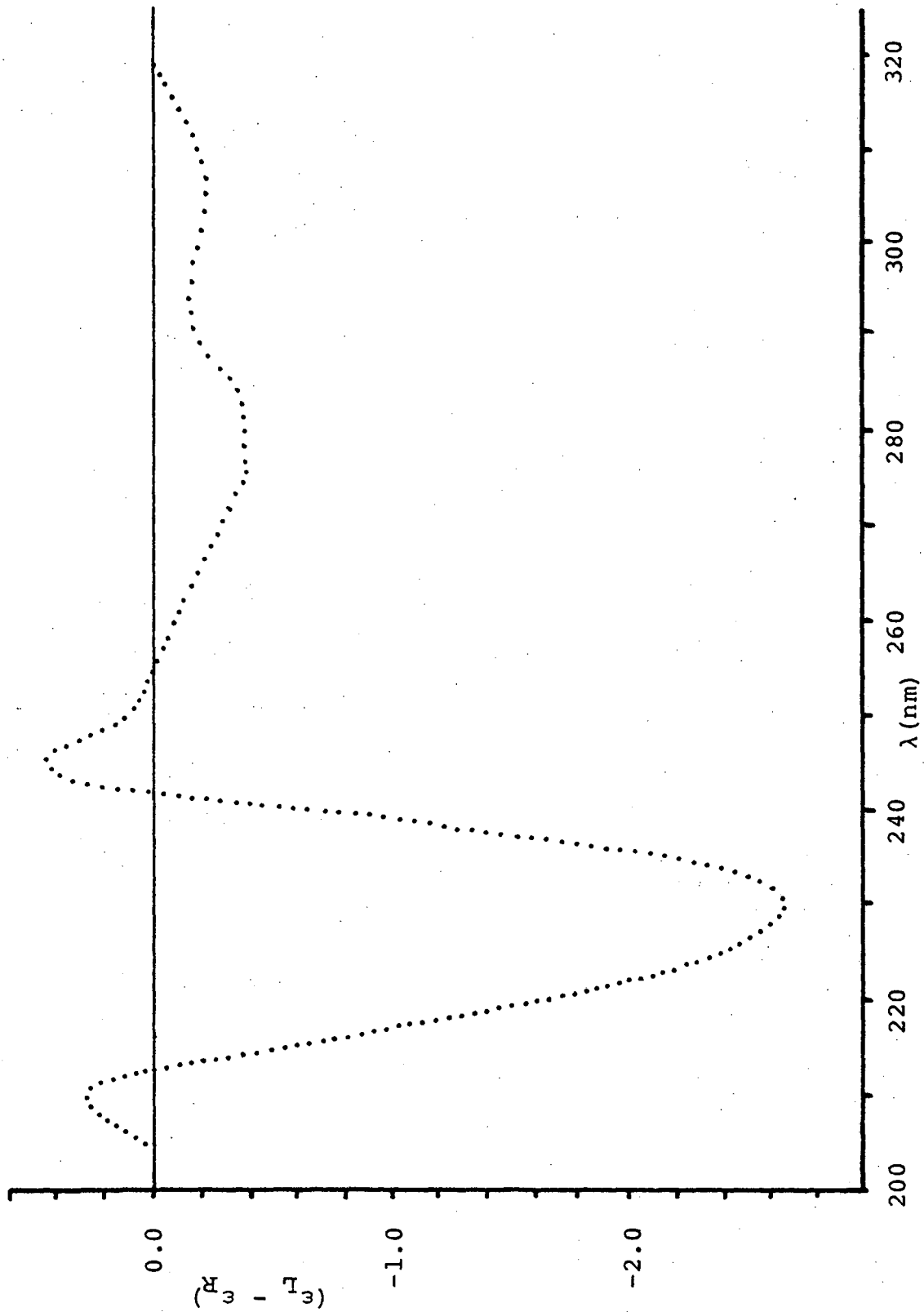

Figure 10: CD of pεA. pH = 7. 20°C.

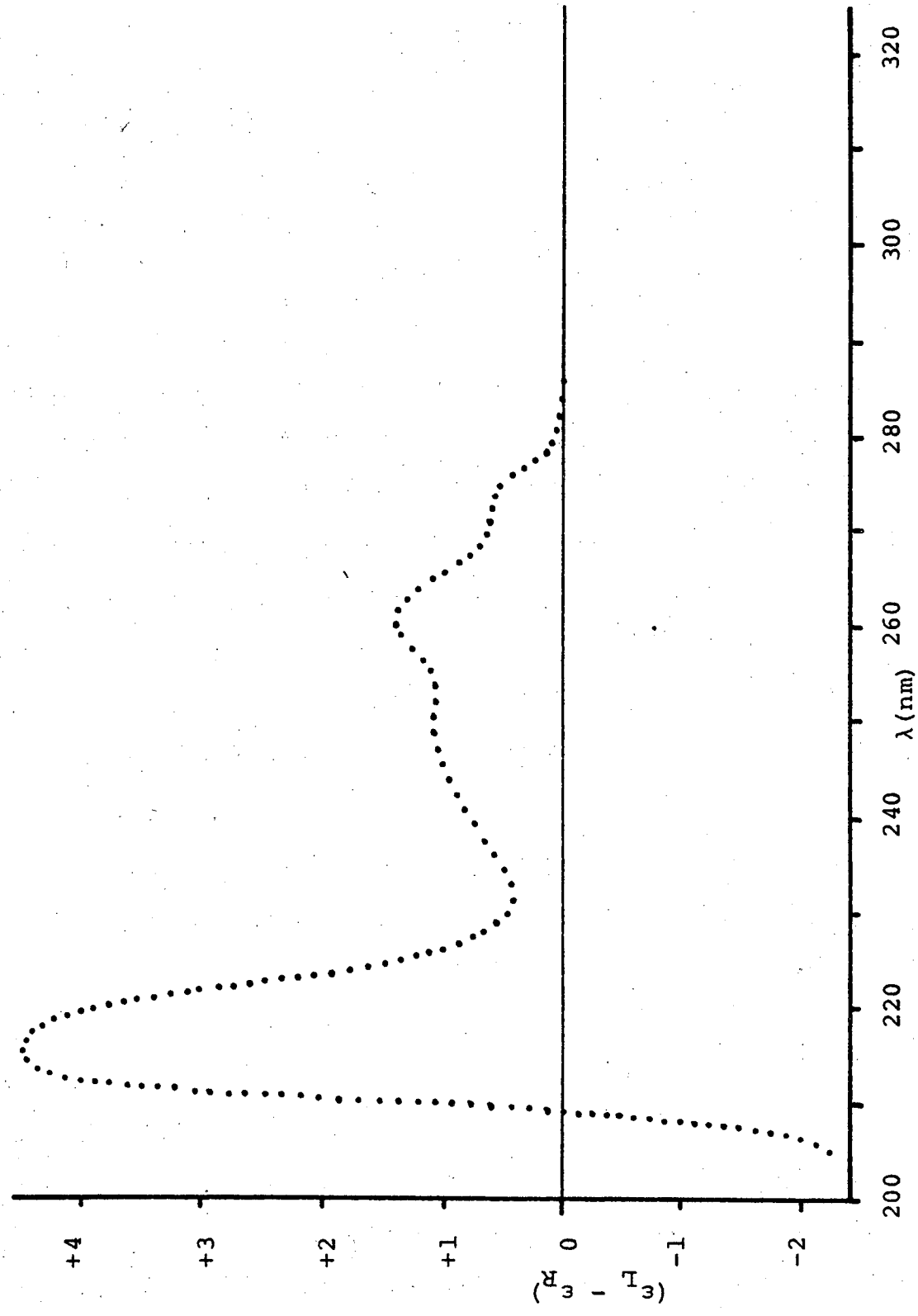

Figure 11: CD of pt^6A, 0°C. pH = 7.

attachment of the asymmetric amino acid threonine.

(ii) Dimers

The CD of the dinucleoside monophosphates studied are shown in Figures 12 - 14. Aside from the spectra of UpA and Upt^{6}A, they are significantly larger than would be expected if we only summed the monomers' spectra. As a matter of fact, the CD of the monomers have been subtracted from the dimers' spectra to obtain these Figures. Thus, the CD pictured is due only to the interaction via stacking of the component base moieties, and the resultant interaction of the electronic transitions on these bases (not the asymmetry of the sugar moieties). The monomer CD is believed not to change as a result of base-base interaction[72].

The quantity which we will be interested in then, is the $(\varepsilon_L - \varepsilon_R)$ of the dimer minus the $(\varepsilon_L - \varepsilon_R)$ of the monomers. From convention, the dimer CD is per residue (divided by 2 in the case of dimers), and hence we subtract 1/2 the sum of the monomers' CDs to obtain the CD due to base-base interaction. This will be referred to herein simply as $\Delta\varepsilon$.

(C) $\Delta\varepsilon$ Temperature Dependence

The PDP8/e yielded the 'smooth data' (SD) which was the ellipticity $\theta°$ (in degrees) multiplied by a factor which was usually 100 (determined simply by the arbitrary numbers fed into the program). Figure 15 illustrates a

Figure 12: CD of some of the hypermodified dimers. pH = 7. Monomer CD's have been subtracted. 25°C. (per residue)

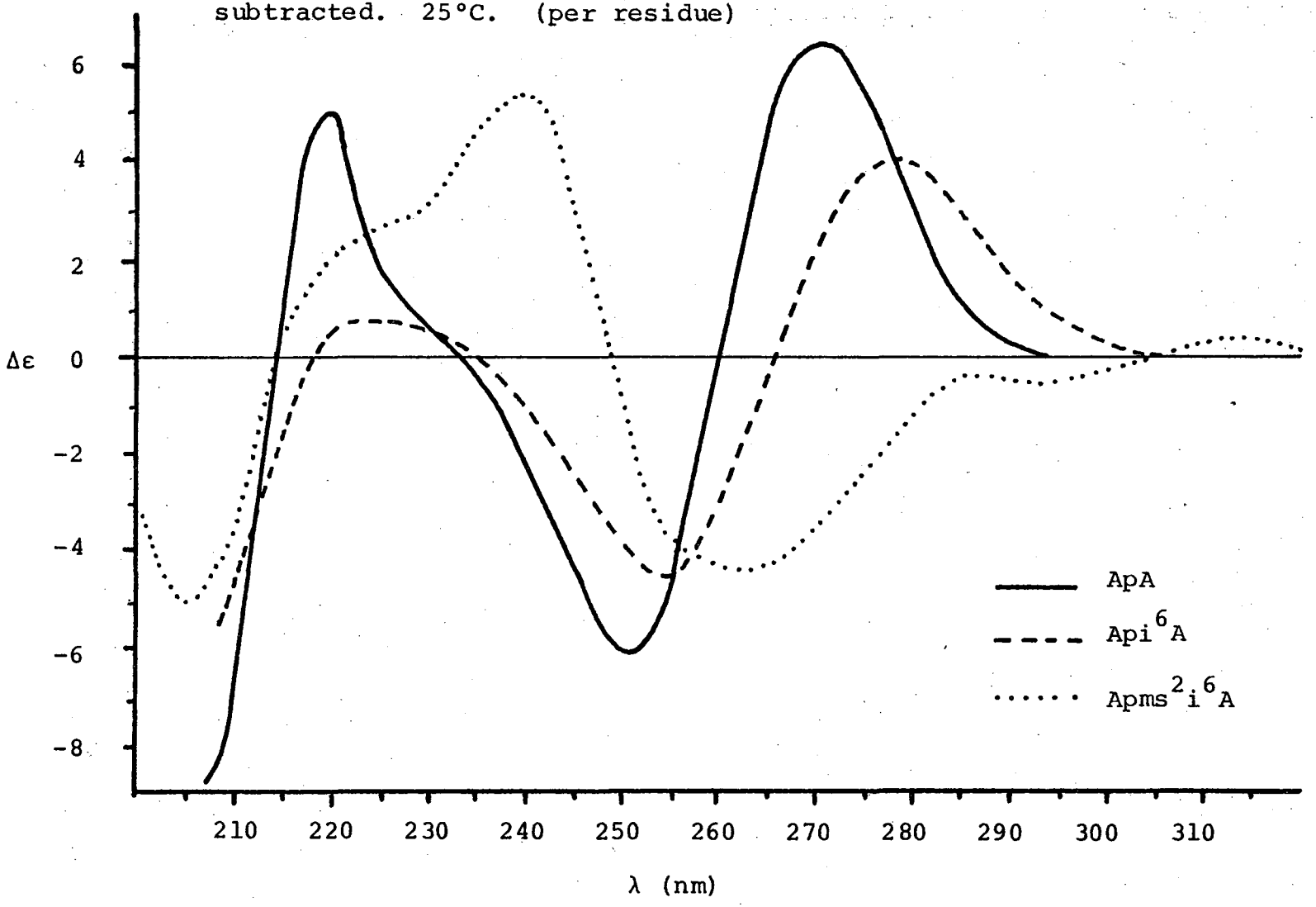

Figure 13: CD of ApεA. pH = 7, 20°C. Monomer Contributions have been subtracted. (per residue)

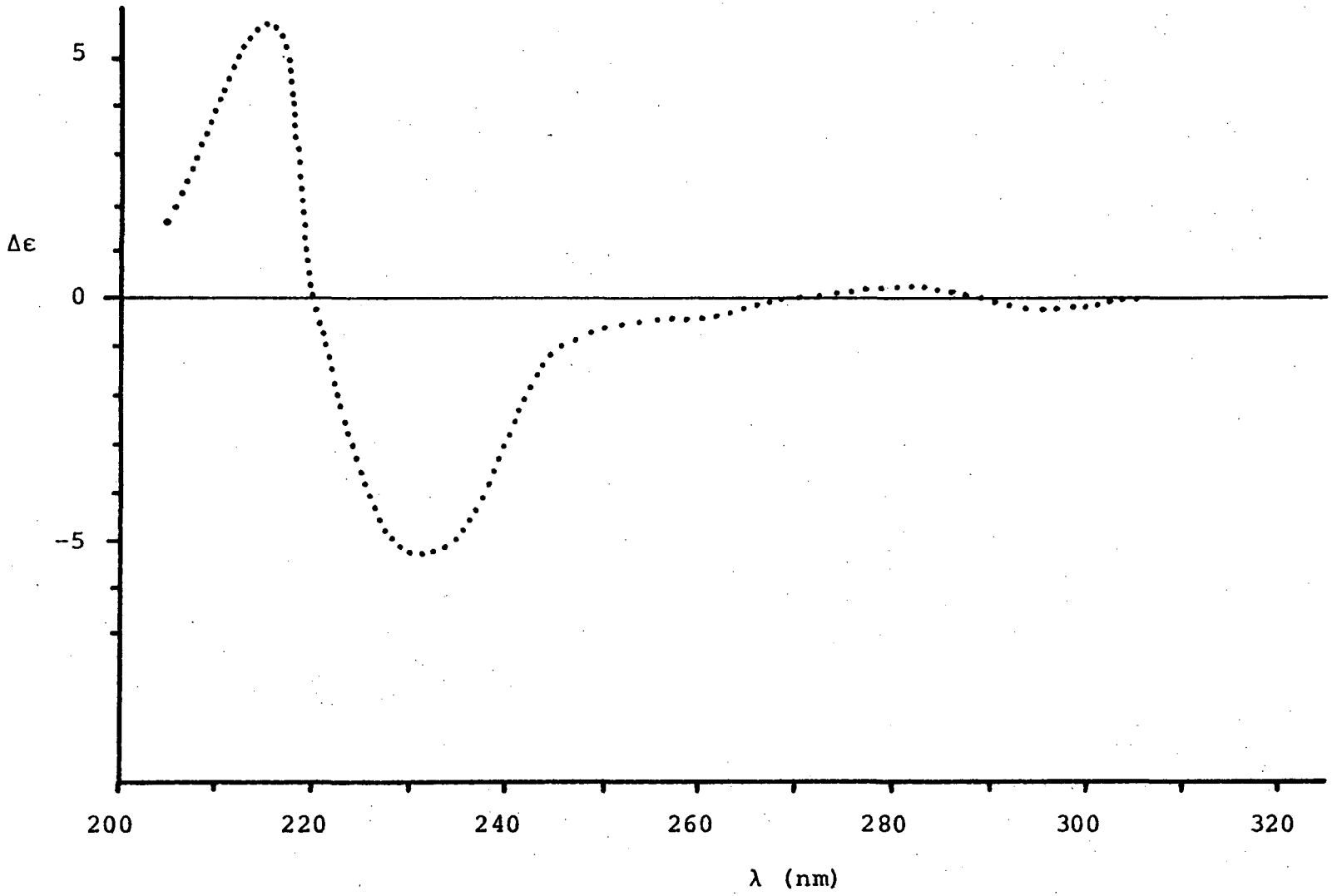

Figure 14: CD of dinucleoside monophosphates. pH 7. 0°C. Monomer contributions have been subtracted. (per residue)

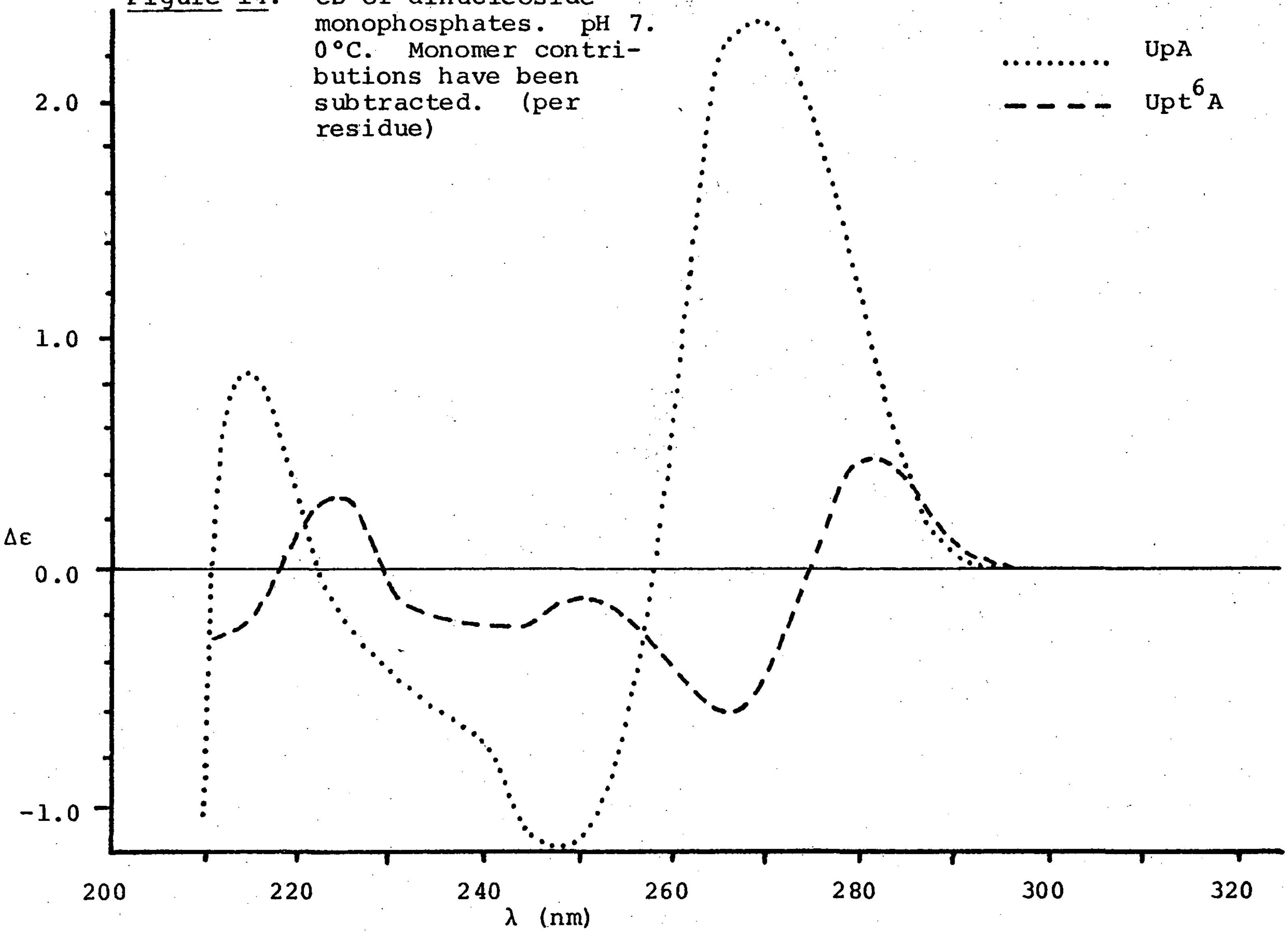

Figure 15: CD 'melt' of Api^{6}A, pH 7. The monomer CD's have not been subtracted.

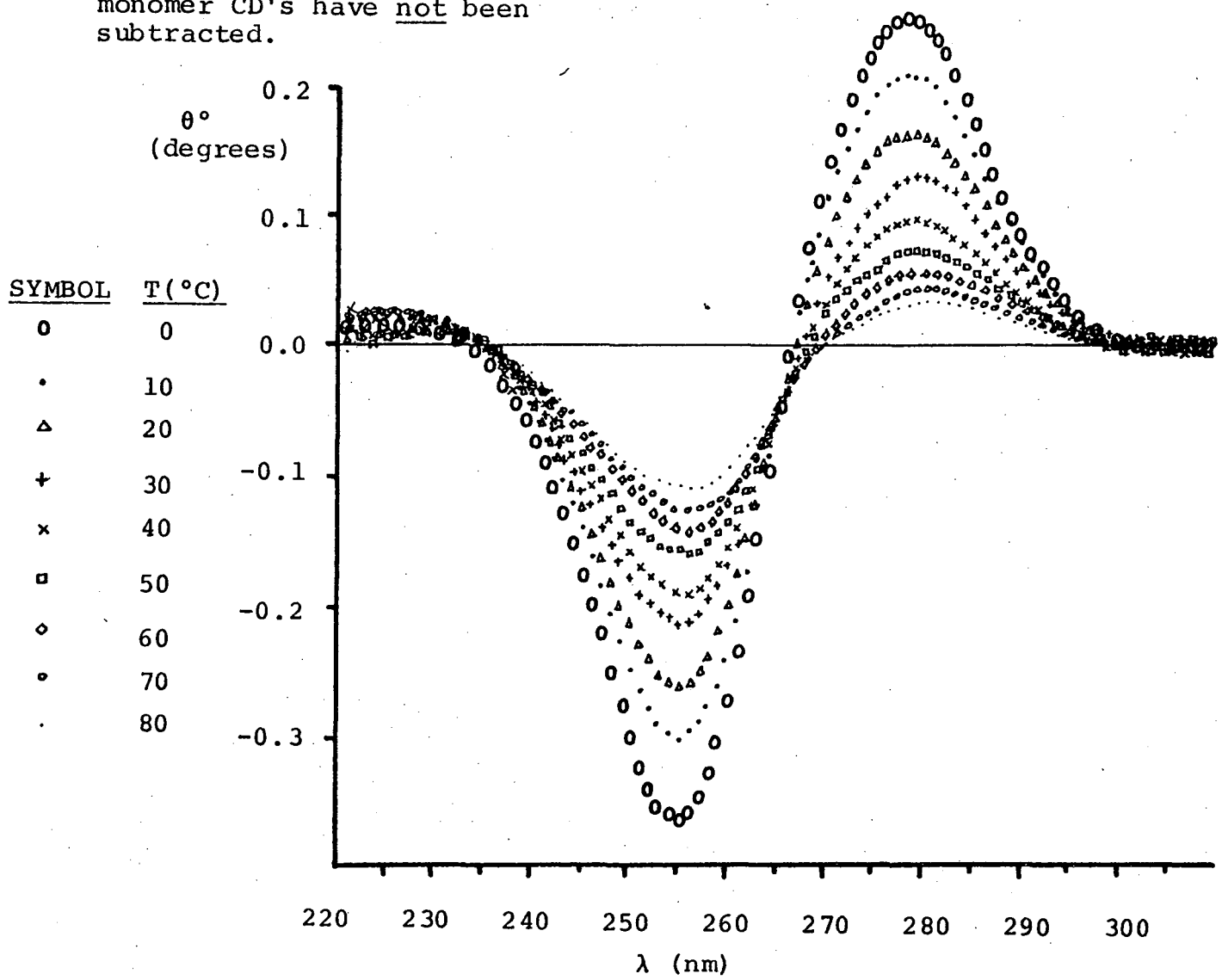

typical CD melt experiment. The $\Delta\varepsilon$ at the wavelength of the dimer's CD max or min vs. temperature was then obtained as follows:

$$(\varepsilon_L - \varepsilon_R)_{dimer}(T) = \frac{\theta°(T)\ 100}{(Conc.)\ 3300} \quad \frac{1}{2} \quad \frac{\rho_{room\ T}}{\rho_T}$$

where the concentration was determined by an absorption measurement (at room temperature) and the extinction coefficient.

Determinations of the $(\varepsilon_L - \varepsilon_R)$ of the component monomers at the same λ used for the dimer were also made. In most of those studied, no temperature dependence within experimental error at the wavelengths chosen could be found. Then,

$$\Delta\varepsilon(T,\lambda) = [(\varepsilon_L - \varepsilon_R)_{dimer}(T,\lambda)] - \frac{1}{2}[(\varepsilon_L - \varepsilon_R)_{monomer\ 1}(\lambda) + (\varepsilon_L - \varepsilon_R)_{monomer\ 2}(\lambda)]$$

However Up showed a marked change with temperature, and this was corrected for in the calculation of $\Delta\varepsilon$ of dimers which contained U. Table III contains the values for $\Delta\varepsilon$ obtained in dilute Na phosphate buffer near pH 7.

(D) $\Delta\varepsilon$ Dependence Upon Salt

Because of the negative results concerning possible effects upon the absorption by the addition of NaCl or $MgCl_2$, only a limited number of studies were performed with the CD. The CD of Api^{6}A was unchanged at room temperature upon the addition of 5 m$\underline{M}$ Na phosphate buffer, or 10 m$\underline{M}$ $MgCl_2$ or 100 m$\underline{M}$ NaCl, or combinations of those. Likewise,

Table III. CD of the dimers minus their monomers' contributions. pH 7. Wavelength chosen shown below dimer. All magnitudes are in error by ~±0.26 - See Appendix 2 for the derivation and explanation of this number.

$$\Delta\varepsilon = 1/2(\varepsilon_L - \varepsilon_R)_{dimer} - 1/2[(\varepsilon_L - \varepsilon_R)_{monomer\ 1} + (\varepsilon_L - \varepsilon_R)_{monomer\ 2}]$$

T(°C)	ApA 271	Api^{6}A 279	Apms^{2}i^{6}A 264	ApεA 231	UpA 270	Upt^{6}A 280
0	11.1				2.34	0.47
1		6.28		-7.83		
2			-5.79			
10	9.29	5.28	-5.49	-6.70		0.18
20	7.66	4.35	-5.17	-5.36		
25					1.31	0.03
30	6.11	3.62	-4.88	-4.13		
40	4.99	2.91	-4.54	-3.18		0.04
50	3.86	2.42	-4.23	-2.72	0.59	-0.05
60	3.00	2.00	-3.79	-1.99		-0.06
70	2.43	1.70	-3.15	-1.69		
75					0.36	
80	1.77	1.45				

the CD melt of Api^{6}A was unaffected by the addition of salt. Similar results were obtained with Upt^{6}A, in which no effects of the addition of 10 m$\underline{M}$ $MgCl_2$ could be discerned.

III. Nuclear Magnetic Resonance (NMR)

(A) Techniques

(i) Instrumentation

High resolution NMR spectra were obtained on a Bruker HFX 360 MHz spectrometer located at the Stanford Magnetic Resonance Laboratory. These spectra were obtained with the help of Dr. Che-Hung Lee of this laboratory and Dr.'s Conover and Patt of the resonance laboratory. Spectra were run at various temperatures in the FT mode. The pulse widths were generally on the order of microseconds with a period between pulses equal to $\sim$1/2 sec. Pulse amplitude, duration, and delay were kept at a level such as not to cause appreciable saturation. Pulses were continued until a good signal to noise ratio was obtained (usually 50 - 150 for the concentrations used). The entire spectrum was then recorded on paper, followed by expansions of the frequency range in order to accurately determine coupling constants.

(ii) Sample Preparation

Unless otherwise specified, samples of both monomers and dimers were run at a concentration of 5 m$\underline{M}$. The reasons for this will be discussed later. The concentration was accurately determined by the measurement of the OD of a

dilution of a stock solution containing the sample in pure water. Using the extinction coefficients, an appropriate amount of the stock solution was then removed for the preparation of the NMR sample. To this was added ∿5λ of 1 N TSP (sodium trimethylsilylpropionate - Stohler Isotope Chemicals) (1 N in protons = 1/9 M)

$(CH_3)_3$-Si-CD_2-CD_2-COO^- Na^+

used as a reference because of its solubility in D_2O and its upfield position (very near TMS). All the samples were made up in 0.5 ml of D_2O, so that the TSP concentration was ∿10 mN. The sample at this point was usually in H_2O and was therefore frozen and lyopholized to remove the water. Then ∿1 ml of 99.8% D_2O (Stohler D320) was added and the freezing and lyopholization repeated.

After 2 or 3 times of repeating the addition of D_2O and lyopholizing, the pD ($-\log[D^+]$) was determined and altered if necessary in the following way. To the lyopholized powder, ∿1 ml of D_2O was again added. A Radiometer electrode (CDC 114), adjusted to either pH 7.00 or 4.01 with standard buffers (the choice depending upon the final pH desired), was then inserted after being carefully rinsed and blotted dried. The pH was then measured on a Radiometer pH meter. The pD = pH measured on the meter + 0.40[93]. For reasons to be given later, mononucleotides were prepared with pD = 5.5 (pH 5.1), and dimers and mononucleosides were prepared with pD ≃ 7 (pH∿6.6). Thus titration of the samples was in generaly required and performed by the addition of 0.1 N DCl or

0.1 N NaOD (Stohler) in D_2O. This was carefully achieved with the help of Hamilton gas tight syringes (#1001) with Teflon needles, while the sample was gently mixed with a vortex mixer. When the pD desired was obtained, the electrode was rinsed with D_2O into the sample below so as not to lose any sample. The sample was then again frozen and lyopholized. The freeze dry cycle was repeated usually 2 or 3 times again after the titration.

Dr. Che-Hung Lee of this lab devised the following steps which were then performed. On the final lyopholization, the samples were placed in a lyopholization bottle equipped with a valve of its own. In this way the entire bottle containing the samples could be removed from the lyopholizer without breaking the vacuum in the bottle. The bottle was then placed in a transparent glove bag (Instruments for Research and Industry X-27-27) along with the NMR tubes and other paraphenalia required for the sample preparation. The bag was sealed, evacuated and then filled with dry N_2 (passed through a condensing trap and NaOH pellets). Several evacuations and fillings were performed in order to insure a dry N_2 atmosphere in the bag.

At this point the bottle was opened and the samples in their polypropylene vials removed. To each was added 0.50 ml of previously unopened 100.0% D_2O (Bio-Rad 710-5008) with a Hamilton syringe. They were then in entirety transfered to the clean (acid washed and extensively rinsed and dried) NMR tubes (Wilmad Glass Co. 527PP). These were sealed with the

tube caps, and then tightly sealed with a small strip of Parafilm. Samples prepared in this were generally kept frozen in the freezer of a refrigerator; deep freezing often cracked the tubes.

This entire procedure was absolutely necessary to remove residual HDO and to prevent H_2O in the air from condensing in the sample. The samples spectrum at a concentration of 5 mM was easily obliterated in the region of 4 - 6 ppm if this procedure was not followed.

(B) Characteristic NMR Information

The information obtainable from NMR investigations of monomers and dimers is well documented[72,93-101]. I have followed essentially in the footsteps of these workers in my approach. Thus, only the highlights of the properties to be measured will be pointed out here.

(i) Monomers

NMR of the nucleosides and nucleotides will contain the information concerning the addition of the side chain to the unmodified base. In all cases this unmodified base was A. This information will include the effect of hypermodification upon the syn-anti equilibrium of A, and upon all the non-exchangeable protons of A. This data is presented in Table VIII, and will be discussed in a following chapter. The monomers' properties studied as a function of temperature were those which would aid in interpreting the dimers'

spectra. These consisted of the chemical shifts of H8 and H2 of the adenine moiety, and the chemical shift and coupling constant of the H1' sugar proton[93,98,99], and the protons of the hypermodified side chain. These are the easiest protons to assign, and their shifts are often monitored as a function of base-base interaction.

Since the mononucleotides protons are affected by the different ionizations of the phosphate group, the spectra of the monophosphates were obtained at a pD = 5.5. At this pD, the phosphate carries essentially a -1 charge, similar to the dimer's charge at pD = 7 (see pK values at the equivalent salt conditions in reference 102 - note that at this pD no significant protonation of the adenine base moiety will occur). Thus changes in chemical shifts between mononucleotides and dimers will not be caused by the influence of the phosphate group.

Nucleosides were studied in some cases, in order to determine the effect of the deletion of the phosphate group upon the hypermodified nucleotides' properties. These were run at a pD ≃ 7.

The assignment of the protons was easy in the case of the monomers, since most had been assigned previously in the literature[14,82,104]. In the case where there was question concerning the base proton assignment, comparisons between nucleoside and nucleotide, or between different pD's were performed[100,101]. Also useful for the assignments is the fact that H2 is more easily saturated than H8, and thus

they are relatively easily differentiated.

(ii) Dinucleoside Monophosphates

The chemical shifts and coupling constants of several of the protons of the nucleotides are changed dramatically by the stacking[93-99]. As with the absorption and CD, these changes resulting from the stacking equilibrium have been measured as a function of temperature.

The concentration chosen to study the stacking was 5 m<u>M</u>. Above 10 m<u>M</u> it is known that significant intermolecular stacking occurs, which also affects the chemical shifts[93,99]. The pD was set at neutrality to ensure that changes observed were due only to intermolecular stacking, and not protonation. The temperature was varied over a similar range as with the absorption and CD experiments ($\sim$0 - 80°C).

Because of the presence of a body of literature dealing with the affect of stacking upon certain protons, and the relative ease of assignment of these certain protons, not all of the protons on the dimer were studied. In general, the base moiety protons H8 and H2 were studied as was the H1' proton of the sugar. The side chain protons were studied when they could be easily assigned (some were in a region containing many sugar protons). Assignments were made by comparing high temperature dimer spectra with their monomer spectra. Since they approached the already characterized monomers' spectra at high temperatures, this

method was generally quite straight forward. The different saturation characteristics of the base protons verified this type of assignment, as did the characteristically varied temperature dependences of the various protons[93-99].

The quantity desired is the change in the NMR property due only to intramolecular interaction. Thus the dimerization change[93] was measured for both the chemical shifts and the coupling constants, as a function of temperature. This is simply the difference between the chemical shifts or coupling constants of the dimer and its constituent monomers.

(C) Temperature Dependence of the Dimerization Changes in the Chemical Shifts

The chemical shifts were easily obtained from the recorded chart. First, the position of the internal reference was noted. (TSP - however, in several instances the residual HDO peak was used as a reference. Since its position is very temperature dependent, the HDO peak was always referenced to samples run at the same temperature which contained TSP - immediately after those samples were run.) Then the various peak positions were obtained and the distance in cm between them calculated. Using the printed scale expansions this was converted into Hz or ppm (δ_{TSP}). Figure 16 illustrates a sample NMR spectrum.

The monomers' protons exhibited relatively small changes in their δ_{TSP}'s as the temperature was changed (typical changes ranged from 0.005 to 0.08 ppm from 0 - 75°C). The

Figure 16: NMR of Upt^{6}A. Bruker 360 MHz; 5 mM; 60°C; pD = 7.37. Boxed insert is a T60 scan, which demonstrates the need for the use of 360 MHz FT spectra. Other expansions are from the complete spectrum at the bottom of the figure.

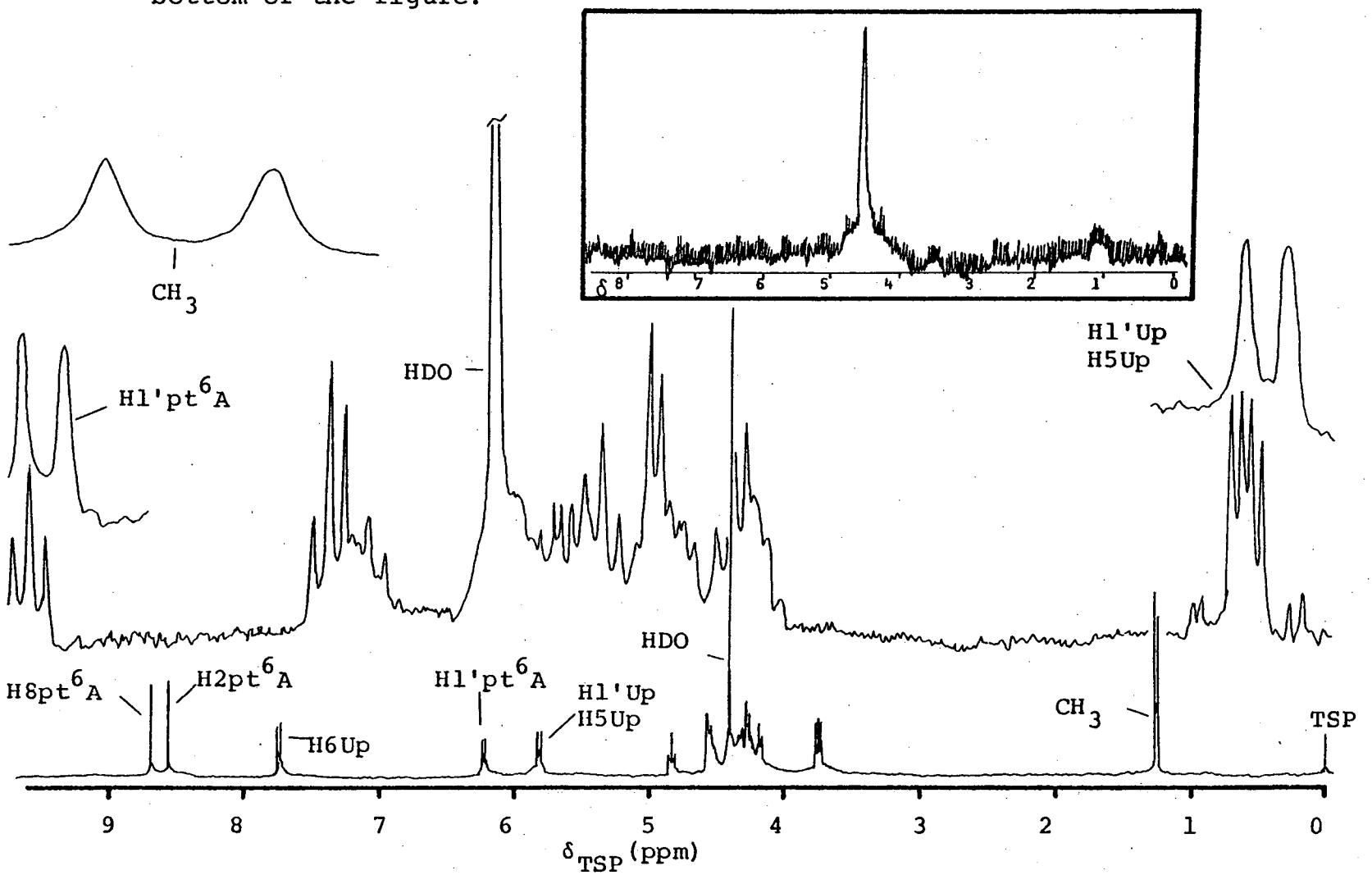

δ_{TSP}'s were plotted vs. temperature and smooth curves were drawn through the points to obtain the values to be used in calculating the dimerization shifts. This was done to obtain more accurate monomer chemical shifts, since their temperature dependences were often linear or with only slight curvatures. The δ_{TSP}'s obtained in this way are given in Table IV.

The dimers' δ_{TSP}'s were then recorded, and the appropriate monomer's δ_{TSP} value (obtained from the smooth graph) was subtracted from it. In this way I obtained the $\Delta\delta_{TSP}$'s shown in Table V.

(D) Temperature Dependence of the Dimerization Changes in the H1' Coupling Constants

The dimerization changes in the coupling constants of the H1' protons were obtained in a fashion similar to that used in the previous section. All coupling constants were obtained from scale expansions on the order of 1 - 2 Hz/cm. The mononucleotides coupling constants were again obtained from a graph of the raw data as they showed little or no temperature dependence. Then, these values (in Hz) were subtracted from those of the dimers at the various temperatures. Table VI lists the $J_{1',2'}$'s of the dimers and Table VII lists the dimerization changes vs. temperature.

Table IV. Chemical Shifts of the Mononucleotides (δ_{TSP}). pD = 5.5 ; Concentration = 5 m<u>M</u>. (δ ±0.005 ppm)

Temp. →	0	10	20	25	37	45	60	75
Proton ↓								
H8Ap	8.381	8.380	8.378	8.378	8.375	8.373	8.369	8.363
H2Ap	8.231	8.247	8.261	8.268	8.283	8.290	8.302	8.308
H1'Ap	6.137	6.134	6.132	6.130	6.127	6.125	6.121	6.117
H8pA	8.527	8.523	8.518	8.515	8.507	8.500	8.484	8.462
H2pA	8.245	8.265	8.277	8.283	8.294	8.298	8.303	8.305
H1'pA	6.161	6.161	6.159	6.157	6.156	6.154	6.150	6.145
H8pi6A	8.473	8.469	8.465	8.462	8.456	8.450	8.440	8.427
H2pi6A	8.254	8.270	8.285	8.291	8.302	8.307	8.312	8.314
H1'pi6A	6.159	6.158	6.156	6.157	6.155	6.154	6.150	6.144
=CH-	5.426	5.428	5.430	5.432	5.434	5.436	5.439	5.442
$-(CH_3)_2$	1.758	1.759	1.760	1.761	1.763	1.764	1.766	1.768
$-CH_2-$	4.132	4.150	4.164	4.171	4.185	4.192	4.202	4.205
H8pms2i6A	8.281	8.278	8.274	8.271	8.264	8.258	8.245	8.229
H1'pms2i6A	6.086	6.088	6.088	6.088	6.086	6.085	6.080	6.074
=CH-	5.382	5.387	5.391	5.392	5.396	5.398	5.401	5.402
$-CH_3$ a	1.764	1.765	1.765	1.765	1.765	1.765	1.766	1.767
$-CH_3$ b	1.753	1.754	1.754	1.754	1.755	1.756	1.757	1.758
$-CH_2-$	4.133	4.155	4.169	4.173	4.183	4.187	4.193	4.197
$-S-CH_3$	2.577	2.584	2.592	2.595	2.602	2.606	2.612	2.616
H8pεA	8.623	8.621	8.617	8.615	8.608	8.602	8.589	8.573
H2pεA	9.126	9.132	9.138	9.141	9.148	9.153	9.162	9.171
H1'pεA	6.288	6.288	6.287	6.286	6.285	6.284	6.282	6.281
H10	7.991	8.006	8.018	8.023	8.032	8.036	8.042	8.045
H11	7.585	7.603	7.615	7.620	7.630	7.636	7.642	7.647
H8pt6A	8.829	8.815	8.801	8.795	8.778	8.767	8.746	8.725
H2pt6A	8.695	8.696	8.696	8.696	8.697	8.697	8.698	8.699
H1'pt6A	6.270	6.264	6.258	6.255	6.247	6.243	6.233	6.224
$-CH_3$	1.283	1.280	1.277	1.275	1.272	1.270	1.265	1.261
H6Up	7.957	7.941		7.917	7.898	7.885	7.861	7.838
H5Up	5.895	5.908		5.921	5.925	5.925	5.924	5.922
H1'Up	5.975	5.973		5.968	5.962	5.955	5.940	5.921

Table V. Dimerization Shifts of the Dinucleoside Monophosphates ($\Delta\delta_{TSP}$). pD = 7 for the dimers; pD = 5.5 for the mononucleotides. ($\sim\pm.010$ ppm)

Temp.	0	4	10	20	25	37	45	60	75
ApA									
H8Ap	.160	.149	.142	.118	.119	.116	.108	.119	.101
H2Ap	.330	.320	.299	.251	.239	.202	.177	.158	.128
H1'Ap	.302	.291	.281	.247	.244	.212	.194	.194	.160
H8pA	.282	.280	.280	.241	.231	.196	.166	.147	.106
H2pA	.137	.133	.131	.114	.097	.099	.085	.080	.065
H1'pA	.209	.209	.197	.153	.153	.116	.101	.100	.069
Api^{6}A									
H8Ap	.221		.210	.192	.180	.162	.160	.159	.143
H2Ap	.336		.314	.266	.253	.212	.194	.174	.142
H1'Ap	.367		.366	.354	.344	.317	.302	.288	.255
H8pi6A	.260		.242	.225	.207	.182	.171	.160	.133
H2pi6A	.192		.183	.162	.150	.126	.114	.102	.082
H1'pi6A	.181		.172	.143	.134	.112	.106	.104	.084
=CH-	.345		.331	.304	.287	.265	.242	.215	.207
-CH_3 a	.158		.149	.137	.127	.111	.112	.112	.101
-CH_3 b	.122		.115	.106	.097	.085	.086	.089	.082
-CH_2-					.322			.231	.193
Apms^{2}i^{6}A									
H8Ap	.154		.154		.147	.157	.150	.159	.155
H2Ap	.165		.167		.141	.149	.130	.131	.117
H1'Ap	.395		.392		.376	.378	.354	.342	.303
H8pms2i6A	.233		.227		.197	.194	.170	.156	.130
H1'pms2i6A	.139		.140		.120	.123	.104	.098	.081
=CH-					.386	.394	.348	.307	.267
-CH_3 a	.091		.096		.085	.110	.093	.102	.096
-CH_3 b	.123		.126		.109	.137	.109	.118	.104
-S-CH_3	.016		.023		.028	.045	.045	.042	.042
ApεA									
H8Ap		.272		.260			.240		.241
H2Ap		.356		.294			.233		.162
H1'Ap		.494		.472			.412		.339
H8pεA		.263		.218			.169		.128
H2pεA		.086		.063			.047		.076
H1'pεA		.158		.126			.098		.080
H10		.221		.229			.210		.176
H11		.265		.259			.230		.178

Table V. (Continued) $\Delta\delta_{TSP}$

Temp.	0	10	20	25	37	45	60	75
UpA								
H6Up	.170	.157	.146	.142	.141	.133	.126	.115
H5Up	.171	.154	.142	.130	.108	.093	.094	.085
H1'Up	.303	.272	.251	.230	.194	.172	.159	.126
H8pA	.087	.072	.067	.062	.066	.064	.063	.049
H2pA	.037	.025	.020	.019	.019	.013	.016	.015
H1'pA	.049	.034	.032	.023	.021	.017	.028	.022
Upt^6A								
H6Up	.166	.159	.158	.150	.136	.141	.136	.118
H5Up	broadened	-	-	-	--	-	-	-
H1'Up	.261	.240	.216	.205	.171	.155	.139	.113
H8pt6A	.227	.216	.209	.198	.184	.188	.186	.171
H2pt6A	.009	.006	.003	-.005	-.013	-.006	.003	.001
H1'pt6A	.044	.037	.029	.024	.016	.016	.017	.020
$-CH_3$	.010	-.002	-.004	-.005	-.009	-.010	.009	.000

Table VI. Coupling Constants of the H1' proton of the dinucleoside monophosphates ($J_{1'2'}$, Hz). pD = 7. (±0.2 Hz)

Temp. (°C)	0	4	10	20	25	37	45	60	75
ApA									
H1'Ap	2.6		3.0	3.4	3.5	3.9	4.0	4.3	4.4
H1'pA	3.1		2.6	3.5	3.8	4.0	4.4	4.8	4.9
Api^{6}A									
H1'Ap	3.6		3.9	4.1	4.2	4.6	4.7	4.8	5.0
H1'pi6A	4.0		4.0	4.1	4.1	4.3	4.4	4.6	4.8
Apms^{2}i^{6}A									
H1'Ap	3.8		4.8		5.7	6.2	5.9	6.2	5.6
H1'pms2i6A	3.6		4.2		4.3	4.9	4.2	4.4	4.3
ApεA									
H1'Ap		3.4		4.5			5.3		5.8
H1'pεA		3.4		3.8			4.2		4.6
UpA									
H1'Up	3.7		4.0		4.4	4.6	4.7	4.8	5.0
H1'pA	4.2		4.3	4.6	4.7	5.0	5.0	5.2	5.2
Upt^{6}A									
H1'Up$_6$			4.1	4.8	4.7	4.9	5.0	5.1	5.2
H1'pt^{6}A	4.3		4.2	4.6	4.5	4.7	4.8	5.0	5.0

Table VII. Dimerization Changes in the H1' Coupling Constants ($\Delta J_{1'2'}$ Hz). ($\pm\sim 0.3$ Hz)

Temp. (°C)	0	4	10	20	25	37	45	60	75
ApA									
Ap	4.1	3.9	3.7	3.2	3.1	2.6	2.4	2.0	1.7
pA	2.8	3.2	3.2	2.3	2.0	1.8	1.3	0.9	0.7
Api^{6}A									
Ap	3.0		2.8	2.5	2.4	1.9	1.7	1.5	
pi6A	1.8		1.8	1.7	1.6	1.4	1.2	1.0	0.7
Apms^{2}i^{6}A									
Ap	2.9		1.9		0.9	0.3	0.5	0.1	0.5
pms2i6A	2.1		1.5		1.4	0.8	1.5	1.2	1.2
Apε A									
Ap		3.3		2.1			1.1		0.3
pε A		2.2		1.7			1.2		0.7
UpA									
Up	0.9		0.7		0.4	0.3	0.3	0.3	0.2
pA	1.7		1.5	1.2	1.1	0.8	0.7	0.5	0.4
Upt^{6}A									
Up			0.6	0.0	0.1	0.0	0.0	0.0	0.0
pt6A	1.5		1.6	1.2	1.3	1.1	1.0	0.8	0.8

Table VIII. NMR chemical shifts (δ_{TSP}) of the naturally occurring hypermodified monomers of A. All are at ∿ room temperature (20 - 25°C). All shifts are in error by ±0.005 ppm.

Monomer	A	i^6A	ms^2i^6A	pA	pi^6A	pi^6A	pms^2i^6A	pt^6A
pD =	8.30	6.89	7	5.43	5.50	5.5	5.5	5.38
Concentration	2 mM	1.4 mM	5 mM in CD_3OD §	5 mM	5 mM synthetic ϕ	3.1 mM SVP ϕ	3 mM	1 mM + EDTA *
Proton								
H8	8.345	8.284	8.121	8.518	8.495	8.465	8.274	8.795
H2	8.265	8.253		8.284	8.316	8.285		8.696
H1'	6.081	6.076	5.927	6.164	6.165	6.156	6.088	6.255
H2'	4.811	4.804	4.762	4.775	4.775	4.779	4.808	4.872
H3'	4.431	4.436	4.346	4.514	4.514	4.507	4.519	4.572
H4'	4.298	4.306	4.159	4.401	4.398	4.395	4.355	4.427
H5'	3.923	3.927	3.886	4.132	4.124	4.121	4.104	4.071
H5"	3.840	3.843	3.757	4.132	4.124	4.121	4.104	4.071
(i^6A, ms^2i^6A)								
=CH-		5.431	5.396		?	5.430	5.391	
$-CH_2-$		4.153	4.196		4.637	4.164	4.169	
$-S-CH_3$			2.576				2.592	
$-CH_3$ a		1.764	1.779		1.927	1.762	1.765	
$-CH_3$ b		1.764	1.767		1.971	1.762	1.754	
(t^6A)								
$>CH-COO^-$								4.305
$-CH_3$								1.241

§ ms^2i^6A is essentially insoluble in D_2O.

ϕ the synthetic pi6A lacked a =CH- proton! Thus all the dimers were referred to the pi6A from the SVP degradation.

* the final pt6A preparation evidently still contained some divalent cations, and small amounts of EDTA were added to sharpen the lines. Essentially no changes in peak positions were observed upon the addition of EDTA.

Chapter 5 ANALYSIS OF THE DATA - THE TWO-STATE MODEL

Chapter 5

ANALYSIS OF THE DATA - THE TWO-STATE MODEL

I. Comparisons of Stacking Abilities - A Dynamic Model

The static properties of dinucleoside monophosphates have often been used to compare their stacking interactions[72,95]. Thus, the %h at a given temperature can be used as a rough measure of the relative stacking abilities of the various unmodified dimers[69]. Likewise, the magnitudes of dimers' CD at a given temperature can also be interpreted in terms of stacking abilities. NMR dimerization shift magnitudes also can be used for a first approximation of relative stacking interactions[93].

The problem with this simple approach is that we are not certain that a given amount of stacking will yield the same values for the measured properties (%h,$\Delta\varepsilon$,$\Delta\delta_{TSP}$) for dimers containing different monomers. This uncertainty is especially true in the case of hypermodifications. For instance, the hypermodified monomers exhibit very different absorption spectra from that of adenosine's. The present theories of hypochromism show that these differences in the monomers' absorption properties (ε, λ_{max}'s, and transition moment directions) will significantly affect the value of the hypochromism (and most likely the %h as well)[72]. Likewise, the ring currents of the hypermodifications may very well be different from that of adenosine's, and thus the dimerization shift magnitudes of the bases adjacent to the

hypermodification may very even without invoking structural changes. CD spectral magnitudes of dimers are also subject to variation with monomer properties, even though the monomers' spectra have been subtracted. New absorption bands or different transition directions caused by hypermodification could greatly affect the dimers' CD[72].

For these reasons, a more detailed analysis is necessary in order to extract information about the relative stacking abilities of the dimers studied. Of course, one way to do this would be to determine the properties of the monomers (electronic transition magnitudes and directions, ring currents, etc.). Then with the proper theories we could relate these static properties and structural information to the properties of the dimers. However, these monomer properties are exceedingly difficult to obtain. Moreover, the existing theories, which utilize these properties in predicting the properties of dimers with given structures, would probably be insufficient in explaining measured differences in terms of structural differences.

Instead, I have chosen the alternative of studying the properties of the dimers as a function of the position of the stacking equilibria. Since we have seen this equilibrium to be temperature dependent, it is possible to extract relative thermodynamic parameters of the stacking interactions through the use of a model which describes this equilibrium. The simplest model that can describe the stacking equilibrium is the two-state model[72,95]. This is the model which I have

chosen to utilize.

II. The Two-State Model

This model consists of a dynamic equilibrium between an unstacked state and a stacked state which can be described by a single equilibrium constant (which is temperature dependent):

$$\text{Unstacked State (U)} \overset{K(T)}{\rightleftharpoons} \text{Stacked State (S)}$$

$$K(T) = [S]/[U] \qquad (1)$$

We can then define:

P_s = Property of the stacked state S

P_u = Property of the unstacked state U

Both of these we will assume to be temperature independent. Then the measured property at any temperature (P(T)) will be some combination of these properties, since the relative amounts of U and S will change with temperature:

$$P(T) = P_u(\text{fraction U}) + P_s(\text{fraction S}) \qquad (2)$$

$$= P_u([U]/([U]+[S])) + P_s([S]/([U]+[S])) \qquad (3)$$

It is known that the properties of dimers closely approach the sum of the properties of their component monomers when the stacking equilibria is sufficiently perturbed[72,95]. In this present study for instance, we have seen the hypochromicity, the CD differences, and the dimerization changes approach zero with increasing temperature (see Chapter 4, Tables II, III, V, VII). Also, the absorptions of ApA and Api^{6}A very closely approach their monomers' absorptions with the addition of ethanol (see Chapter 4, Figure 8). Likewise,

protonation of the bases tends to change the dimers' absorption almost completely to their monomers absorption (see Chapter 4, Section I E ii).

For these reasons, and since the monomers' properties have been subtracted from all of the dimers' measured properties, I have chosen the value zero for the property of the unstacked state, P_u. Then, using this assumption, and combining equations 1 and 3, we arrive at:

$$K(T) = [P(T)/(P_s - P(T))] \qquad (4)$$

Thus, we maesure P(T):

Absorption $\%h(\lambda)$

CD $(\varepsilon_L - \varepsilon_R)_{dimer} - \Sigma(\varepsilon_L - \varepsilon_R)_{monomers}$

NMR $\delta_{dimer} - \delta_{monomer}$; $J_{dimer} - J_{monomer}$

Unfortunately however, P_s is very difficult, if not impossible, to obtain experimentally. One can see from the Tables in Chapter 4 that none of the properties at the lowest temperatures have begun to even level out to some final value for a 100% stacked state. Some workers have used high salt concentrations in order to look at the very low temperature properties[70,92]. This type of experiment is not only difficult to perform, but seems undesirable in light of the possible effects of the high salt upon the stacking equilibrium[70,95].

What I have instead chosen to do is make one more assumption about the physical model such that I could arrive at a value for P_s via a data fitting procedure[104,70]. The idea is to assume that the $\Delta H°$ for the stacking equilibrium

is temperature independent. There is some basis for this in the literature[104,70].

Then, the van't Hoff equation applies

$$\ell n\ K(T) = -\Delta H°/(RT) + \Delta S°/R \qquad (5)$$

and ℓn K(T) vs. 1/T should yield a straight line. Thus, the criteria of fit will simply be to choose the value of P_s which when substituted into equation 4 will result in a set of K's which form the best straight line in a van't Hoff plot[104]:

1) Choose a value for P_s - Obtain K vs. T (equation 4).
2) Plot ℓn K vs. 1/T - Calculate least squares line and note least squares deviation.
3) Choose a new P_s.
4) Repeat steps 1 - 3 until minimize the deviation from the least squares line.

(Appendix 1 gives the Fortran program used to perform this type of fit. The deviation used was the average deviation from the least squares line of each of the ℓn K values, divided by the total Y range. This was done because the value chosen for P_s greatly affected the size of the Y range - see the program listing.)

From the straight line of best fit I obtained $\Delta H°$, $\Delta S°$, P_s and a calculated set of equilibrium constants $K_c(T)$ (these latter were calculated from the $\Delta H°$ and $\Delta S°$ values). Then we could obtain the actual calculated fit through the experimental data $P_c(T)$:

$$P_c(T) = [P_s \cdot K_c(T)/(1 + K_c(T)]$$

The listing for the Fortran programs used in calculating and plotting these fits is also shown in Appendix 1.

To summarize the two state analysis then, the assumptions are:

1) Only two states, which are in equilibrium with one another, are present.
2) The values of the properties of these two states are temperature independent - only the ratio of the states' populations change with temperature.
3) The unstacked dimers' properties are identical with the sum of the respective monomers' properties, and our choice of measured properties thus yields $P_u = 0.0$
4) The heat capacities of U and S are the same and hence $\Delta H^\circ \neq f(T)$.

The weaknesses of this approach will best be discussed after we have looked at the results obtained from its use (see the following chapters).

III. An Additional Analysis - The 3'-Endo Method

Another approach utilizing the two-state model has been used with the $J_{1',2'}$ coupling constants. In this case, the value for P_s was chosen from a consideration of x-ray data of stacked double strands, and NMR theory. It is known that the sugar conformation of monomers is an equilibrium between 2' and 3' endo[96,97]. Upon formation of a double stranded stacked helix, the sugar conformation changes

to essentially 100% 3' endo. This has been observed by x-ray[96]. In this sugar conformation, the vicinal angle between the 1' and 2' sugar protons is 90°. According to the modified Karplus equation[96], this will eliminate the coupling between these protons and hence $J_{1'2'} = 0.0$.

Thus for this model, we take as our fully stacked state the stacked conformation found in double stranded stacked helices. The geometry found for the sugar residues in this conformation, coupled with the pertinent NMR theory, leads to the value for the stacked state's coupling = 0.0. Once again, the unstacked state's properties are taken as equal to the monomers' properties. Then, we can define

A(T) = observed splitting in the dimer

B(T) = splitting of the monomer

X = fraction of stacked form = $\frac{[S]}{[U] + [S]}$

Then,

$$A(T) = X \cdot P_s + (1 - X)B(T) \qquad (6)$$

Combining equation 1 and 6 we arrive at

$$K(T) = [(B(T) - A(T))/A(T)] \qquad (7)$$

Using this equation, which relates only measured properties with the equilibrium constant, we can at every temperature obtain a K. From a least squares line of the ℓn K's vs. 1/T, I have arrived at a 'best' set of K's.

This method differs from that in section II of this chapter in that the value of P_s is obtained in a different manner. Thus, the assumption of $\Delta H°$ being independent of temperature did not have to be invoked in order to arrive

at P_s or the set of equilibrium constants (it was invoked to obtain the 'best' K's). Otherwise, the methods are identical in their basic assumptions.

IV. Summary

In this chapter I have described the analysis method used in treating the primary data. I have chosen the two-state model to simulate the dynamic stacking equilibrium. I did so in order that I could arrive at more meaningful comparisons of the stacking abilities of the various dimers than could be made simply by a study of the static properties of the dimers. This of course requires the use of a model, and I have in this chapter carefully pointed out the assumptions made in using the model, so that we will have a realistic view of the results obtained from its use. The next chapter describes these results.

Chapter 6 RESULTS

I. Introduction

II. Absorption Results

III. Circular Dichroism Results

IV. Proton Resonance Results

(A) Two-State Fitting Results

(B) 3'-Endo Method Results

Chapter 6

RESULTS

I. Introduction

This chapter is essentially only a tabulation of the 'thermodynamic' results obtained from the analyses of the primary data presented in Chapter 4. Also included are figures which illustrate some of the representative fits obtained. The next chapter will deal with the interpretations of the results presented here.

II. Absorption Results

The parameters obtained from the two-state model analysis of the percent hypochromicity vs. temperature data are presented in this section. Figure 1 illustrates typical types of plots generated in obtaining the best fit (ℓn K vs. 1/T). Figure 2 gives some examples of the actual data and the calculated curves fitted to the data points.

The fact that there exists a mathematically best fit is demonstrated in Figure 3. This figure illustrates examples of how the best fit was determined by minimizing the deviations from the least squares line (see Chapter 5). Care was always taken to check that there was only one minimum as a function of the P_s chosen.

Table 1 presents the absorption results. The interpretations of the various parameters will be discussed in the following chapter. The values for the probable lower

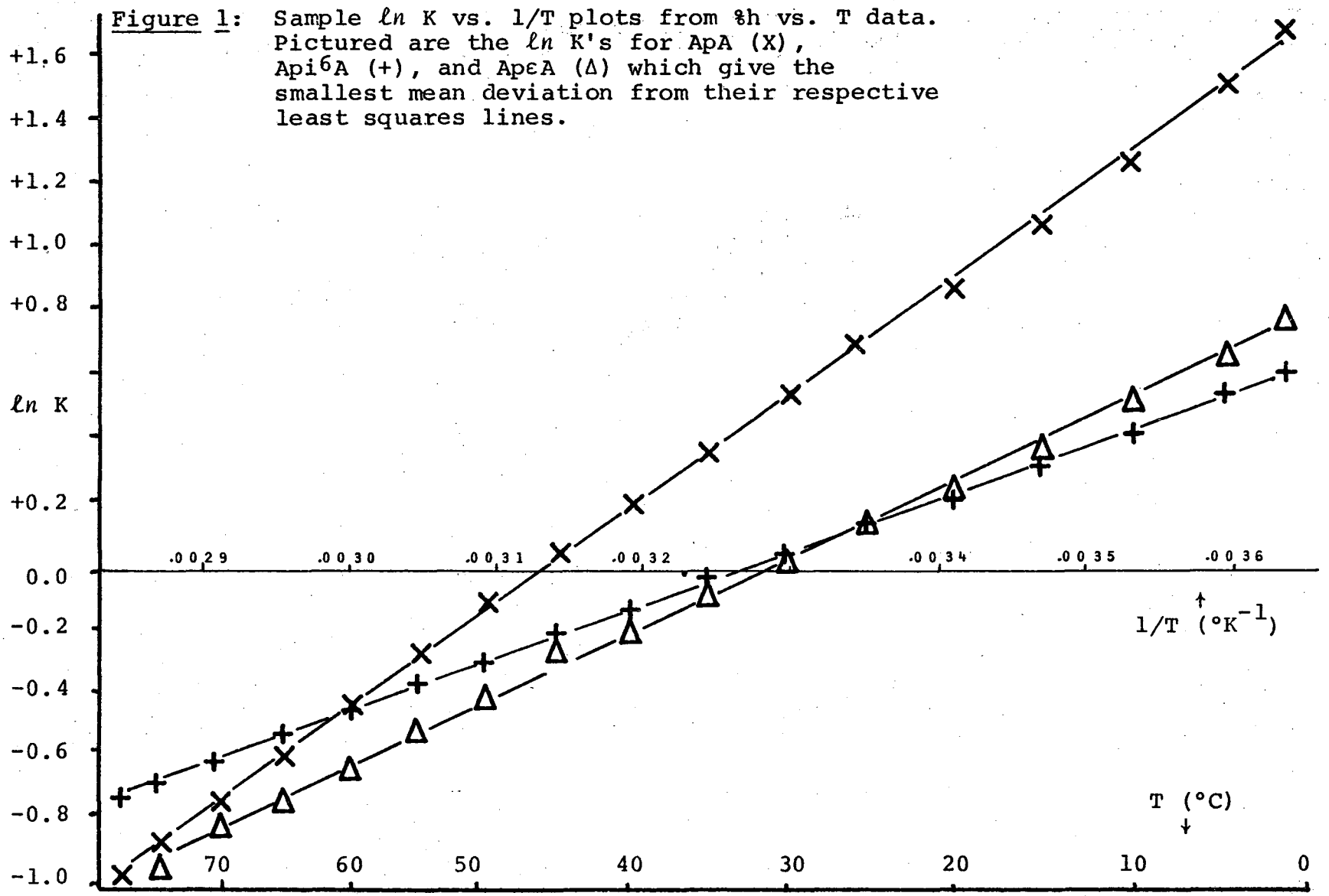

Figure 1: Sample ℓn K vs. 1/T plots from %h vs. T data. Pictured are the ℓn K's for ApA (X), Api^{6}A (+), and Apε A (Δ) which give the smallest mean deviation from their respective least squares lines.

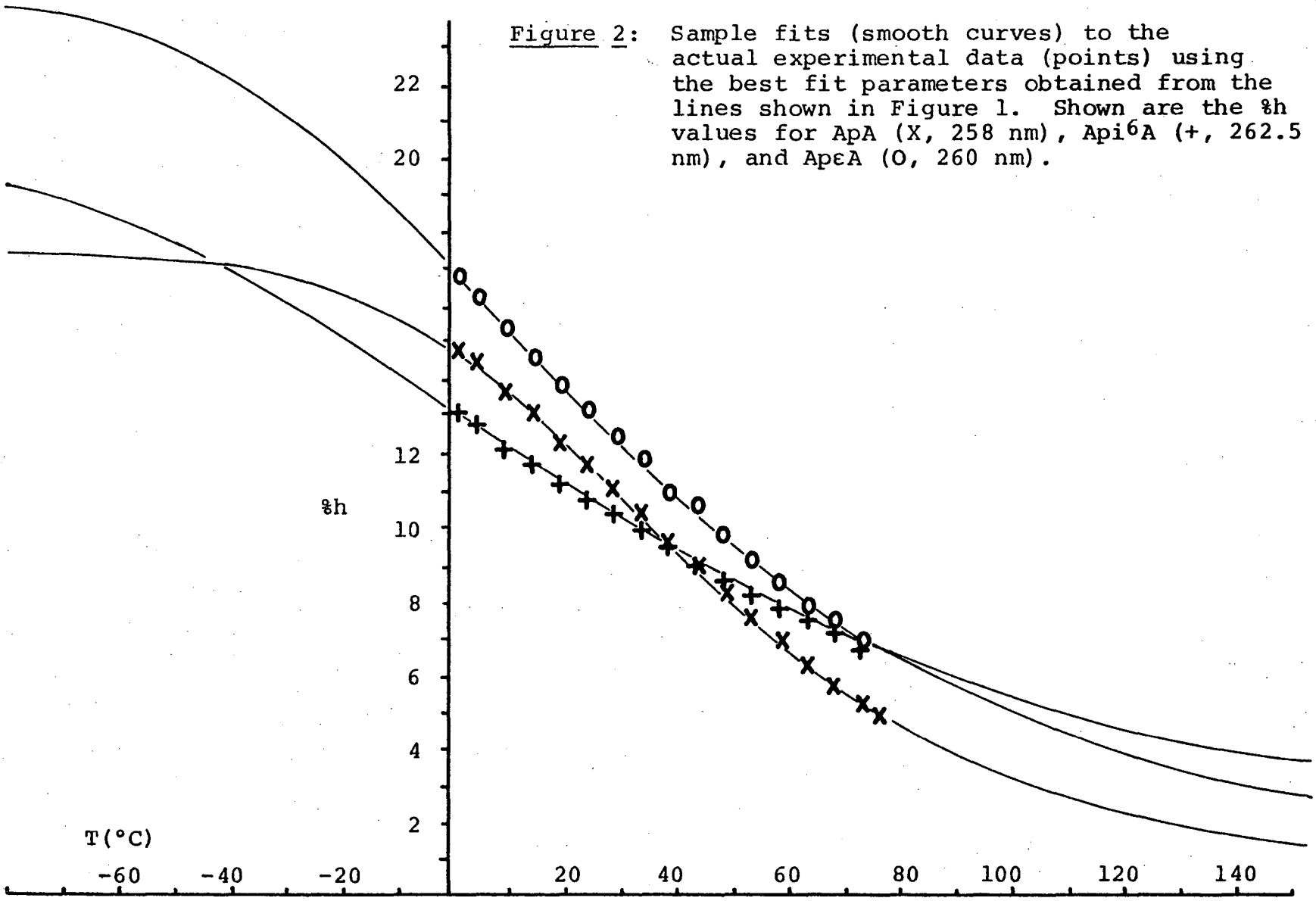

Figure 2: Sample fits (smooth curves) to the actual experimental data (points) using the best fit parameters obtained from the lines shown in Figure 1. Shown are the %h values for ApA (X, 258 nm), Api^{6}A (+, 262.5 nm), and ApεA (O, 260 nm).

Figure 3: Error from least squares line (ℓn K vs. 1/T - see Figure 1, and see Chapter 5 for definition of the error) as a function of the P_s value chosen. This, as in Figures 1 and 2, is for the %h vs. T data for ApA (——), Api^{6}A (····) and ApεA (- - -). Arrows point to the best $\%h_s$ values.

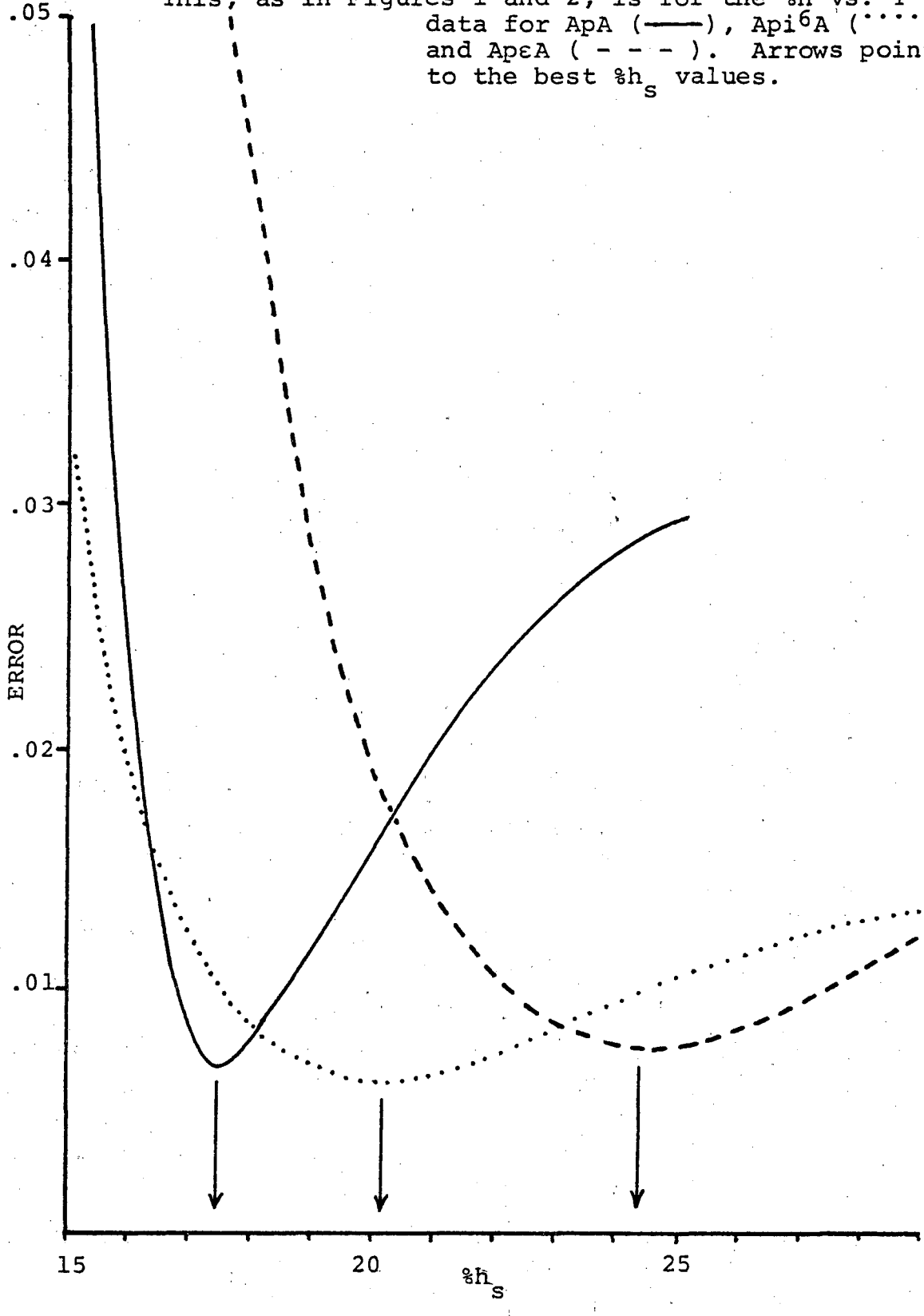

Table I. The results from absorption data (%h (λ) vs. T) for the two-state model. Listed are the best fit parameters obtained as described in Chapter 5. Listed in parentheses are the likely lower and upper limits for each value. These numbers were obtained as described in Appendix 2. They do not relate to the accuracy of the two-state model in describing the dimers' stacking.

Dimer	$\Delta H°$ (kcal/mole)	$\Delta S°$ (cal/°mole)	$K_{37°C}$	P_s ($\%h_s$)	Error * ($\times 10^2$)
ApA	-7 (-5,-9)	-20 (-17,-27)	1.4 (0.9,1.8)	18 (15,21)	0.7
Api^{6}A	-3 (-2,-5)	-11 (-9,-15)	0.9 (0.4,1.8)	20 (15,37)	0.6
Apms^{2}i^{6}A	-6 (-4,-9)	-18 (-10,-27)	2.9 (1.1,4.5)	10 (7,13)	0.7
ApεA	-4 (-3,-6)	-14 (-12,-20)	0.9 (0.5,1.3)	24 (18,36)	0.8
UpA	-2 (-2,-6)	-8 (-8,-17)	0.3 (0.1,2,8)	13 (4,25)	1.5
Upt^{6}A	-3 (-1,-5)	-8 (-6,-16)	1.4 (1.0,3.9)	18 (12,37)	1.6
CpA	-6 (-4,-10)	-19 (-14,-30)	0.9 (0.6,1.9)	12 (9,19)	1.4

* Error = error in best fit, defined in program (see Appendix 1 and Chapter 5) as the mean deviation of all of the points from the least squares line, divided by the total range of the ordinate.

and upper limits (shown in parentheses) were obtained via a detailed graphical analysis which is discussed in Appendix 2. They do not represent any error inherent in the choice of the two-state model itself.

III. Circular Dichroism Results

Parameters from the two-state model analysis of the data for ApA, Api^{6}A, Apms^{2}i^{6}A, and ApεA are presented here. Unfortunately, because of the small CD magnitudes observed for UpA and Upt^{6}A and the small changes in these magnitudes with temperature variation, their CD melting curves could not be fit using this method (i.e. no minimum in the Error vs. P_s plot could be obtained).

Figure 4 illustrates some typical best fits to the actual experimental data. Table II presents the results along with probable lower and upper limits (again see Appendix 2).

IV. Proton Magnetic Resonance Results

(A) Two-State Fitting Results

It is possible to obtain minima in the Error vs. P_s curves for many of the protons for the various dimers. However, many of the protons exhibited such small dimerization changes or small changes with temperature variation, that no minima could be obtained. These latter include most of the protons of Apms^{2}i^{6}A, UpA, and Upt^{6}A. Even those protons whose changes could be fit exhibited large fitting

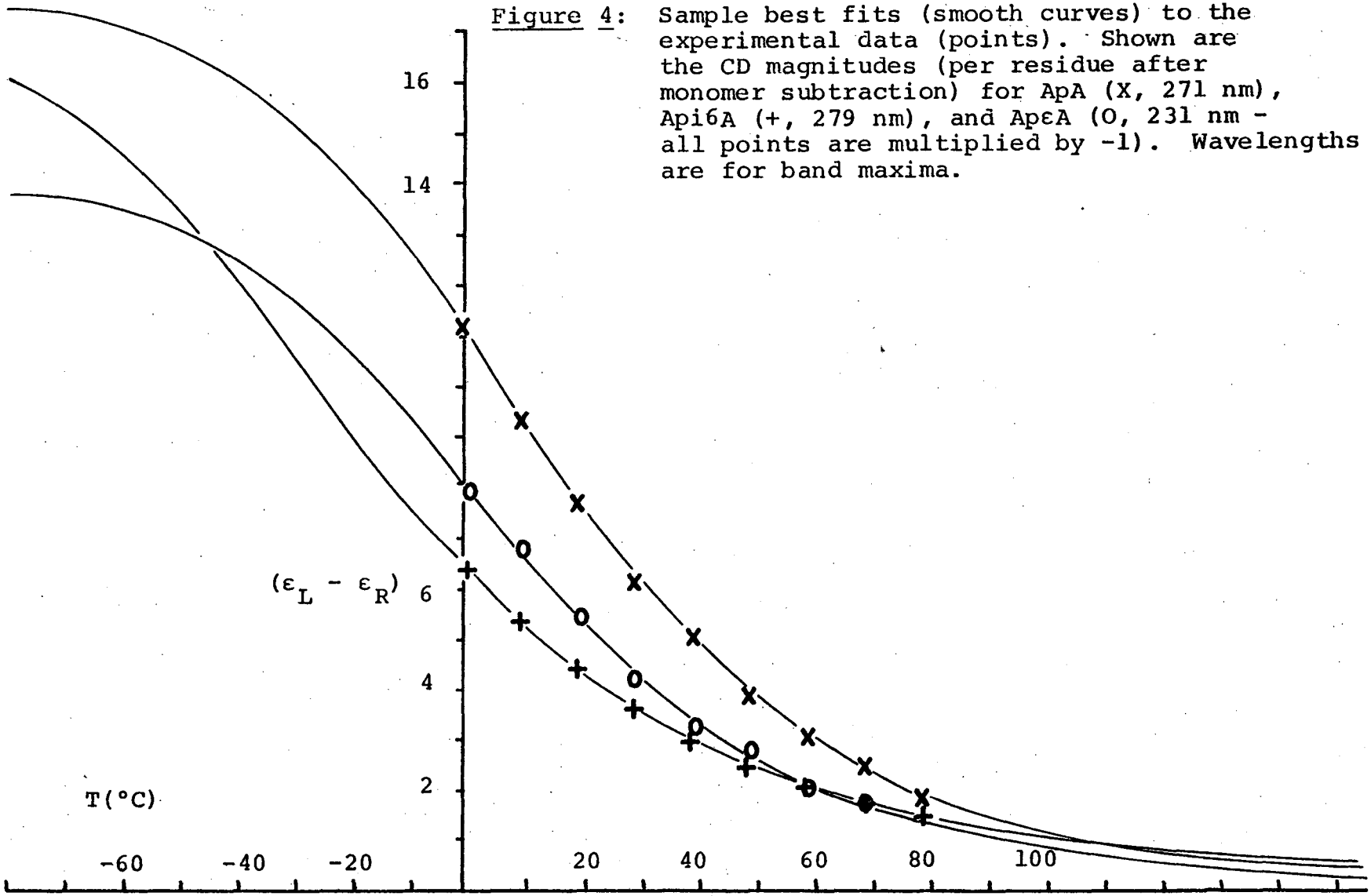

Figure 4: Sample best fits (smooth curves) to the experimental data (points). Shown are the CD magnitudes (per residue after monomer subtraction) for ApA (X, 271 nm), Api6A (+, 279 nm), and ApεA (O, 231 nm - all points are multiplied by -1). Wavelengths are for band maxima.

Table II. The results from the CD data (Chapter 4, Table III) for the two-state model. Listed are the best fit parameters obtained as described in Chapter 5. Also listed in parentheses are the probable lower and upper limits for each parameter (see Appendix 2).

Dimer	$\Delta H°$ (kcal/mole)	$\Delta S°$ (cal/°mole)	$K_{37°C}$	P_s $(\Delta\varepsilon_s)$	Error * $(x10^2)$
ApA	-6.5 (-6,-7.5)	-23 (-21,-25)	0.4 (0.3,0.6)	17 (14,20)	0.7
Api^6A	-4.5 (-4,-5.5)	-18 (-17,-20)	0.2 (0.1,0.5)	17 (10,30)	0.4
$Apms^2i^6A$	-5 (-3,-9)	-16 (-9,-25)	2.4 (0.7,4.0)	-7 (-6,-11)	2.8
Apε A	-6 (-5,-7)	-22 (-20,-25)	0.4 (0.2,0.5)	-14 (-11,-21)	1.4

* Error = error in best fit, defined in program (see Chapter 5 and Appendix 1) as the mean deviation of all of the points from the least squares line, divided by the total range of the ordinate.

errors compared with those of absorption or CD fits. The protons of ApεA were not fit because of an insufficient number of data points with temperature.

The results from the analyses of the proton changes that were fit are given in Table III. The likely errors in the parameters are listed for a few cases of the data which gave better fits. The reader is referred to Appendix 2 for a short discussion of the error analysis of the NMR data.

(B) 3'Endo Method Results

Presented here are the results of the 3'-Endo method of analysis of the $J_{1'2'}$ coupling constants. This method has not been applied to the 3' Up residues of UpA or $Upt^{6}A^{97}$. The results are listed in Table IV. Figure 5 illustrates some of the van't Hoff plots used to arrive at the 'best' parameters in Table IV.

Table III. The results from the two-state fitting of the NMR data. Listed are the best fit parameters obtained as described in Chapter 5, Section II. The reader is referred to Appendix 2 for a brief description of the probable errors in the parameters listed.

Dimer	ΔH° (kcal/mole)	ΔS° (cal/°mole)	$K_{37°C}$	P_s	Error * ($x10^2$)
ApA					
H2Ap	-3 ± 2	-13 ± 5	0.3 (0.1,1.0)	0.9 ± 0.8	1.7
H8pA	-6 ± 2	-20 ± 6	1.4 (0.6,2.2)	0.3 ± 0.2	3.0
H1'Ap	-2	-9	0.3	1.0	3.7
H2pA	-3	-12	0.8	0.2	4.4
H1'pA	-5	-16	0.6	0.4	4.9
$\Delta J_{1',2'}$,Ap	-3 ± 2	-13 ± 5	0.5 (0.2,1.6)	8 ± 8	1.0
$\Delta J_{1',2'}$,pA	-5	-19	0.2	10	5.4
Api^{6}A					
H2Ap	-3 ± 2	-12 ± 2	0.4 (0.1,1.0)	0.7 ± 0.8	2.3
H2pi^{6}A	-4	-13	0.7	0.3	2.8
H8pi^{6}A	-3 ±2	-11 ± 3	0.9 (0.1,1.8)	0.4 ± 0.8	2.9
H1'Ap	-5	-14	4.2	0.4	5.4
H1'pi^{6}A	-2	-11	0.2	0.8	8.1
$\Delta J_{1',2'}$,pi^{6}A	-8	-24	2.3	2	4.7
$\Delta J_{1',2'}$,Ap	-7	-21	1.1	4	4.6

Table III. (Continued)

Dimer	ΔH° (kcal/mole)	ΔS° (cal/°mole)	$K_{37°C}$	P_s	Error * ($x10^2$)
Apms^{2}i^{6}A					
H8pms^{2}i^{6}A	-5	-16	2.6	0.3	3.9
UpA					
H1'Up	-4	-13	0.7	0.5	2.2
Upt^{6}A					
H1'Up	-4	-14	0.9	0.4	2.0
H6Up	-3	-8	2.5	0.2	6.8
$\Delta J_{1',2'}$pt^{6}A	-2	-11	0.1	9	7.8

* Error = error in best fit, defined in program (see Chapter 5 and Appendix 1) as the mean deviation of all of the points from the least squares line, divided by the total range of the ordinate.

Table IV. Results from the 3'-Endo Method. See Appendix 2 for a discussion of the K ± values. They do not include uncertainty due to the choice of the model.

Dimer	ΔH° (kcal/mole)	ΔS° (cal/°mole)	$K_{37°C}$ (±0.08)
3' Residues			
ApA (Ap)	-3.5	-12	0.71
Api^{6}A (Ap)	-3.0	-11	0.45
Apms^{2}i^{6}A (Ap)	-7.5	-29	0.10
Apε A (Ap)	-7.5	-27	0.22
5' Residues			
ApA (pA)	-5.5	-20	0.38
Api^{6}A (pi^{6}A)	-2.9	-12	0.30
Apms^{2}i^{6}A (pms^{2}i^{6}A)	-2.2	-10	0.24
Apε A (pε A)	-3.9	-15	0.31
UpA (pA)	-4.4	-18	0.17
Upt^{6}A (pt^{6}A)	-2.3	-11	0.22

Figure 5: Van't Hoff plots of ℓn K's derived from the 3'-Endo method. The lines are the least squares lines for ApA (Ap, ——), and Api^{6}A (Ap, - - -). See Appendix 2 for derivation of error bars.

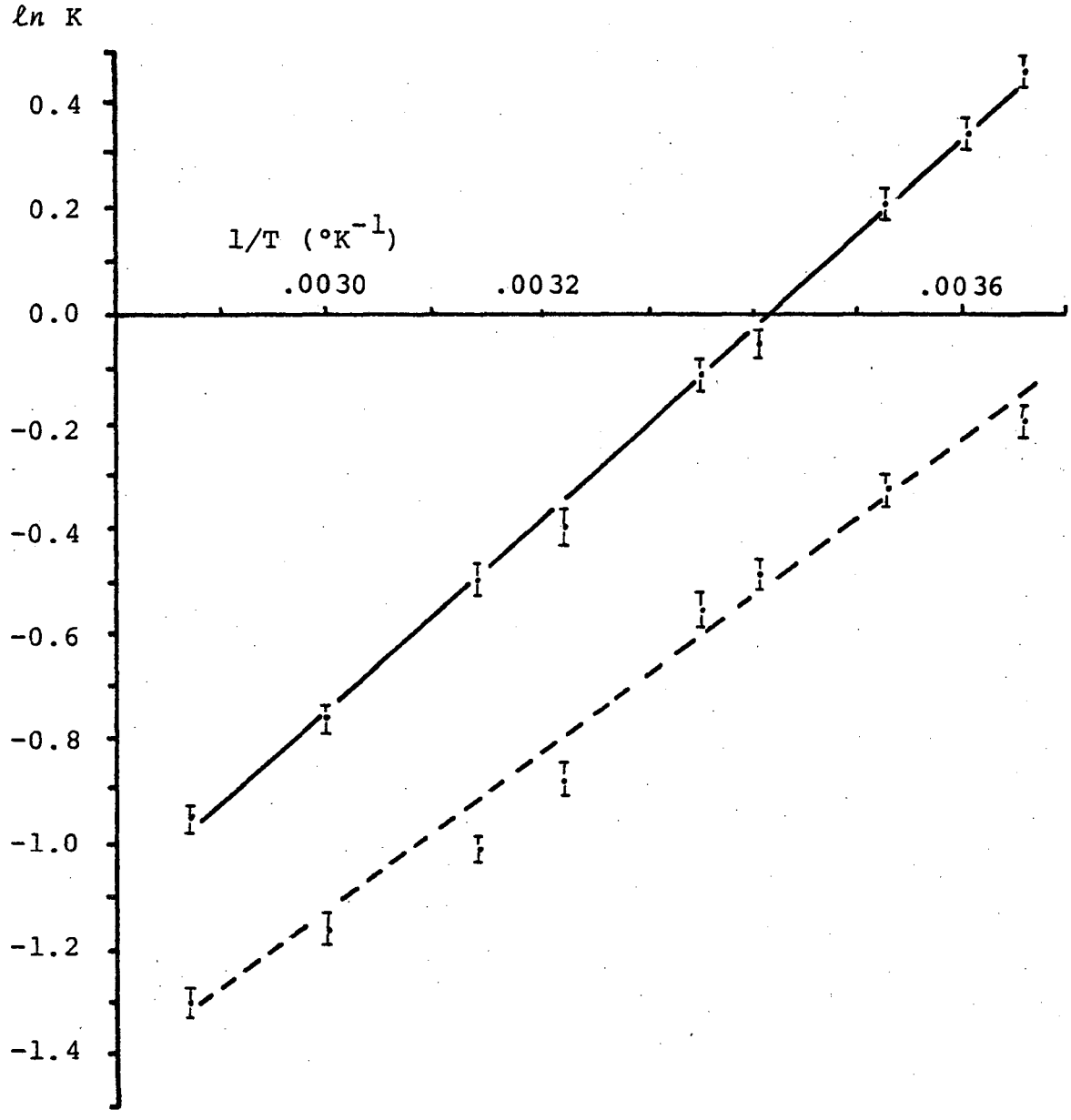

Chapter 7 DISCUSSION

I. Dynamic Stacking

(A) Literature Comparison

(B) The Property of the Stacked State, P_s

(C) $\Delta H°$ and $\Delta S°$

(D) Two-State Stacking Equilibrium Constants

(i) Differences in K's Between Dimers

(ii) Differences in the K's Between Techniques

(iii) Trends in the Equilibrium Constants

(E) Deficiencies of the Two-State Model

(F) Errors

(G) Summary of the Dynamic Stacking

II. Static Properties

(A) Monomer Properties

(B) Dimer Properties

(i) Absorption

(ii) CD

(iii) NMR

a) Api^6A

b) $Apms^2i^6A$

c) $Ap\varepsilon A$

d) Upt^6A

(C) Summary of the Static Properties

III. Summary

Chapter 7

DISCUSSION

I. Dynamic Stacking

(A) Literature Comparison

Before discussing the stacking properties of the molecules studied in this thesis, it is necessary to compare the results obtained herein to those reported in the literature. No reports have been made of the dynamic stacking properties of any dinucleotide containing hypermodifications. However, numerous studies have been made of the unmodified dimers, ApA and UpA. Table 1 summarizes the pertinent thermodynamic parameters obtained for these dimers (most arrived at via a two-state model analysis of some sort).

That this is not a very useful comparison is rather obvious when one notices the large variations in the values from one author to the next, and from one property to the next. There is essentially no comparison to make with the NMR data. The authors reporting the -11 kcal/mole for $\Delta H°^{99}$, obtained the value from a very questionable 'sigmoidal' dimerization shift vs. temperature curve. Of all the dimerization shift curves of the various protons of the numerous dimers studied here, sigmoidal curves were never observed. The analysis of their data naturally yielded high $\Delta H°$ values.

The absorption and CD (or ORD) literature values offer a better, but still not a very useful comparison. With the absorption of ApA, the $\Delta H°$'s vary as might be expected from

Table I. Literature Comparison. Thermodynamic parameters for models describing the stacking equilibrium of ApA and UpA. Most authors have utilized a two-state model in arriving at these values.

Dimer	Property	ΔH°	ΔS°	$K_{37°C}$	Reference
ApA					
	Absorption	-7	-20	1.4	This Work
	Absorption	-8.5	-28	0.7	70,92
	Absorption	-9.4	-29	1.9	105
	Absorption	-10.2	-33	0.9	106
	CD	-6.5	-23	0.4	This Work
	CD	-8.5	-30	0.3	107
	ORD	-8.0	-28	0.3	108
	ORD	-5.3	-20	0.2	70,92
	NMR(H2Apδ$_{TSP}$)	-3	-13	0.3	This Work
	NMR(H2Apδ$_{TSP}$)	-11	---	---	99
	NMR(all dimerization changes)	-2→-6	-9→-20	0.2→1.4	This Work
	NMR(3'-Endo Method)				
	Ap	-3.5	-12	0.71	This Work
	pA	-5.5	-20	0.38	This Work
	Absorption Titration	---	---	5.0	71
	Calorimetry	-3.4	---	---	109
UpA					
	Absorption	-2	-8	0.3	This Work
	ORD	-5.1	-21	0.10	70,92
	NMR(H1'Upδ$_{TSP}$)	-4	-13	0.7	This Work
	NMR(3'-Endo Method)				
	pA	-4.4	-18	0.17	This Work
	Absorption Titration	---	---	0.00	71

the error analysis presented here. The same is true with the $\Delta S°$ values. In general, the $K_{37°C}$'s don't show as much scatter as the $\Delta H°$'s or $\Delta S°$'s. The value obtained here is in the range of those found by others, within the error limits reported here. The same story is true of the CD and ORD data. The $K_{37°C}$'s in these cases however are actually rather close.

An interesting trend in the literature that seems to be rather constant is that the K's from the absorption are generally higher than those from the CD. The data in this thesis also bear this out.

Thus in light of the variation found by the different authors, let it suffice to say that the values obtained in this thesis fall within experimental error of those in the literature. This is not a good confimation of the data, considering the size of the experimental errors reported here and the scatter found in the literature.

(B) The Property of the Stacked State, P_s

Aside from the choice of the two-state model, the major difficulty in arriving at thermodynamic parameters is in the attainment of values of P_s. Since this property has not been measured for the two-state fits, one can attempt to ascertain that the value obtained from the fit is physically reasonable. This of course is not easy, or we would simply have chosen a P_s from physical intuition. However, some things can be said about the possible values, and about the

trend of P_s values from one molecule to the next.

For the absorption, one might expect the %h of the stacked state of the dimer to approach that of a longer polymer, in which the stacking is believed to be greater at measurable temperatures. High molecular weight poly A is believed to be almost fully stacked near zero degrees[105,110]. Its %h at 0°C at 257 nm was found to be between ∿25 - 35%[105,110]. The $\%h_s$ determined in this thesis for ApA was 18%. Since the hypochromism is chain length dependent, this roughly corresponds to a %h for an infinite polymer of A to be (assuming nearest neighbor interactions only)[72]

$$H(n) = [(n - 1)/n]\ H(\infty)$$

$$\%h(\text{dimer, } n=2) = 1/2\ \%h(\text{infinite polymer, } n=\infty)$$

$$\text{or} \quad \%h(\text{poly A}) = 2 \times 18 = 36\%$$

Thus, the $\%h_s$ found for ApA is certainly reasonable. No such data have been obtained for polymers containing the other dimers.

However, the theory of hypochromism can be used to deduce how changes in the monomers' properties will affect the %H (or %h). Assuming that a set of dimers have identical geometries in the stacked state and identical monomer transition directions, the dimer which contains a monomer having higher extinction coefficients in its UV bands will have the higher %h[72]. In the case of the hypermodifications of A, the monomers extinctions are generally significantly larger than those of A's. If the UV bands are indeed an indication of the sizes of the bands at the lower λ's (whose interactions

with the 260 transitions greatly influence the %h), then one could on the basis of these assumptions expect dimers containing them to exhibit larger %h's than their unmodified counterparts. In fact, this is found to be the case with Api^{6}A, ApϵA, and Upt^{6}A (see Table I, Chapter 6). It is not the case with Apms^{2}i^{6}A, and one might well wonder if a value of ~10% for its $\%h_s$ is physically reasonable.

A check of the P_s values for the CD band maxima is more complicated. CD bands can superimpose onto one another and often cancel each other. The band shapes and sizes are thus dependent not only upon the stacking, but also upon the sequence and the monomers' properties. It happens that 3 of the 4 dimers studied (ApA, Api^{6}A and ApϵA) show similar P_s magnitudes while that of Apms^{2}i^{6}A is smaller than the rest (as was the the case with the absorption). However, it is difficult to argue over the significance of this because of the factors already mentioned.

Using a simple nearest neighbor approach, the $\Delta\epsilon_s$ for ApA of 17 translates into a $\Delta\epsilon \simeq 35$ for a poly A 100 units in length. Poly A at 0°C gives a $\Delta\epsilon \simeq 23$[111]. It is not known whether this difference is significant.

Values for dimerization shifts of fully stacked states can be derived from calculations of ring current fields[112]. Of course this requires a knowledge of the geometry, and moreover, the theoretical values of the ring currents tend to change with time[112,113]. If we assume that the base adjacent to an A approaches within van der Waals radii of

that A, and that a proton on that base falls in the region of highest ring current, then its $\Delta\delta_{TSP}$ could be no greater than 1.6 ppm. This is rather high, and it is not surprising that all of the P_s's found for $\Delta\delta_{TSP}$'s fall within that limit. The dimerization changes in the $J_{1',2'}$ coupling constants are expected to be approximately that of the monomers at low temperature for the fully stacked dimer (This is because the fully stacked dimer will exhibit essentially no coupling in its pure 3'-Endo state, as described in Chapter 5.). There is somewhat of a scatter of these P_s values. pA of Upt^{6}A and ApA give high values while Ap of Api^{6}A gives a low value. The derived K's may thus be in question.

Thus in summary, the P_s values arrived at by the fitting procedures appear for the most part to be physically reasonable. However, for the variation which could be allowed in the P_s values and still be considered 'reasonable', the scatter in the resultant fit parameters is high. This section has contained only some necessary checks upon the P_s values, and does not constitute a sufficient verification.

(C) $\Delta H°$ and $\Delta S°$

In order to arrive at two-state equilibrium constants, the stacking equilibria have been studied as a function of temperature. This then also yields values for the standard changes in the enthalpy ($\Delta H°$) and entropy ($\Delta S°$). Since stacking is mainly caused by attractive forces[94], it has often been described in terms of its ΔH[94]. However, mostly

because of our lack of knowledge of the role of the solvent (H_2O) in stacking, it is very difficult to interpret the counterbalancing effects of the ΔH or ΔS in terms of molecular models.

It is interesting to note however, that with few exceptions the hypermodified counterparts of ApA have been found here to have less favorable enthalpic contributions relative to ApA. That their free energies are not widely different from ApA's is a result of a more favorable entropic contribution in each case. (The exceptions are results for Apms^{2}i^{6}A and ApεA from the 3'-Endo analysis of their Ap residues). It is evident that these trends are difficult to interpret in terms of the properties of the additional side chains when one considers the available data on monomer interactions. For instance, methylation of the base moiety of nucleosides generally increases the favorable enthalpic contribution to the stacking[94]. This is in direct contrast to what is found here for the hypermodifications if they were to be considered simply as 'methylations'. Changes in the entropic contributions are even more difficult to interpret[72, 94]. It is also difficult to assess the effects upon the ΔH or ΔS of the hypermodifications when one considers both the stacked state and the unstacked state.

Unfortunately because of the large experimental errors in both the $\Delta H°$'s and $\Delta S°$'s (not to mention the uncertainty due to the choice of the two-state model), this discussion may be academic. In fact, the experimental error alone in

almost all cases allows an overlap of the values of $\Delta H°$ and $\Delta S°$ for ApA and its hypermodified dimers. Thus, within experimental error these parameters could be equal for all of the dimers. Also, although the mentioned trends are the same from one technique to the next, the absolute values of the $\Delta H°$'s and $\Delta S°$'s are in general different for the absorption, CD or NMR results.

(D) Two-State Stacking Equilibrium Constants

Because of the difficulty in interpreting changes in the separate contributions to the free energies, the remainder of the discussion of the dynamic stacking abilities will be centered about the equilibrium constants. This is also advantageous in light of the experimental errors in the K's relative to those in the $\Delta H°$'s and $\Delta S°$'s. Because of the restrictions put on the parameters as a result of the experimental curve shapes, the errors listed for the $\Delta H°$'s and $\Delta S°$'s do not propagate into the K's. Thus, it is generally found that when the $\Delta H°$ becomes less favorable the $\Delta S°$ will somewhat compensate and become more favorable. The limits tabulated for the K's in Chapter 6 were derived from the curve shape errors described in Appendix 2, and not from a propagation of the total separate errors possible in the $\Delta H°$'s or $\Delta S°$'s.

(i) Differences in K's Between Dimers

I have mentioned that the absolute values of the equi-

librium constants fall within ranges found by others in the literature. Of more interest for this study are the differences between the K's for the various dimers.

In fact, the most important finding in this dissertation is that the dimers containing hypermodifications do have different stacking equilibrium constants than their unmodified counterparts. Thus even on the small scale of the dimer, hypermodification appears to affect the physical interactions between the neighboring residues. As a first step then, the design of the dimer approach is sound for the study of the role of hypermodifications.

The conclusion that the dimers exhibit different stacking abilities is of course subject to the assumptions made in arriving at the K's (two-state model, P_s, etc.), as well as to the experimental errors. The effects upon the K's of the choice of the model are difficult to assess in terms of ± values. Indeed, a simple equilibrium constant may not be justifiable if more than two states are involved in the stacking. And although the experimental errors are less than those in the enthalpy and entropy, there is enough overlap between the ranges of the K's that the equilibria could be the same regardless of the extent of hypermodification. However, because of certain trends in the 'best' K's that emerge from all of the properties monitored, I will discuss these best values in relation to the affect of hypermodification upon dimer stacking. This data set taken as a whole strongly indicate that the dimers containing hypermodifi-

cations exhibit different stacking properties than the unmodified dimers.

(ii) Differences in the K's Between Techniques

Aside from the differences in the K's amoung the dimers, the next most obvious observation of the results in Chapter 6 is that the K's for a <u>given</u> dimer are different from technique to technique. Hence, one notices different K's for ApA from the absorption (1.4), the CD (0.4), and the NMR (0.7, 3'-Endo). Even within the realms of one technique, NMR, there is a variance of K's depending upon the particular dimerization change (proton shift or coupling constant) monitored (0.2 - 1.4).

It is possible that in some of these cases, the discrepancies can be explained by experimental error. However, because of the general lack of agreement in the best values for the various dimers from technique to technique, it is believed that the discrepancy is the result of the choice of the two-state model. This is also suspected because of the trends in the K's from technique to technique. The K's from absorption tend to be generally higher than those found by CD or NMR (3'-Endo).

(iii) Trends in the Equilibrium Constants

With only a few exceptions, certain trends are evident from technique to technique in the K's for ApA, Api^{6}A, Apms^{2}i^{6}A and ApεA. It appears from the best K's in Tables

I, II and IV that these hypermodifications slightly decrease the stacking ability relative to ApA. The notable exceptions to this are the rather abnormally high K's found for $Apms^2i^6A$ with absorption (2.9) and CD (2.4). It was mentioned in section I B that the P_s values for this dimer with CD and absorption could possibly be unreasonable, this possibility being very likely for the $\%h_s$. Even without invoking this question, the experimental errors found with the K's for $Apms^2i^6A$ were generally large ($\sim\pm 1.7$ for both the absorption and the CD). This is a result of the fact that the properties monitored for $Apms^2i^6A$ generally showed small changes with temperature relative to the changes observed for the other dimers (see Tables II and II in Chapter 4). This is also evidenced in the large fitting error for the $Apms^2i^6A$ CD data (0.028). The small changes with temperature might lead one to suspect a lower $\Delta H°$, but the P_s values obtained from the fits yield relatively high $\Delta H°$ values. If one quite arbitrarily picks values of P_s close to those found with the other dimers (18 - 24 for $\%h_s$, 14 - 17 for $\Delta\varepsilon_s$ - this is admittedly dangerous with the CD) then values for the K's obtained with both the absorption and the CD are less than that for ApA. Considering the large experimental errors in the K's of $Apms^2i^6A$, the large CD fitting error, and the possibility of unreasonable P_s values, it is easily conceivable that the actual data are consistent with the trend of lower stacking stabilities with the extent of hypermodification. Certainly the 3'-Endo results of $Apms^2i^6A$

are consistent with this trend.

Because of the large variation between the K's for the various protons of a given dimer, it is impossible to judge whether the dimerization change fits agree with this trend (Table III, Chapter 6). Also, large fitting errors relative to the absorption or CD fits were observed with almost all protons. Likewise, for a given proton (even those with the better fitting errors) the ± values for the K's are large. Even if one compares corresponding protons from ApA to Api^{6}A, no consistent trend is observed:

Proton	$K_{37°C}$(ApA)		$K_{37°C}$(Api^{6}A)
H2Ap	0.3	<	0.4
H2pA (pi^{6}A)	0.8	>	0.7
H8pA (pi^{6}A)	1.4	>	0.9
H1'Ap	0.3	<	4.2
H1'pA (pi^{6}A)	0.6	>	0.2

All this stems from the fact that the changes from the extremes of the temperature range were generally no more than only ∿0.15 ppm and often only 0.1 ppm or less. Thus, the dimerization changes unfortunately cannot be taken as either supporting or conflicting evidence for the trend mentioned above.

The other important trend to be noticed in Tables I, III and IV is the fact that with all the techniques used, Upt^{6}A appears to be stabilized relative to UpA. The absorption yields a large difference in the K's (1.4 vs. 0.3) while the NMR shows a smaller but consistent difference (0.22 vs. 0.17,

3'-Endo). The H1'Up dimerization change fit also yields the same trend (0.9 vs. 0.7), but is unreliable considering the discussion above.

The results taken together indicate that i^6A, ms^2i^6A and ϵA destabilize the stacking of ApA, while t^6A stabilizes the stacking of UpA. The fact that these trends appear in all of the techniques used adds weight to their validity.

(E) Deficiencies of the Two-State Model

There is a large body of literature dealing with the two-state model and its use in describing dimer stacking equilibria (see references 72,95 and references therein). The basic arguement against the use of the two-state model for this system is that different thermodynamic parameters are obtained for different properties monitored. It is my opinion after conducting these experiments, analyses and error analyses, that disagreement between parameters from different authors using different techniques is not a sufficient arguement against the validity of the two-state model. I have shown in Appendix 2 that simply experimental and fitting errors can account for large variances in the thermodynamic parameters. Thus, differences in experimental techniques and analysis procedures could possible explain many of the differences found in the literature.

However, I have presented in this thesis parameters obtained from absorption, CD and NMR utilizing the same analysis technique. I have found with several dimers that

the parameters obtained with the different methods are not equivalent. In fact, even certain trends are followed in the differences (absorption K's > CD or NMR K's). Thus, as the previous literature has time and again suggested, the work presented here indicates that more than two states are involved in the dimer stacking.

More recently, static NMR measurements have been interpreted in terms of a stacking equilibrium involving more than one stable stacked state[97,98].

In light of all this, it is somewhat surprising that clean isosbestic points were obtained in the CD melting curves (e.g. see Figure 15, Chapter 4). These isosbestic points were observed for all of the dimers studied by CD. This type of observation has been studied by Powell et al.[114] for absorption and CD of ApA and CpC. These authors conclude that for optical data, thermodynamic parameters can be obtained from a two-state model. They state that if there are more than 2 states, the "intermediates between the stacked and unstacked forms do not have recognizable identities in terms of spectroscopic properties". It is possible that there exists a set of stacked states which exhibit indistinguishable absorptions. Likewise there may be a set of states with similar CD spectra. That these two sets of states might not overlap would be conceivable when one considers the different geometry dependences of the absorption and CD[72,92]. The absorption tends to be less geometry dependent, and depends more on simply the distance between the

bases than does the CD. Perhaps this is why the CD appears to 'melt' out with increasing temperature before the absorption does ($K_{abs.} > K_{CD}$ in general). NMR, with its probes (protons) on various portions of the dimer, may be more sensitive to the nature of the stacked states[97,95]. This could explain the differences between results from different protons. Each proton may 'melt' away in a different fashion.

Thus, it is clear that there exist more than two states for the dimer stacking. It is not clear whether the use of a two-state model is a valid means of obtaining thermodynamic parameters from temperature data. Ts'o[95] points out that it is not a bad approximation to use for optical spectroscopy, while obtaining overall thermodynamics for the stacking from NMR fit procedure is not valid.

The 3'-Endo method is also a two-state model, and is a specific probe on only one portion of the dimer. From the above discussion, the results from the 3'-Endo method probably do not reflect how the dimer melts - only the sugar region. However, if we are only to compare that region from dimer to dimer (and not from property to property), then the trends obtained in the parameters may very well describe the trends in the 'overall' stacking of the different dimers. It is of interest to note that the parameters from the 3'-Endo analysis of the Ap residue of ApA agree quite well with the fit parameters from the dimerization change $\Delta J_{1',2'}$,Ap (which has the smallest fit error - 0.010):

ApA	$\Delta H°$	$\Delta S°$	$K_{37°C}$	Table (Ch.6)
3'-Endo (Ap)	-3.5	-12	0.71	IV
$\Delta J_{1',2'}$ (Ap) (fit)	-3	-13	0.5	III

(The differences in the two analyses is in the choice of P_s and the assumption of $\Delta H \neq f(T)$ - see Chapter 5.)

The other major assumption used in fitting the data to the two-state model is that $\Delta H°$ must be independent of temperature. Aside from the rationale given in Chapter 5, Figure 5 in Chapter 6 presents data which supports this. The ℓn K's from the 3'-Endo method (which places no restrictions upon $\Delta H°$) plotted vs. 1/T give very reasonable straight lines.

In conclusion of this discussion, although there are difficulties in using the two-state model to analyze the data, it is worth while to use in obtaining relative thermodynamic parameters. One should not expect the values to be consistent from technique to technique. For a series of dimers however, the two-state model when applied to a single property should yield meaningful relative stabilities. Thus, it should be useful in attempting to learn of differences in stacking abilities - not absolute stacking abilities.

(F) Errors

The errors for a set of K's derived from a single property should then arise mostly from experimental and calculational errors - not, as was discussed above, the choice

of the model (i.e. the error of the absolute values of the K's will of course include the error due to the choice of the model - the error of the 'relative' K's should not). However as we have seen, even the experimental and fitting errors are substantial. This is the reason for the importance of monitoring several different properties.

Some of the properties measured have shown smaller errors than others. This can be seen first of all by the fitting error of the best fit (last column of Tables I, II and III, Chapter 6). Those curves yielding larger fit errors generally gave higher errors in the final parameters. With the absorption the error ranged from 0.006 to 0.016. The CD fit errors ranged from 0.004 to 0.028. The NMR fit errors ranged from 0.010 to 0.078. The relative confidence that one places in the values obtained from the fits should be based upon these relative error magnitudes. Absorption (with the most data points) is probably safer than CD, with both of these being much more reliable than the NMR fits.

The 3'-Endo method is however an altogether different approach to the NMR, and the relative confidence level is not clear. In Table IV though, the same types of trends in stability are observed for both the Ap and pA (pA*) residues (ApA being more stable than its hypermodified counterparts). Also the agreement with the good $\Delta J_{1',2'}$,Ap fit (fit error = 0.010) is also encouraging. Finally, assuming that the model is correct, the experimental propagated error in the K's is small.

(G) Summary of the Dynamic Stacking

In this section I have presented the major findings of this dissertation. It has been pointed out that the results obtained generally agree with those thermodynamic values reported in the literature. It is important to remember in this regard that an agreement with literature values is probably only a necessary criteria for the validity of the values, and does not constitute a sufficient check upon the parameters.

I have discussed the values arrived at for the properties of the stacked states and have concluded that in most cases the values obtained from the fits are physically reasonable. The choice of the P_s values however, remains as one of the most difficult problems in this type of analysis.

The $\Delta H°$'s and $\Delta S°$'s are difficult to interpret in molecular terms. Thus, the possible trend that hypermodifications of ApA exhibit less favorable enthalpy contributions and more favorable entropic contributions to the stacking free energy, can not be readily explained in terms of the side chains' properties. Another difficulty is the quite large uncertainty in the values obtained.

For these reasons and others which I have discussed, it is most useful to compare the equilibrium constants of the stacking equilibria. While it is difficult to attain absolute K's because of the use of a model, it appears that relative values of K's can be derived. Thus stacking differences have been deduced between dimers containing hypermodifica-

tions and those without modification. Because the trends have been observed from technique to technique it is believed that i^6A, ms^2i^6A and εA destabilize the stacking of ApA, while t^6A stabilizes the stacking of UpA.

Finally, the use of the two-state model has been discussed in detail, along with the effects of the experimental and calculational errors upon the thermodynamic parameters. I have concluded that the two-state model is a useful model in detecting stacking differences, but only when used with several techniques. The inherent errors of a model and of the experiment itself require one to check by different experiments the resultant trends which may be apparent from the analysis of a single technique.

This has been performed in this dissertation, and the stability trends observed are felt to be an accurate description of the stystem. In the next section, we will see if the static properties of the dimers are consistent with the thermodynamic results presented here.

II. Static Properties

Up to now I have made no attempts to construct molecular models for the stacked states of the dimers. This is a difficult problem, especially because of the likely presence of more than one stacked state. This is one of the reasons why the preceeding thermodynamic approach has been used. With that type of analysis no real detail of the molecular states are specified, aside from the fact that the

stacked state is characterized by considerable base-base interaction, and the unstacked state has properties similar to the monomers.

Certainly however, conformational information can be obtained from the static properties. This section describes the effects of hypermodification upon the properties of the monomers and dimers, in an effort to learn of the effects of hypermodification upon the conformations of the monomers and dimers.

(A) Monomer Properties

It is important in a study of dimer properties to investigate the constituent monomers' properties. The optical and NMR properties of the monomers have been tabulated and briefly discussed in Chapter 4. In this section, I will interpret as much as possible these properties in terms of conformational differences.

The absorption is of course markedly changed as the side chains are added to adenosine. Unfortunately because of the complex changes in the electronic properties of the base moieties, it is impossible to extract conformational information from this. For example, it is not possible to learn from the absorption about the affect of the side chain's addition upon the glycosidic bond angle (syn-anti equilibrium). Nor is it possible to deduce the position of the side chain relative to the base or sugar moiety. Of course, detailed theoretical calculations could yield more information about

the relative geometry of the side chain, but the difficulties are numerous.

Because of the changes in the absorption bands, the hypermodifications of A will exhibit different CD spectra as well. As mentioned in Chapter 4 though, the only conclusion that can be drawn in the absence of more detailed theoretical considerations, is that the syn-anti equilibrium is not greatly influenced by the addition of the side chain.

The NMR of the monomers (nucleosides and nucleotides) is by far the best technique to learn about changes in the conformations brought about by hypermodification. Table VIII in Chapter 4 gave the pertinent NMR shifts of the hypermodified monomers. Here, In Table II, are presented these data in a more useful manner - the changes caused by hypermodification. The differences between the shifts of A and A*, or pA and pA*, will yield information about the affect of the modification (*) of (p)A upon its chemical shifts. The difference between A* and pA* tells us about the effects of the phosphate upon the protons' shifts of A*.

From the 1st column in Table II, i^6A - A, we can note two things. First, the base protons of i^6A are shielded relative to those of A. This is the trend expected from the addition of the electron donating alkyl group[115-117]. H8 is more shielded than H2, even though H8 is further away from the influence of the side chain's inductive effect than H2. It is suspected from the small magnitudes of the shifts however, that the shielding is due to the inductive effects,

Table II. Differences in chemical shifts ($\Delta\delta_{TSP}$) for the naturally occurring monomers at room temperature. Original shifts are in Table VIII, Chapter 4. A (-) number denotes an upfield shift relative to the compound being subtracted. Error in difference propagates to ∿±0.010 ppm.

	DIFFERENCE BETWEEN MONOMERS								
Proton	1 i^6A minus A	2 ms^2i^6A minus A *	3 pi^6A minus pA	4 pms^2i^6A minus pA	5 pt^6A minus pA	6 pA minus A	7 pi^6A minus i6A	8 pms^2i^6A minus ms2i6A *	9 pi^6A (synthetic) minus pi6A (SVP)
H8	-.061	-.224	-.053	-.244	+.280	+.173	+.181	+.153	+.030
H2	-.012		+.001		+.410	+.019	+.032		+.030
H1'	-.005	-.154	-.008	-.076	+.091	+.083	+.080	+.161	+.009
H2'	-.007	-.049	+.004	+.033	+.097	-.036	-.025	+.046	-.004
H3'	+.005	-.085	-.007	+.005	+.058	+.083	+.071	+.173	+.007
H4'	+.008	-.139	-.006	-.046	+.026	+.103	+.089	+.196	+.003
H5'	+.004	-.037	-.011	-.028	-.061	+.209	+.194	+.218	+.003
H5"	+.003	-.083	-.011	-.028	-.061	+.292	+.278	+.347	+.003
=CH-							-.001	-.005	?
$-CH_2-$							+.011	-.027	+.473
$-S-CH_3$								-.016	
$-CH_3$ a							-.002	-.014	+.165
$-CH_3$ b							-.002	-.013	+.109

* ms^2i^6A was insoluble in D_2O and was dissolved instead in CD_3OD.

rather than through-space interaction of the side chain with the base near H2 which could possibly conteract the inductive effects. The second thing to notice is that within experimental error, the shifts of the sugar protons are not changed. Thus no significant interaction of the side chain with the sugar is occurring.

The pi^6A - pA data verifies the information derived from the i^6A - A data. Again H8 is shielded more than H2 while the sugar protons are essentially unaffected.

In the second column, ms^2i^6A - A, the rather large changes can probably be attributed to the solvent effect. Because of its insolubility in D_2O, ms^2i^6A was run in CD_3OD. However, H8 of ms^2i^6A is shielded relative to A significantly more than the sugar protons, and this is again probably due to the electron releasing inductive effects of the isopentenyl group and the thio-methyl group[115-117]. The availability of the pms^2i^6A - pA data (below) allows us to learn about the side chain in the absence of data for A in CD_3OD.

Column four, pms^2i^6A - pA, yields more information than ms^2i^6A - A. Again, we see the H8 shielded relative to pA. The value is much greater than that for pi^6A, and is more than likely due to the combined inductive effects of the 2 side chains. In this case, the sugar protons do show some changes which cannot be experimental error. Possibly the glycosidic bond angle has changed, or the side chain is interacting somewhat with the sugar, but the effects are small.

pt^6A - pA yields large changes in the base and sugar protons. The H8 and H2 are deshielded as expected from a combination of the inductive and resonance effects of the side chain[115-117]. This is supported by the difference in pK_a values for the N1 nitrogen. pt^6A and pA were spectrophotometrically titrated at $\mu = 0.1$. The pK_a's from the midpoints of the titration curves were 3.4 for pt^6A and 3.8 for ApA. Thus the electron donation from the side chain makes N1 more basic. However, the sugar protons also exhibit changes which can not be explained simply in terms of through-bond effects of the side chain. A comparison between pD 5.5 and pD 7 spectra shows that the H2 and $-CH_3$ protons are not affected by the phosphate ionization. Thus the syn-anti equilibrium is probably not affected by the addition of the threonine side chain. This comparison also shows that the side chain is probably not extending back twoard the H8 portion of the ring. This is as expected from crystal structure studies, which show the side chain extending away from the base moiety[55,56]. Also, the NMR of t^6A base in pyridine showed with one exception the side chain's protons not to be different from those of free threonine[14]. The exception was the αN-H proton which the authors felt was H-bonding to the ring nitrogen of t^6A (see also the x-ray structure references above).

The effects of the phosphate group also yield useful information. Column 6 demonstrates the well-known effect of the phosphate group[94,100,101], which is the selective

deshielding of H8. This is evidence for the anti conformation. Also, the sugar protons adjacent to the phosphate are deshielded from the electron withdrawel of the phosphate group.

pi^6A - i^6A exhibits almost identical values as with pA - A. Thus, as has been found by others[90], the side chain does not affect the syn-anti equilibrium. Also however, the side chain protons are not affected at all which would suggest that they are not near the H8 side of the ring.

Although pms^2i^6A - ms^2i^6A is somewhat complicated by the solvent difference, the relevant information can be obtained. Since columns 2 and 4 show essentially identical differences for H8, the solvent probably does not affect this proton's shift. Then, the difference noted in column 8 is similar to those in 6 and 7, indicating that the syn-anti equilibrium has not been affected. It is interesting to note that the combination of the solvent difference and the phosphate group have very little affect upon the side chain protons. Unless the two effects of solvent and phosphate fortuitously cancel one another, this also points to an anti conformation ($-S-CH_3$ is more restricted than the isopentenyl). Moreover, the isopentenyl group must not be in the region of the H8 portion of the base, or it would be deshielded by the phosphate.

The final column (9) demonstrates why pi^6A had to be obtained from an SVP degradation. The synthetic pi^6A for some reason lacked a =CH- proton. The $-CH_2-$ protons appeared

then as a singlet. The possibility of a D replacing the H in =CH- was tested by heating the sample in H_2O. No exchange was observed. Also, the $-CH_2-$ protons and $-CH_3$ protons were shifted downfield very much. The $-CH_3$ resonances of the synthetic sample were also less equivalent than those of the SVP sample. It is suspected that an electronegative bromine atom is in place of the vinylic hydrogen. The synthetic sample was thus rejected. All shifts in Chapter 4 are for the SVP pi^6A. (Incidentally, the absorption spectra of the two different pi^6A's were identical.)

A further point to note in Table VIII of Chapter 4 is that the non-equivalences of the $-CH_3$ groups in the isopentenyl chains are different for pi^6A and pms^2i^6A. A broad singlet is observed for pi^6A and i^6A, while a definite doublet appears for pms^2i^6A and ms^2i^6A. This is most likely due to the closeness of the $-S-CH_3$ group and the isopentenyl group. This is again suggestive of the isopentenyl side chain being swung away from the H8 side of the base moiety.

In summary of this section, it appears that in general the additions of the large side chains do not greatly alter the conformation of adenosine or adenosine monophosphate. The CD and NMR data consistently give the picture that the syn-anti equilibrium is not noticeably affected. Also, as is consistent with the crystal structures of some of the base moieties[51-56], the side chains do not seem to interact significantly with the base or sugar portions (with the possible exception of t^6A). The chains apparently do not fold

back toward the H8 portion of the ring as judged by the lack of effects upon the chains caused by the phosphate's addition or ionization.

(B) Dimer Properties

(i) Absorption

The static absorption property of interest is the %h at 25°C (see Table I, Chapter 4). This property has in the past been used in comparing the stacking abilities of dimers[69,72]. It should be of interest then to see if the values are consistent with the dynamic stacking results discussed in this chapter.

The value for Apms^{2}i^{6}A (7.7%) is below that of ApA, Api^{6}A and ApεA. Based on this alone, we would predict the base-base interaction to be smaller, with the possibility of diminished stacking strength. This is in disagreement with the thermodynamic analysis of the absorption and the CD, in which Apms^{2}i^{6}A was found to stack more than ApA, Api^{6}A and ApεA. However, I have pointed out the abnormally high K's derived for Apms^{2}i^{6}A from both the absorption and the CD. These are probably a result of an incorrect P_s value, as discussed in section I B of this chapter. In light of the small error in the %h's as compared to those large errors found with the absorption and CD K's for Apms^{2}i^{6}A, the static data in this case may be a more reliable measure of stacking. Furthermore the diminished %h is consistent with the thermodynamic 3'-Endo method results. From the

3'-Endo analysis of both the 3' and 5' residues, Apms^{2}i^{6}A is found to stack less than ApA, Api^{6}A and ApεA. Thus, this %h for Apms^{2}i^{6}A is consistent with the trend of stacking abilities of ApA type dimers found by the dynamic analyses. Hypermodification of ApA seems to diminish the stacking ability.

The value of 13.1% for ApεA is on the other hand inconsistent with the trend. The use of the simple arguement that the higher %h means a higher stacking gives a picture which is inconsistent with the thermodynamic parameters found from absorption, CD, and NMR. One can argue however, that the %h is also affected by the strength of the monomer absorption band strengths, and in this case, εA has a band at ∿230 nm of $\varepsilon \simeq 32 \times 10^3$. This is much larger than the bands of A, and in fact the fit of the absorption data predicts a high value of the $\%h_s$ (24 as opposed to 18 for ApA). Hence for a given amount of stacking we might expect a higher %h for ApεA; then, the %h value could be consistent with the trend that εA destabilizes the stacking of ApA.

The data for Api^{6}A as compared to ApA, and for Upt^{6}A as compared to UpA agree with the trends found from the dynamic analysis of all the techniques. The Api^{6}A data presented here is in disagreement with the results found for synthetic models of this dimer[122]. Compounds with trimethylene bridges between the base moieties (instead of sugars and a phosphate) showed stronger stacking for (A)C_3(i^{6}A) than for (A)C_3(A). Thus these type compounds do not appear

to be good models for dinucleoside phosphates.

The ethanol denaturation experiment, though not exactly a static measurement, yields some information about possible conformations. Api^{6}A and ApA exhibited identical melts with EtOH. Thus the interactions stabilizing the stacked states (as 'seen' by the EtOH) must be approximztely the same. It seems unreasonable then that the isopentenyl side chain could be inserted between the bases as proposed by Schweizer et al.[90].

The salt binding experiments described in Chapter 4 demonstrated no affect upon the absorption from the addition of salt or Mg^{++}. The results for Api^{6}A are in contradiction to the experiments with poly i^{6}A in which the authors attributed Mg^{++} induced changes in the optical melts to specific interaction of the ion with the base moiety[121]. Upt^{6}A does not appear to bind any cations that affect the absorption. That salt binding to the $-COO^-$ might change the absorption at all, was supported by the large absorption changes observed when the $-COO^-$ group was protonated. (In fact, it was observed during the spectrophotometric titration of pt^{6}A that the absorption change due to the $-COO^-$ protonation was greater than that for the N1 protonation.) On the basis of these observations, the Mg^{++} binding to t^{6}A in E. coli tRNA^{Ile} proposed by Miller et al.[39] may be in question. The melt data of the various dimers also show the stacking not to be influenced by salt or Mg^{++}.

In summary, the kinds of arguements used for Apms^{2}i^{6}A

and ApεA demonstrate the difficulties described in Chapter 5 in relying on the static properties alone in comparing stacking abilities. The conclusion I have reached concerning the agreement between the static absorption, and the dynamic analyses from the absorption, CD and NMR, is that they are not inconsistent. In some cases they agree, and the other differences can be rationalized, but only when we consider the entire set of data from various methods. Thus, we will also consider the static properties of the CD and the NMR.

(ii) CD

The CD of ApA, Api^{6}A, Apms^{2}i^{6}A and ApεA at room temperature (Figures 12 and 13, Chapter 4) are consistent in their magnitudes with the hypermodifications causing decreased stacking of ApA. The differences are not very large, but in no case does the CD of the hypermodified dimers equal or exceed that of ApA.

The CD of UpA and Upt^{6}A (shown in Figure 14 of Chapter 4) however are far from what would be expected on the basis of the trends observed so far. On the other hand, the extremely small CD of the Upt^{6}A may be the result of a cancellation of larger positive and negative CD bands. Also, since the CD is much more geometry dependent than the absorption, tilting of the residues could explain the variance in the two methods. Certainly though, on the basis of the CD alone, Upt^{6}A would not be predicted to exhibit larger base-base interactions than UpA.

As with the absorption no affects upon the CD (and most likely then upon the stacking) of Api^{6}A or Upt^{6}A were observed after the addition of salt or Mg^{++} (Section II D, Chapter 4).

Thus, the CD static spectra are like the static absorption properties in that they often afford both supporting and conflicting evidence for the relative stacking abilities obtained from the dynamic analyses. It is clear that in the absence of the knowledge of the optical properties of the 'fully-stacked' states, the static absorption or CD cannot in themselves offer conclusive evidence for stacking abilities.

(iii) NMR

With its many probes on the various portions of the dimers, NMR remains as the most detailed conformational analysis technique. Because of its specific nature however, the true complexities of the stacking reaction and conformations become evident. The ability to make simple comparisons of base-base interactions or of stacking abilities can easily be erased by the complications of rationalizing all the chemical shift or coupling constant changes. It is clear that the base proton and H1' shifts of dimers "can not lead to a conclusive solution of the detailed dynamic conformations of these molecules"[97].

Thus, I will not in this section describe conformations of the dimers. However, one can obtain from the shifts monitored here some information about conformational changes

between dimers, as well as information concerning the hyper-modified side chain's environment in the stacked state. A final analysis would require the assignment, shifts and coupling constants of all the protons of the dimers, not to mention the more difficult consideration of the several possible stable conformations of stacked dimers[97].

The major points for a simple discussion of the base protons and the H1' protons are the following. First, if dimerization shifts are different for a given proton on an unmodified dimer and a modified dimer, then a) there is a difference in the conformations, and/or b) there is a difference in ring current or anisotropy of the modified monomer relative to the unmodified monomer. Second, if we compare just the protons on the pA* residue of ApA* (where * refers to the various modifications), the second factor above (b) is removed. In all cases, the neighboring residue is Ap. Finally, increased (or decreased) dimerization shifts of even the pA* residue do not necessarily indicate more or less base-base overlap. If one examines a typical calculated ring current diagram, it is apparent that simple twisting of two bases relative to one another can cause base protons to move into different shift contours. Thus, the base-base overlap could remain essentially unchanged, while (according to the most recent values[112]) most of the changes observed in this thesis could be explained by a change of only contour line ($\sim$0.4 ppm). With these factors in mind, I will not present the salient differences observed between

the modified and unmodified dimers (see Table V, Chapter 4).

a) Api^6A

Protons H8pA*, H1'pA* and H2Ap exhibit identical dimerization shifts within experimental error for ApA and Api^6A ($\sim\pm0.01$ ppm for each dimerization shift - the error in the difference is even larger $\sim\pm0.02$ ppm). Protons H8Ap, H2pA* and H1'Ap exhibit larger dimerization shifts with Api^6A (at low temperatures, $\sim$0.06, 0.05, and 0.07 respectively). The changes in H8Ap and H1'Ap could be due to ring current changes, but H2Ap has not changed, and thus this would seem unlikely. Furthermore H2pA* has also changed. Hence, the differences must be attributed to conformational differences. H8pA* and H2Ap are the protons generally giving the largest effects upon stacking for these types of dimers ($\Delta\delta_{TSP}$'s $\sim$0.3 ppm), and these are the very protons that show no change upon the addition of the isopentenyl side chain. It seems then that the change in base-base overlap must be a small one. This is also evident from the %h and CD at 25°C (see previous sections), which indicate slightly less base-base interaction.

According to recent proposed models, the H1'Ap change could represent a change from conformation I to II and III[97] (see Figure 1). However, the changes (and lack of changes) observed for the base protons are not consistent with any transformation between the different conformations.

The side chain protons exhibit large dimerization changes. The order of shifting is $-CH_2- > =CH- > -CH_3$. In

Figure 1: Proposed conformations for dimers. The examples shown are pictured as ApA dimers. View is perpendicular to the planes of the bases. RNA 11 geometry is shown for comparison 123. Conformations I, II and III are those proposed by Lee 97. Ap residue (fine line), pA residue (dark line).

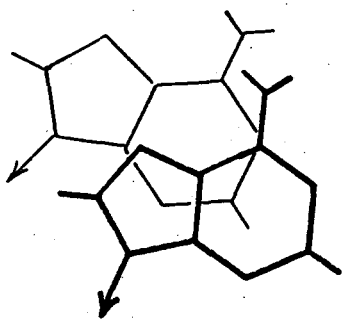

RNA 11

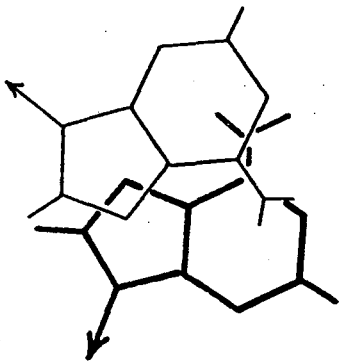

II

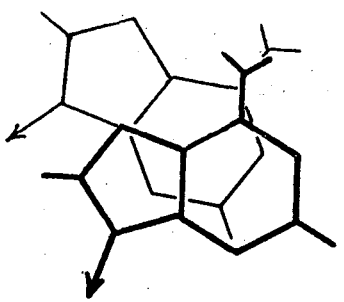

I

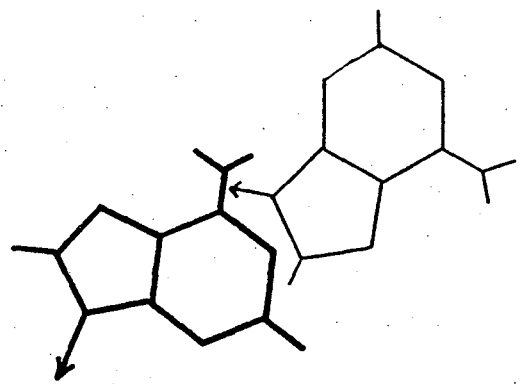

III

agreement with the EtOH 'denaturation' data, this order is not to be expected from a situation where the chain is folded between the bases[90]. Here, the further the proton is from the attachment to the base, the less its shift. This is not to say there is no interaction of the chain with the neighboring base, for even the methyl groups show significant shifts (∿0.15 ppm, as compared to the base protons ∿0.2 - 0.3 ppm). Furthermore, the two methyl groups are now very much more inequivalent than in the monomer. Thus the side chain certainly feels the ring currents of the neighboring A.

All of these results are generally in large variance with those reported by Schweizer et al.[90]. These authors generally found smaller dimerization shifts for Api^{6}A than ApA. These workers ran their spectra at 20 m<u>M</u> concentrations after having themselves shown large concentration dependent shifts. All the spectra recorded in this thesis were obtained at concentrations of 5 m<u>M</u> of less, where concentration dependent shifts were not observed.

Api^{6}A then exhibits some change in conformation relative to ApA, though the base-base overlap is not greatly affected. The side chain is in close proximity to the neighboring A residue, but does not appear to be inserted between the bases.

b) Apms^{2}i^{6}A

Protons H8pA*, H1'pA*, and H8Ap show similar if not

identical dimerization shifts for Apms^{2}i^{6}A and ApA. H2Ap of Apms^{2}i^{6}A is significantly deshielded relative to ApA (0.17 ppm). Since it is one of the protons most sensitive to stacking, Apms^{2}i^{6}A must have some significant change in the base-base orientation (a change in ring current due to electron donation would affect the shift of H2Ap in the opposite direction). The overlap must not be seriously affected though, since H8pA* remains unchanged.

Hl'Ap is shielded much more in Apms^{2}i^{6}A. This taken with the change in H2Ap could suggest a higher population of conformation II for Apms^{2}i^{6}A (see Figure 1 and reference 97). This conformation has less base-base overlap than that of I (which is expected to be the major form for ApA[97, 98]), as was noted with the %h and CD at 25°C.

The -S-CH_3 protons are essentially not shifted at all. This is not too surprising since the H2pA* protons in general show the smallest effect from stacking of all of the base protons (-S-CH_3 is attached to C2 of pA*). The isopentenyl chain again shows some large dimerization shifts. As with Api^{6}A, =CH- is shifted much more than the -CH_3 protons and thus the chain is probably extending into solution rather than between the bases. The =CH- experiences a very large shift (larger than in Api^{6}A) while the methyl groups are again more inequivalent than in the monomer (but shifted less than in Api^{6}A).

In summary, the ms^{2}i^{6}A modification changes the conformation of ApA, with this most likely resulting in a slight

reduction in the base-base overlap. While the thio-methyl group does not feel the effects of the neighboring A residue, the portions of the isopentenyl side chain nearest the attachment to N6 greatly feel the influence of the neighbor. The free end of the isopentenyl chain appears to be further away.

c) ApεA

Protons H8pA*, H1'pA* and H2Ap are not affected by the εA modification. H8Ap and H1'Ap are shielded much more with ApεA. The additional ring certainly adds more ring current in a particular location. It is not inconceivable that H2Ap would be unaffected by the addition ring current while H8Ap and Hk'Ap were affected. However, H2pA* is deshielded somewhat in ApεA, and all of the changes probably result from both factors - a change in conformation and ring current. Lee[97] has proposed from the large H1'Ap changes, that ApεA has larger populations of conformations II and III. However, the base proton changes (and lack of changes) are not entirely consistent with this picture. H10 and H11 are shifted essentially as much as the other base protons.

Thus ApεA appears also to have a different conformation than ApA, though the extent of change in base-base interaction is difficult to estimate.

d) Upt^{6}A

Protons H6Up, H1'pA* and H2pA* all exhibit similar dimerization changes with UpA and Upt^{6}A. H5Up was unfortunately

broadened out enough to make accurate chemical shift measurements impossible. The cause of this is not known. H1'Up of UpA is slightly shielded relative to Upt^{6}A (0.04 ppm). The only large difference between the two molecules is with H8pA*. In Upt^{6}A this proton is shielded much more than in UpA (0.14 ppm). The dimerization shift is still relatively small ($\sim$0.23 ppm) compared to other dimers. This is expected on the basis of the weaker ring current of Up[93,95]. Nevertheless, the <u>difference</u> cannot be attributed to a difference in ring current since Up is the shielder in UpA and Upt^{6}A. Thus there appears to be greater base-base interaction with Upt^{6}A. This agrees with the %h but not with the very low CD magnitudes. The -CH_3 protons of Upt^{6}A are completely unaffected by the presence of the neighboring U.

Again, hypermodification has caused conformational changes. Upt^{6}A seems to have more base-base overlap than UpA. The free end of the side chain threonine does not interact at all with the U residue.

(C) Summary of the Static Properties

Unlike the dynamic analysis, a study of the static properties can yield conformational information. The NMR evidence indicates that hypermodification induces conformational changes. The sum of the techniques point to an increased base-base interaction of Upt^{6}A relative to UpA. Api^{6}A and Apms^{2}i^{6}A appear to exhibit slightly smaller base-base interactions than ApA. The conclusion for Api^{6}A is in

agreement with the conclusions reached by Schweizer et al.[90] on the basis of some static properties. The relative base-base interaction of ApεA has been difficult to determine because of the large change in electronic properties upon modification. The isopentenyl side chains of i^6A and ms^2i^6A may interact to stabilize (or destabilize) a conformation, but probably not by the insertion of the chain between the base moieties.

Since the different methods occasionally yield conflicting evidence for the amount of base-base interaction, it is evident that a study of the base stacking properties must be approached from as many different avenues as possible. Obtaining detailed conformational pictures appears unlikely at present, but the attainment of information concerning conformational changes represents a feasible task.

III. Summary

The static and dynamic properties of the dimers studied have been discussed. More realistically, I have discussed differences in the static and dynamic properties between UpA, ApA and their hypermodified counterparts. The thermodynamic results point to a situation in which i^6A, ms^2i^6A and εA destabilize the stacking of ApA. t^6A stabilizes the stacking of UpA. These differences are probably brought about by the conformational changes induced by hypermodifications. From most indications Api^6A and $Apms^2i^6A$ have less base-base interaction than ApA. The large ε modification

gives rise to conflicting results with the different techniques, and hence ApεA may have more or less base-base interaction than ApA. Most of the properties of Upt^{6}A point to a greater base-base interaction than that of UpA. Thus, if base-base interaction is the determining stabilizing factor in the stacking of these dimers, the static properties for the most part agree with the trend found from the dynamic analysis.

Thus, with t^{6}A stabilizing UpA, and i^{6}A, ms^{2}i^{6}A and εA destabilizing ApA, the large difference in stacking ability between UpA and ApA may be removed by hypermodification. The implications of these dimer results to the possible role of the hypermodified bases in tRNAs will be discussed in the next and concluding chapter.

Chapter 8 CONCLUSIONS

I. The Hypothesis

II. An Additional Hypothesis

III. Anticodon Loop Conformations

IV. Further Questions

V. Summary

Chapter 8

CONCLUSIONS

I. The Hypothesis

We must now consider the relation between the results obtained with the dimers, and the hypothesis proposed in Chapter 2: *Through their stacking interactions with the first letter of the anticodon triplet, hypermodifications function to lock the terminal A·U base-pair into a correct reading frame, thus promoting mRNA binding, eliminating wobble, and perhaps regulating translation.* If a correct reading frame is enhanced by stronger stacking of the dimer immediately adjacent to the anticodon triplet, then the results with Api^{6}A, Apms^{2}i^{6}A, and Apεa (a model of ApyW) are not consistent with the hypothesis. Each of these hypermodified dimers exhibits somewhat less stacking than ApA.

On the other hand, the stronger stacking of Upt^{6}A compared to UpA is consistent with the hypothesis. The enhanced stacking observed here may offer the explanation of why wobble is not allowed on the 3' side of the anticodon triplet. As mentioned in Chapter 1, there is always a pyrimidine (and usually a U) next to the 5' side of the anticodon triplet. UpX dimers are known to exhibit very little stacking relative to dimers not containing U[69,72,95]. Thus in all tRNAs there exists a very flexible linkage adjacent to the 5' side of the anticodon triplet[73]. However, on the 3' side of the anticodon triplet, the only UpX dimer

found is Upt^{6}A, which exhibits less flexibility than UpA. Hence on the basis of this work, the t^{6}A modification of A may be necessary to prevent the flexibility which is believed to be the cause of wobble[73].

It may very well be that the stabilization of the ApA dimer is not required to prevent wobble on the 3' side. Since Api^{6}A, Apms^{2}i^{6}A and ApεA appear to be only slightly less stable than ApA, they are all still significantly more stacked than a UpX dimer. Thus, in the presence or absence of hypermodification, the flexibility next to the 3' terminal A·U base pair of the codon-anticodon complex may be small enough to prevent the mismatching of wobble at that point.

On the basis of the work of Martin, et al.[75], Grosjean, et al.[47], and Yoon, et al.[80,118], the stacking of single stranded residues next to a double stranded helix enhances the stability of the duplex. Using this simple thinking, in order for the tRNA to bind more efficiently to the mRNA when hypermodifications are present, would require the stacking interaction of the non-H-bonded hypermodified base to be stronger than were it not modified. Again, the results for Api^{6}A, Apms^{2}i^{6}A and ApεA are not consistent with the hypothesis in this regard. The t^{6}A modification however, through its stronger stacking with the terminal U·A base-pair, may enhance the stability of the codon-anticodon duplex. Yet, no experiments with dangling ends have shown whether weaker or stronger stacking of the non-H-bonded residues

enhance the duplex stability. Only the presence of these residues has been shown to be important. In fact, the enhancement of the stability of the anticodon-codon interaction is believed to be caused by entropic effects, and not enthalpic effects which might be expected from a stronger stacking of the hypermodified base onto the duplex[118].

II. An Additional Hypothesis

If one agrees that there is indeed a function for the i^6A, ms^2i^6A and yW modifications, then we must formulate a new hypothesis to explain the dimer results. Also, it is my feeling that all of the hypermodifications (t^6 included) will have a related function.

Therefore, it is important to remember that with t^6A stabilizing UpA, and i^6A, ms^2i^6A and εA destabilizing ApA, the large difference in stacking ability between UpA and ApA may be removed by hypermodification. Then, if the dimer stacking stabilities are a good indication of the flexibilities allowed in the linkage adjacent to the anticodon triplet, tRNAs containing these hypermodifications will have similar flexibilities at this crucial point in the anticodon loop.

With this in mind, I examined the relative stacking ability of CpA, the next most prevalent dimer found in this position in tRNAs (see Table II, Chapter 1). The results of both the static and dynamic analyses (Table I, Chapter 4 and Table I, Chapter 6) indicate that the stack-

ing ability of CpA is between those of ApA and UpA. In fact, it is close in stability to those of Api^{6}A and ApεA found by absorption. Thus, 38 of the 65 tRNAs in Tables I and II of Chapter 1 contain dimers in the region adjacent to the 1st letter of the anticodon triplet which exhibit very similar stacking abilities (if ApεA is a reasonable model for ApyW type dimers). It may very well be that the small modifications of A, G and I shown in Table II of Chapter 1 (m^2A, m^6A, m^1G, m^1I), confer on the dimers containing them stacking abilities similar to the other 38.

Assuming that the similar stacking abilities of the dimers studied here accurately represent the flexibility of the region in the anticodon loop of <u>all</u> tRNAs, we must ask why (or if) hypermodification and thus constant flexibility is desirable. One distinct possibility is that a constant flexibility at this point can aid in making the anticodon-codon complex proceed with the same efficiency or rate in <u>all</u> tRNAs. This could be of help in the regulation of protein synthesis by allowing a smoother progression of codon-anticodon interactions. However, similar flexibilities and similar reaction dynamics may be in contradiction if one considers only the nearest neighbor calculations of duplex stabilities[74]. Thus, for A·U 'rich' codon-anticodon complexes (of which those containing hypermodifications would be classified) one would expect different stabilities than those with more G·C pairs. But in light of the large effects of dangling ends[47,118,75], it is possible that the

maintenance of a particular conformation near the 3' side is more important in keeping the duplex stability constant than the nearest neighbor contributions.

Therefore, an additional hypothesis which is consistent with the data presented here is: *Hypermodifications serve to maintain the flexibility of the linkage immediately adjacent to the first letter of the anticodon in all tRNAs. Thereby, all codon-anticodon interactions will have nearly corresponding geometries at this point, which will result in similar interaction dynamics.*

One test of this hypothesis would be to synthesize and examine the other dimers such as Gpm^2A, Gpm^1G and Cpm^1I. However, the real test will be to compare anticodon-codon interactions of tRNAs with and without modifications for a series of different hyper- and smaller modifications. Whether or not the constant flexibility results in a step of regulation is more difficult to assess.

III. Anticodon Loop Conformations

While the step from dimer results to a role of hypermodifications in affecting protein synthesis is rather large, we can with more confidence relate these results to the hypermodifications' role in affecting the loop conformation. Thus, there does seem to be a constant asymmetry of stacking abilities on the 3' and 5' sides of the anticodon triplet. The 3' side of the triplet is less flexible than the 5' side. Two interesting exceptions to this may

be the dipyrimidine dimers found on the 3' side of two Staph. Gly tRNAs (CpU and CpC, Table II, Chapter 1). These dimers may be present in order to allow base-pairing of the C and G residues occurring as the 1st and 7th letters in their anticodon loops. Thus these two tRNAs may have 5-membered anticodon loops.

What I have completely neglected in this study are the properties of the dimers A*pA (* meaning all hypermodifications). The properties of these dimers will also affect the conformation of the anticodon loop. Studies by Lee[97] have shown dimers of the type (Pu)p(Pu*) to be less stable than (Pu*)p(Pu) (where Pu* is a larger purine than Pu - e.g. GpεA vs. εApG). Likewise, Kan et al.[119] reached the conclusion from some oligomer studies that ApyW was less stable than yWpA. Finally, the work of Schweizer et al.[90] may indicate more interaction of i^6ApA as compared to Api^{6}A. Each of the dimers, (Pu*)p(Pu), may be more stable than (Pu)p(Pu)[97,119]. Careful studies of the actual dimers occurring in tRNA are necessary in order to verify these trends. In their absence however, it seems that the hypermodification may serve to form a <u>less</u> flexible linkage on the 3' side of the hypermodification, and a <u>more</u> flexible linkage on their 5' side (both relative to an ApA linkage).

IV. <u>Further Questions</u>

Because of the little data available on the effects of dangling ends upon duplex stabilities, it is difficult to

relate the dimers' results to the results observed on the larger scales of tRNAs. In Chapter 1, it was pointed out that the effect of hypermodifications upon in vitro polypeptide synthesis was caused in part by a more efficient binding of the tRNA to the ribosome-mRNA complex. Whether or not a destabilization of the region around i^6A or ms^2i^6A is responsible for enhanced binding is not known. Perhaps the properties of i^6ApA or ms^2i^6ApA influence this function. The effects of the stabilization by t^6A upon tRNA-mRNA binding are also unknown.

Hence, the pressing problem is to be able to relate the conformational properties of the tRNA and mRNA to their interaction. This present work has served as a study of the influence of the hypermodification upon the properties of the anticodon loop. (In this regard, another pressing question is the applicability of dimer results to polynucleotide conformations.) The effect of hypermodification upon the codon-anticodon interaction is purely by inference, as was pointed out in Chapter 2. Also neglected of necessity in this study were the possible physical interactions of the hypermodified base with the mRNA (or the ribosomes). The best test of the hypothesis put forth here will then be one in which the codon-anticodon interaction (or a reasonable facsimile) is studied as a function of the extent of hypermodification.

V. Summary

This work has progressed from observations of the literature to hypothesis, from hypothesis to experiment, and finally from these new observations to a new hypothesis. The initial observations in the literature pointed out the affects of hypermodification upon translation. From these observations a testable hypothesis for the functions of the hypermodifications was formulated, which suggested experiments to perform on a smaller scale than attempted before.

Studies of the stacking abilities of dinucleoside monophosphates showed that differences in the stacking upon hypermodification were present. These stacking differences are attributed to changes in the dimers' conformations. It was found that i^6A, ms^2i^6A and εA (a model for yW) destabilize the stacking of ApA, while t^6A stabilizes the stacking of Upt^6A.

The t^6A stabilization effect points to its role in preventing incorrect wobble on the 3' side of the anticodon triplet. The hypermodifications as a group remove the stacking differences between ApA and UpA, the dimers which would be present in the absence of hypermodification. Furthermore, the stacking abilities of the hypermodified dimers are similar to those of another very prevalent dimer, CpA. The flexibility next to the 1st letter in the anticodon triplet may then be the same throughout all tRNAs, with the possibility of a better regulated translation step.

Because of the necessity of making inferences from small scale studies to translation, the dimer work is only the first step in understanding the functions of hypermodifications. However, they have served as important in dispelling certain beliefs of their properties, and in proposing new hypotheses for the functions of hypermodifications. Hopefully these hypotheses will be tested by further observations on the scale of tRNA and mRNA interactions.

BIBLIOGRAPHY

1. Hall, R.H. The Modified Nucleosides in Nucleic Acids, Columbia University Press, New York (1971).
2. Martin, D.M.G and Reese, C.B. J. Chem. Soc., 1731 (1968C).
3. Chheda, G.B., Hall, R.H., and Tanna, P.M. J. Org. Chem. 34(11), 3498(1969).
4. Kasai, H., Goto, M., Ikeda, K., Zama, M., Mizuno, Y., Takemura, S., Matsuura, S., Sugimoto, T., and Goto. T. Biochemistry 15(4), 898(1976).
5. Hall, R.H., Csonka. L., David, H., and McLennan, B. Science 156, 69(1967).
6. Hecht, S.M., Leonard, N.J., Burrows, W.J., Skoog, F., Armstrong, D.J., and Occolowitz, T. Science 166, 1272(1969).
7. Kimura-Harada, F., von Mindon, D.L., McCloskey, J.A., and Nishimura, S. Biochemistry 11(21), 3910 (1972).
8. Schweizer, M.P., McGrath, K., and Baczynskyj, L. Biochem. Biophys. Res. Comm. 40(5), 1046(1970).
9. Chheda, G.B., and Mittelman, A. 172nd ACS National Meeting, Division of Biological Chemistry, Abstract #123(1976).
10. Hall, R.H., Robins, M.J., Stasiuk, L., and Thedford, R. J. Amer. Chem. Soc. 88(11), 2614(1966).
11. Biemann, K., Tsunakawa, S., Sonnenbichler, J., Feldman, H., Dütting, D., and Zachau, H.G. Angew. Chem. 78, 600(1966).
12. Harada, F., Gross, H.J., Kimura, F., Chang, S.H., Nishimura, S., and RajBhandary, U.L. Biochem. Biophys. Res. Comm. 33(2), 299(1968).
13. Chheda, B.G., Hall, R.H., Magrath, D.I., Mozejko, J., Shcweizer, M.P., Stasiuk, L., and Taylor, P.R. Biochemistry 8(8), 3278(1969).
14. Schweizer, M.P., Chheda, B.G., Baczynskyj, L., and Hall, R.H. Biochemistry 8(8), 3283(1969).
15. Nakanishi, K., Furutachi, N., Funamizu, M., Grunberger, D., and Weinstein, I.B. J. Amer. Chem. Soc. 92(26), 7617(1970).
16. Hayashi, H., Fisher, H., and Söll, D. Biochemistry 8(9), 3680(1969).
17. Söll, D. Science 173, 293(1971).
18. Bartz, J.K., Kline, L.K., and Söll, D. Biochem. Biophys. Res. Comm. 40(16), 1481(1970).
19. Körner, A. and Söll, D. FEBS Let. 39(3), 301(1974).
20. Fitler, F., Kline, L.K., and Hall, R.H. Biochemistry 7(3), 940(1968).
21. Gefter, M.L. Biochem. Biophys. Res. Comm. 36(3) 435(1969).

22. Agris, P.F., Armstrong, D.J., Schäfer, K.P., and Söll, D. Nucleic Acids Res. 2(5), 691(1975).
23. Chheda, G.B., Hong, C.I., Piskolz, C.F., and Harmon, G.A. Biochem. J. 127, 515(1972).
24. Roberts, J.W. and Carbon, J. Nature 250(5465), 412 (1974).
25. Fleissner, E. Biochemistry 6(2), 621(1967).
26. Faulkner, R.D., and Uziel, M. Biochem. Biophys. Acta 238, 464(1971).
27. Kitchingman, G.R., Webb, E., and Fournier, M.J. Biochemistry 15(9), 1848(1976).
28. Fittler, F., and Hall, R.H. Biochem. Biophys. Res. Comm. 25(4), 441(1966).
29. Furuichi, Y., Wafay, A.Y., Hayatsu, H., and Ukita, T. Biochem. Biophys. Res. Comm. 41(5), 1185(1970).
30. Stern, R., Gonano, F., Fleissner, E., and Littauer, V.Z. Biochemistry 9(1), 10(1970).
31. Gefter, M.L., and Russell, R.L. J. Mol. Biol. 39, 145(1969).
32. Theibe, R., and Zachau, H.G. Eur. J. Biochem. 5, 546(1968).
33. Ghosh, K., and Ghosh, H.P. Biochem. Biophys. Res. Comm. 40(1), 135(1970).
34. Wintermeyer, W., and Zachau, H.G. FEBS Let. 18(2), 214(1971).
35. Odom, O.W., Hardesty, B., Wintermeyer, W., and Zachau, H.G. Arch. Biochem. Biophys. 162(2), 536(1974).
36. Yoshikami, D. and Keller, E.B. Biochemistry 10, 2969(1971).
37. Grunberger, D., Weinstein, I.B., and Mushinski, J.F. Nature 253, 66(1975).
38. Miller, J.P., and Schweizer, M.P. Fed. Proc. 31, 450(1972).
39. Miller, J.P., Hussian, Z., and Schweizer, M.P. Nucleic Acids Res. 3(5), 1185(1976).
40. Hecht, S.M., Kirkegaard, L.H., and Bock, R.M. Proc. Nat. Acad. Sci. 68(1), 48(1971).
41. Thiebe, R., and Zachau, H.G. Biochem. Biophys. Acta 217, 294(1970).
42. White, B., and Tener, G.M. Biochem. Biophys. Acta 312, 267(1973).
43. Krauss, G., Peters, F., and Maass, G. Nucleic Acids Res. 3(3), 631(1976).
44. Litwack, M.D., and Peterkofsky, A. Biochemistry 10(6), 994(1971).
45. Kimball, M., and Söll, D. Nucleic Acids Res. 1(12), 1713(1974).
46. Högenauer, G., Tumowsky, F., and Unger, F.M. Biochem. Biophys. Res. Comm. 46(6), 2100(1972).
47. Grosjean, H., Söll, D.G., and Crothers, D.M. J. Mol. Biol. 103, 499(1976).

48. Münch, H.-J. and Thiebe, R. FEBS Let. 51(1), 257 (1975).
49. Li, H.J., Nakanishi, K., Grunberger, D., and Weinstein, I.B. Biochem. Biophys. Res. Comm. 55(3), 818(1973).
50. Miller, J.P., and Schweizer, M.P. Analy. Biochem. 50, 327(1972).
51. Parthasarathy, R., Ohrt, J.M., and Chheda, G.B. Biochem. Biophys. Res. Comm. 60(1), 211(1974).
52. Parthasarathy, R., Ohrt, J.M., and Chheda, G.B. Biochem. Biophys. Res. Comm. 57(3), 649(1974).
53. Bugg, C.E. and Thewalt, U. Biochem. Biophys. Res. Comm. 46, 779(1972).
54. McMullan, R.K. and Sundaralingam, M. J. Amer. Chem. Soc. 93(25), 7050(1971).
55. Parthasarathy, R., Ohrt, J.M., and Chheda, G.B. J. Amer. Chem. Soc. 96(26), 8087(1974).
56. Adamiak, D.A., Blundell, T.L., Tickle, I.J., and Kosturkiewicz, Z. Acta Cryst. B31(5), 1242 (1975).
57. Nygjerd, G., McAlister, J., Sundarlingam, M., and Matsuura, S. Acta Cryst. B31(2), 413(1975).
58. Nishimura, S. Prog. Nucl. Acid Res. Mol. Biol. 12, 49(1972).
59. Jukes, T.H. Nature 246, 22(1973).
60. Elkins, B.N. and Keller, E.B. Biochemistry 13(22), 4622(1974).
61. Dube, S.K., Marcker, K.A., Clark, B.F.C., and Cory, S. Nature 218, 232(1968).
62. Stewart, J.H., Sherman, F., Shipman, N.A., and Jackson, M. J. Biol. Chem. 246(24), 7429(1971).
63. Takeishi, K., Ukita, T., and Nishimura, S. J. Biol. Chem. 243, 5761(1968).
64. Ghosh, H.P., Söll, D., and Khorana, H.G. J. Mol. Biol. 25, 275(1967).
65. Uhlenbeck, O.C., Baller, J., and Doty, P. Nature 225(7), 508(1970).
66. Freier, S.M. and Tinoco, I. Biochemistry 14(15), 3310 (1975).
67. Clark, B.F.C. and Marcker, K.A. J. Mol. Biol. 17, 394 (1966).
68. Watson, J.D. Molecular Biology of the Gene, W.A. Benjamin, Inc., Menlo Park, Cal, 2nd Ed.(1970).
69. Warshaw, M.M. and Tinoco, I. J. Mol. Biol. 19, 29 (1966).
70. Davis, R.C. and Tinoco, I. Biopolymers 6, 223(1968).
71. Simpkins, H. and Richards, E.G. Biochemistry 6(8),
72. Bloomfield, V.A., Crothers, D.M., and Tinoco, I. Physical Chemistry of Nucleic Acids, Harper & Row, San Francisco (1974).
73. Fuller, W. and Hodgson, A. Nature 215, 817(1967).
74. Borer, P.N., Dengler, B., Tinoco, I. and Uhlenbeck, O.C. J. Mol. Biol. 86, 843(1974).

75. Martin, F.H., Uhlenbeck, O.C., and Doty, P. J. Mol. Biol. 57, 201(1971).
76. Hall, R.H. Prog. Nucl. Acid Res. Mol. Biol. 10, 57 (1970).
77. Sussman, J. and Kim, S. Biochem. Biophys. Res. Comm. 50, 351(1975).
78. Quigley, G.J., Seeman, N.C., Wary, A.H.-J., Suddath, F.L., and Rich, A. Nucl. Acids Res. 2, 2329 (1975).
79. Ladner, J.E., Jack, A., Robertus, J.D., Brown, R.S., Rhodes, D., Clark, B.F.C., and Klug, A. Nucl. Acids Res. 2, 1629(1975).
80. Yoon, K. Ph.D. Thesis, University of California, Berkeley(1976) (and references therein).
81. Robillard, G.T., Tarr, C.E., Vosman, R., and Berendsen, H.J.C. Nature 262, 363(1976).
82. Secrist, J.A., Barrio, J.R., Leonard, N.J., and Weber, G. Biochemistry 11(19), 3499(1972).
83. Borer, P.N. Ph.D. Thesis, University of California, Berkeley (1972).
84. Cunningham, R.S. and Gray, M.W. Biochemistry 13(3), 543(1974).
85. Follman, H. Tetr. Lett. 22, 2113(1967).
86. Freier, S.M. Ph.D. Thesis, University of California, Berkeley (1976).
87. Freier, S.M. and Tinoco, I. Biochemistry 14(15), 3310(1975).
88. Walker, G.C. and Uhlenbeck, O.C. Biochemistry 14(4), 817(1975).
89. Grimm, W.A.H. and Leonard, N.J. Biochemistry 6(12), 3625(1967).
90. Schweizer, M.P., Thedford, R., and Slama, J. Biochem. Biophys. Acta 232, 217(1971).
91. P.L. Biochemicals' Ultraviolet Absorption Spectra, Circular OR-10, 7th printing (1973).
92. Davis, R.C. Ph.D. Thesis, University of California, Berkeley (1967).
93. Ts'o, P.O.P., Kondo, N.S., Schweizer, M.P., and Hollis, D.P. Biochemistry 8(3), 997(1967).
94. Ts'o, P.O.P., Basic Principles in Nucleic Acid Chemistry, Vol. I, Academic Press, New York(1974).
95. Ts'o, P.O.P., Basic Principles in Nucleic Acid Chemistry, Vol. II, Academic Press, New York(1974).
96. Lee, C.-H., Ezra, F.S., Kondo, N.S., Sarma, R.H., and Danyluk, S.S. Biochemistry 15(16), 3627(1976).
97. Lee, C.-H. Manuscript submitted to Biochemistry(1977).
98. Kondo, N.S. and Danyluk, S.S Biochemistry 15(4), 756 (1976).
99. Chan, S.I. and Nelson, J.H. J. Amer. Chem. Soc. 91(1), 168(1969).
100. Schweizer, M.P., Broom, A.D., Ts'o, P.O.P., and Hollis, D.P. J. Amer. Chem. Soc. 90(4), 1042(1960).

101. Danyluk, S.S. and Hruska, F.E. Biochemistry 7(3), 1038(1968).
102. Izatt, R.M., Christensen, J.J., and Rytting, J.H. Chem. Reviews 71(5), 439(1971).
103. Robins, M.J., Hall, R.H. and Thedford, R. Biochemistry 6(6), 1837(1967).
104. Topal, M.D. Ph.D. Thesis, New York University, New York(1974).
105. Applequist, J. and Damle, V. J. Amer. Chem. Soc. 88,3895(1966).
106. Leng, M. and Felsenfeld, G. J. Mol. Biol. 15, 455 (1966).
107. Johnson, N.P. and Schleich, T. Biochemistry 13(5), 981(1974).
108. Brahms, J., Maurizot, J.C. and Michleson, A.M. J. Mol. Biol. 25, 481(1967).
109. Breslauer, K.J. and Sturtevant, J.M. Personal Communication.
110. Applequist, J. and Damle, V. J. Amer. Chem. Soc. 87(7), 1450(1965).
111. Cech, C. Ph.D. Thesis, University of California, Berkeley(1975).
112. Giessner-Prettre, C. and Pullman, B. Biochem. Biophys. Res. Comm. 70(2), 578(1976).
113. Giessner-Prettre, C. and Pullman, B. J. Theor. Biol. 27, 92(1970).
114. Powell, J.T., Richards, E.G., and Gratzer, W.B. Biopolymers 11, 235(1972).
115. Morrison, R.T., and Boyd, R.N. Organic Chemistry, 2nd Ed., Allyn and Bacon, Inc., Boston(1970).
116. March, J. Advanced Organic Chemistry: Reactions, Mechanism, and Structure, McGraw-Hill Co., San Francisco(1968).
117. Pasto, J.D., and Johnson, C.R. Organic Structure Determination, Prentice Hall, Inc., N.J.(1969).
118. Yoon, K., Turner, D.H., Tinoco, I. Jr., von der Haar, F., and Cramer, F. Nucleic Acids Res. 3(9), 2233(1976).
119. Kan, L.S., Ts'o, P.O.P., von der Haar, F., Sprinzl, M. and Cramer, F. Biochemistry 14(14), 3278 (1975).
120. Bettelheim, F.A. Experimental Physical Chemistry, W.B. Saunders, Co., Philadelphia(1971).
121. Thedford, R. and Straus, D.B. Biochem. Biophys. Res. Comm. 47(5), 1237(1972).
122. Leonard, N.J., Iwamura, H., and Eisenger, J. Proc. Nat. Acad. Sci. 64, 352(1969).
123. Rosenberg, J.M., Seeman, N.C., Kim, J.J.P., Suddath, F.L., Nicholas, H.B., and Rich, A. Nature 243, 152(1973).

APPENDIXES

Appendix 1

COMPUTER PROGRAMS

The Fortran program used in obtaining the best fit parameters was WATTSK. Illustrated here is the listing of this program (using a PDP8/e) containing the %h vs. T data of ApA. Following the listing is a sample run of the program with the data for ApA. Once the program has been edited to contain new data (PH(I)), then the only variable is the 'PERCENT HYPOCHROMICITY' which is entered upon request in the run mode. In performing a fit then, the user must enter his data, PH(I) vs. T(I), in the edit mode. Then upon calling the program - R WATTSK - the user is instructed to 'INPUT HYPOCHROMICITY OF THE STACKED STATE'. Then upon entering a value for the stacked state property, the program lists the results of the best fit.

The program used in matching the actual experimental curve (i.e. the calculation of $P_c(T)$) was WATTSH. Following the WATTSH listing is a sample run, again using the parameters for ApA which were obtained from the results of the WATTSK program. Thus, the input of the WATTSH program is a portion of the output of WATTSK.

Plotting was done with the program PLTTR (Dr. Alan Levin).

```
 R EDIT
*WATTSK.FT<WATTSK.FT

#R

#L
      DIMENSION T(20),PH(20),EQK(20),TI(20),AEQK(20),DX(20)
      DIMENSION DY(20),DXX(20),TIX(20),DXDY(20),XY(20),Y(20)
      DIMENSION YB(20),TT(20)
      X=17.
      N=17
      T(1)=2.
      T(2)=5.0
      DO 1 I=3,N
1     T(I)=T(I-1)+5.
      T(N)=78.0
      DO 2 I=1,N
      T(I)=T(I)+273.16
2     TI(I)=1.0/T(I)
      PH(1)=14.8
      PH(2)=14.4
      PH(3)=13.7
      PH(4)=13.1
      PH(5)=12.4
      PH(6)=11.7
      PH(7)=11.1
      PH(8)=10.4
      PH(9)=9.67
      PH(10)=9.03
      PH(11)=8.33
      PH(12)=7.62
      PH(13)=6.94
      PH(14)=6.30
      PH(15)=5.75
      PH(16)=5.26
      PH(17)=4.87
      WRITE(1,4)
      READ (1,3),PHS
4     FORMAT('INPUT HYPOCHROMICITY OF STACKED STATE')
3     FORMAT(F10.5)
      STI=0.0
      SAEQK=0.0
      DO 5 I=1,N
40    CONTINUE
      EQK(I)=PH(I)/(PHS-PH(I))
      AEQK(I)=ALOG(EQK(I))
      STI=STI+TI(I)
5     SAEQK=SAEQK+AEQK(I)
      GO TO 200
      WRITE(1,11),(TI(I),AEQK(I),I=1,N)
11    FORMAT(1X,F10.6,5X,F8.4)
200   CONTINUE
```

```
      TIB=STI/X
      AEQKB=SAEQK/X
      DO 6 I=1,N
50    CONTINUE
      DX(I)=(TI(I)-TIB)
      DY(I)=(AEQK(I)-AEQKB)
      DXX(I)=DX(I)**2
      TIX(I)=TI(I)**2
      DXDY(I)=DX(I)*DY(I)
      XY(I)=TI(I)*AEQK(I)
6     CONTINUE
      SDX=0.0
      SDY=0.0
60    CONTINUE
      SDXX=0.0
      STIX=0.0
      SDXDY=0.0
      SXY=0.0
      DO 7 I=1,N
      SDX=SDX+DX(I)
      SDY=SDY+DY(I)
      SDXX=SDXX+DXX(I)
      STIX=STIX+TIX(I)
70    CONTINUE
      SDXDY=SDXDY+DXDY(I)
7     SXY=SXY+XY(I)
      B=(AEQKB*STIX-TIB*SXY)/SDXX
      BM=SDXDY/SDXX
      DH=-BM*1.9872
      DS=B*1.9872
      WRITE(1,9),DH,DS
9     FORMAT('DELTAH = ',F6.0,5X,'DELTAS = ',F6.1)
      SYB=0.0
80    CONTINUE
      DO 8 I=1,N
      Y(I)=BM*TI(I)+B
      TT(I)=TI(I)-1./(80.+273.16)
      YB(I)=ABS(AEQK(I)-Y(I))
8     SYB=SYB+YB(I)
      YBX=SYB/X
      ALNK37=BM/310.16   + B
      AK37=EXP(ALNK37)
      WRITE(1,14),AK37
14    FORMAT('EQUILIBRIUM CONSTANT AT 37 DEGREES = ',F10.5)
90    CONTINUE
      WRITE(1,12),YBX
12    FORMAT('AVERAGE Y DEVIATION = ',E12.5)
      YX=Y(N)-Y(1)
      YY=YBX/YX
      WRITE(1,13),YX,YY
13    FORMAT('Y RANGE = ',F10.6,/,'AVE.  Y DEV./Y RAN. =',E12.5)
```

```
      CALL OOPEN('SYS','WATTSA')
      WRITE(4,100)(TT(I),I=1,N),(AEQK(I),I=1,N)
      CALL OCLOSE
100   FORMAT(5E12.4)
      CALL OOPEN('SYS','WATTSB')
      WRITE(4,100)(TT(I),I=1,N)(Y(I),I=1,N)
      CALL OCLOSE
      STOP
      END
```

```
 R WATTSK

INPUT HYPOCHROMICITY OF STACKED STATE
17.5
DELTAH = -6523.      DELTAS =  -20.4
EQUILIBRIUM CONSTANT AT 37 DEGREES =    1.35788
AVERAGE Y DEVIATION =  0.17408E-01
Y RANGE =  -2.581780
AVE.  Y DEV./Y RAN. =-0.67427E-02
```

```
 R EDIT
*WATTSH.FT<WATTSH.FT

#R

#L
      DIMENSION T(50),TC(50),PH(50),X(50),EX(50)
      T(0)=163.16
      DO 1 I=1,31
      T(I)=T(I-1)+10.0
      TC(I)=T(I)-273.16
1     CONTINUE
      TT=310.16
      TTI=-1.0/TT
      XX=4.58
      WRITE (1,6)
6       FORMAT('INPUT DELTAH, EQK AND PHS')
      READ (1,2), DELTAH, EQK, PHS
2       FORMAT (3F10.5)
      DO 3 I=1,31
      X(I)=((1.0/T(I))+TTI)*(DELTAH/XX)
      EX(I)=(10.**X(I))*EQK
3       PH(I)=PHS*(EX(I)/(1.0+EX(I)))
      DO 4 I=1,31
4       WRITE(1,5),TC(I),EX(I),PH(I)
5       FORMAT(1X,F5.0,F8.3,F9.3)
      CALL OOPEN('SYS','WATTSH')
      WRITE(4,100)(TC(I),I=10,21),(PH(I),I=10,21)
100   FORMAT(5E12.4)
      CALL OCLOSE
      STOP
      END

#E
```

R WATTSH

INPUT DELTAH, EQK AND PHS

6523.	1.358	17.5
-100.	5833.523	17.497
-90.	2074.300	17.492
-80.	820.934	17.479
-70.	355.939	17.451
-60.	166.915	17.396
-50.	83.770	17.294
-40.	44.603	17.116
-30.	25.012	16.827
-20.	14.682	16.384
-10.	8.975	15.746
0.	5.687	14.883
10.	3.722	13.794
20.	2.507	12.510
30.	1.734	11.098
40.	1.227	9.643
50.	0.888	8.229
60.	0.654	6.923
70.	0.491	5.765
80.	0.375	4.771
90.	0.290	3.937
100.	0.228	3.247
110.	0.181	2.684
120.	0.146	2.226
130.	0.118	1.854
140.	0.097	1.552
150.	0.081	1.306
160.	0.067	1.106
170.	0.057	0.941
180.	0.048	0.806
190.	0.041	0.694
200.	0.036	0.601

Appendix 2

ERROR ANALYSES

I. Errorin the $\delta h(\lambda)$ at 25°C

II. Error in the Absorption Two-State Fit Parameters

(A) The Scaling Error

(B) The Shape Error

(C) Total Error

III. Error in the CD Two-State Fit Parameters

IV. NMR Parameters Error Analysis

(A) Two-State Fit Parameters

(B) 3'-Endo Method Errors

Appendix 2

ERROR ANALYSES

All errors have been estimated by the formula[120]:

mean deviation for a function, $f(x_i)$, = Δf

$$= [\Sigma(\partial f/\partial x_i)^2 \delta x_i^2]^{1/2}$$

where δx_i is the estimated error in each of the variables of the function.

I. Error in the $\%h(\lambda)$ at 25°C

$$\%h - (1 - \varepsilon_d/\varepsilon_m)100 = 100 - 100\varepsilon_d/\varepsilon_m$$

$$\Delta\%h = [(-100/\varepsilon_m)^2 \delta\varepsilon_d^2 + (100\varepsilon_d/\varepsilon_m^2)^2 \delta\varepsilon_m^2]^{1/2}$$

Then substitute in the appropriate values for each dimer

ε_d, ε_m, $\delta\varepsilon_m$, $\delta\varepsilon_d$

$\delta\varepsilon_m$ was estimated at ±0.1 for each monomer, or ±0.2 for the sum of the two monomers.

$\delta\varepsilon_d$ was taken as the standard deviation of the mean from the several measurements of the ε_d:

$$\delta\varepsilon_d = [\Sigma d_i^2/(N(N-1))]^{1/2}$$

N, the number of measurements, was usually 5 - 10. This is assuming no error in the monomer ε's and thus is probably an underestimate of the total error. Thus, for example with ApA:

$$\varepsilon_d = 27.1 \times 10^3$$

$$\varepsilon_m = 30.8 \times 10^3$$

$$\delta\varepsilon_m = \pm 0.2 \times 10^3$$

$$\delta\varepsilon_d = \pm 0.1 \times 10^3$$

The error in the %h for each dimer was thus calculated.

II. Error in the Absorption Two-State Fit Parameters

The errors in the fit parameters will originate from the error in the shape of the %h vs. T curve and from the scaling of the %h axis. Assuming error only in the ordinate (i.e. not temperature), the two sources of these errors are the errors in the

1) %h at 25°C,

and 2) % change in the absorption with temperature.

The 2nd source dictates the error in the shape of the %h vs. T curve, while the sum of the 1st and the 2nd determines the scaling error (with the 1st being >> 2nd). Thus, I have separately determined the errors in the parameters from the scaling error and the shape error via graphical procedures. These errors have been summed in order to obtain the total likely errors in the fit parameters.

(A) The Scaling Error

I have added and subtracted from each %h value the sum of the #1 and #2 errors. Then I obtained the best fits of these '+' and '-' curves. The parameters obtained from the 2 new %h vs. T curves served as limits for the error allowed by scaling errors:

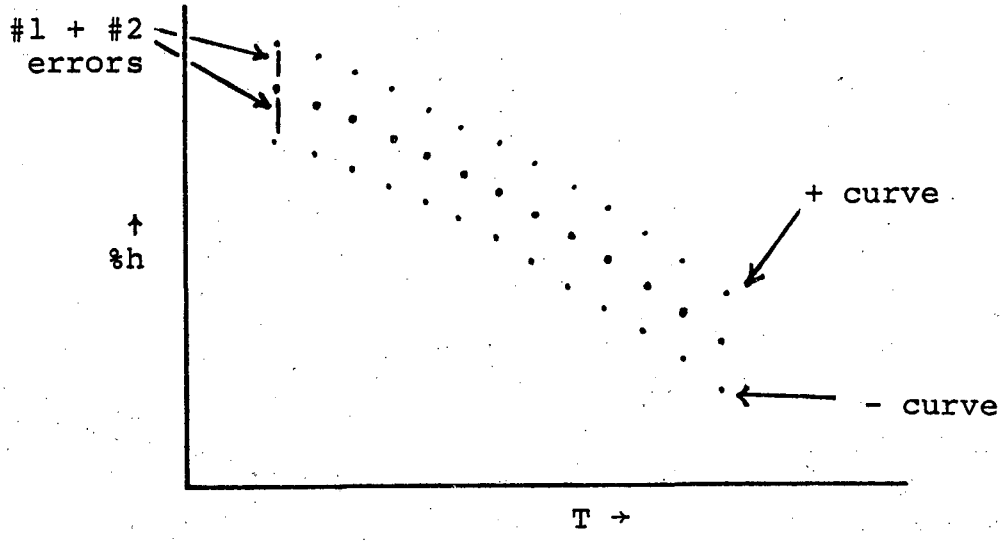

Thus, for each dimer two new sets of data were fit with the program WATTSK. For example the high and low fits of ApA are shown here:

	High	Low
$\Delta H°$	-6.0	-7.2
$\Delta S°$	-19	-23
$K_{37°C}$	1.4	1.3
$\%h_s$	19	16

These were determined by adding and subtracting the total of source 1 error (±0.7) and source 2 error (±0.3, see below).

The attainment of the #1 error was shown in the section I of this Appendix. The derivation of the source #2 error is as follows:

For two of the dimers I calculated the average deviation for the % change in the absorption. This was not a standard deviation, just an average deviation

$$\Sigma(x_i - \bar{x})/N$$

This ranged from a low value near zero at the start of a run (2°C) to ±0.2 for the dimer and monomers at the high

temperatures. For the % change at 25°C the error was

±0.1 for the dimer

±0.05 for the monomers

This has to be translated into $\pm\varepsilon$ values in order to arrive at the Δ%h values. For the monomers and dimers both then,

$$\varepsilon_T = [\varepsilon_{25}/(1 + \%_{L-25}/100)][1 + \%_{L-T}/100]$$

Neglecting the source #1 error ($\delta\varepsilon_{25}$),

$$\Delta\varepsilon_T = [(\partial\varepsilon_T/\partial\%_{L-25})^2(\delta\%_{L-25})^2 + (\partial\varepsilon_T/\partial\%_{L-T})^2(\delta\%_{L-T})^2]^{1/2}$$

And typical values for the dimers and monomers were chosen:

For the Dimers

$$\varepsilon_{25} = 25 \times 10^3$$
$$\%_{L-25} = 1.5$$
$$\%_{L-T} = 4.0 \quad \text{(where T is the highest used, } \sim 75°C)$$
$$\delta\%_{L-25} = \pm 0.1$$
$$\delta\%_{L-T} = \pm 0.2$$

For the Monomers

$$\varepsilon_{25} = 28 \times 10^3$$
$$\%_{L-25} = -1.0$$
$$\%_{L-T} = -3.0 \quad (T = \text{highest})$$
$$\delta\%_{L-25} = \pm 0.05$$
$$\delta\%_{L-T} = \pm 0.2$$

For both monomers and dimers the $\Delta\varepsilon$ worked out to be $\pm 0.06 \times 10^3$. This propagated into the %h (as in section I) as an error = ±0.3.

(B) The Shape Error

In order to determine the error in the parameters due

to shape errors, various values of P_s ($\%h_s$) were inserted into the WATTSK program and then plotted. When these curves just fell outside of the error bars allowed by the shaping errors (±0.3), the parameters obtained were considered as limits. Figure 1 illustrates this approach for ApA. The limits obtained in this example were

$\Delta H°$ -5.4 → -7.9

$\Delta S°$ -18 → -24

$K_{37°C}$ 0.97 → 1.8

$\%h_s$ 20 → 16

This procedure was followed for each dimer.

(C) Total Error

In order to tabulate estimated total errors in the fit parameters the errors from the shaping and the scaling were simply added. Since however the error around the best value was not symmetrical (e.g. the lower limit of the $\Delta H°$'s and K's were often further from the best than the upper limits), ranges are listed in the tables in Chapter 6, rather than ± values. Thus with the example of ApA:

		Scale Limits		Shape Limits	
	best	'high'	'low'	'high'	'low'
$\Delta H°$	-6.5	-7.2	-6.0	-7.9	-5.4
Difference		-0.7	+0.5	-1.4	+1.1

total 'high' limit = -6.5 - 0.7 - 1.4 = -8.6

total 'low' limit = -6.5 + 0.5 + 1.1 = -4.9

Thus,

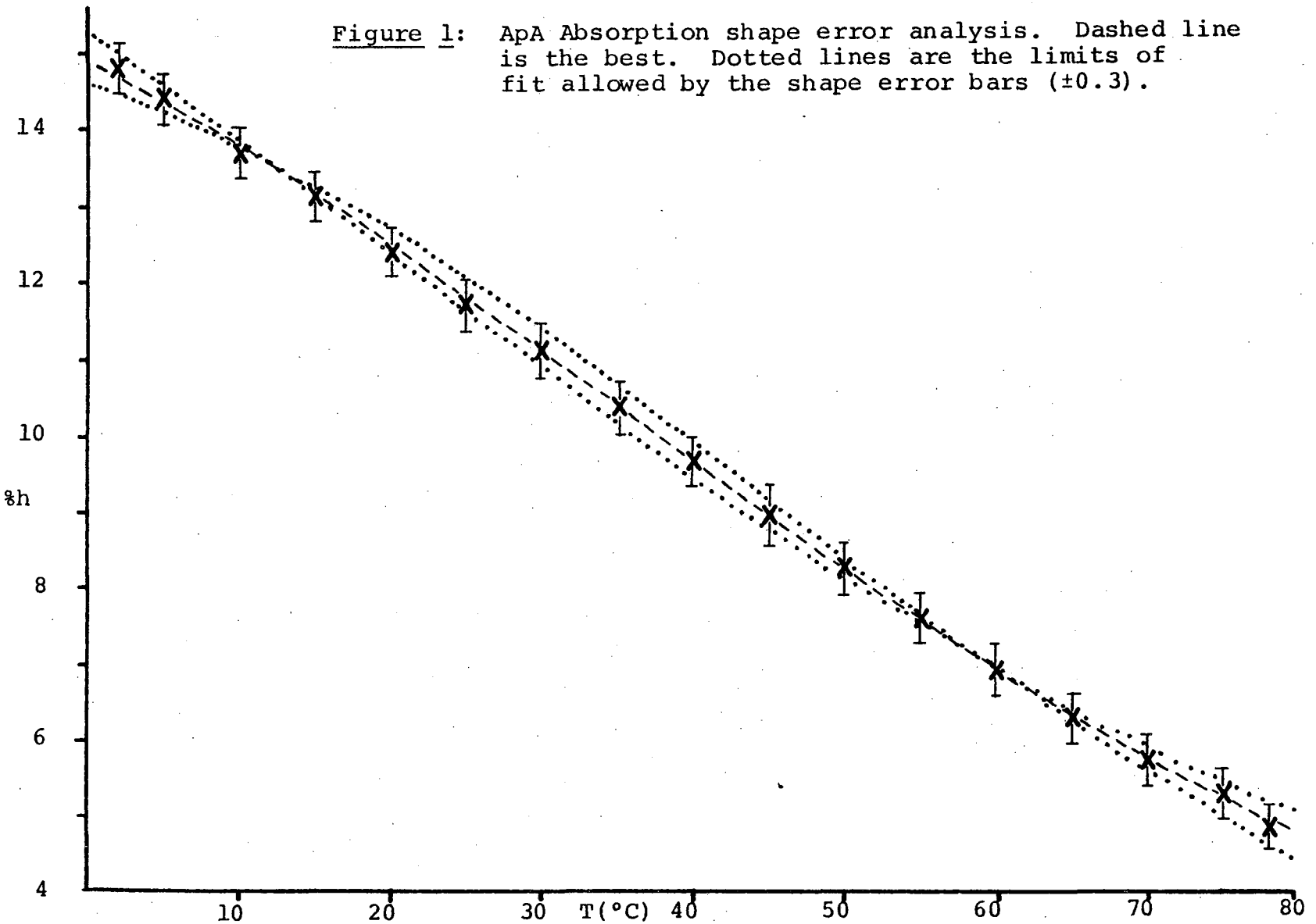

Figure 1: ApA Absorption shape error analysis. Dashed line is the best. Dotted lines are the limits of fit allowed by the shape error bars (±0.3).

$\Delta H° = -6.5$ (-4.9, -8.6)

This addition method of errors was checked by adding the scale error only to the ApA data (±0.7). The best fit was obtained, then the shape error analysis on these sets of data was performed. The 'high' limit to the $\Delta H°$ came to be -8.5, in very close agreement to the -8.6 from the addition method. Likewise, the errors in the $\Delta S°$, $K_{37°C}$ and $\%h_s$ corresponded very closely to those obtained by the simple addition of the scale and shape errors.

In general, the shaping errors were larger than the scaling errors for all the parameters, even though source #1 error was greater than source #2 error.

III. Error in the CD Two-State Fit Parameters

A graphical analysis similar to that used for the shape error analysis in the absorption parameters was utilized for the CD curves.

$$\Delta(\varepsilon_L - \varepsilon_R)_{\substack{\text{dimer or} \\ \text{monomer}}} = [((1/2)(100/3300)(1/\text{Conc.}))^2(\delta\theta°)^2 + (-\theta°(100/3300)(1/2)(1/\text{Conc.}^2)^2 \cdot (\delta\text{Conc.})^2]^{1/2}$$

For δConc.

$$\Delta\text{Conc.} = [(1/\varepsilon b)^2(\delta A)^2 + (-A/\varepsilon^2 b)^2(\delta\varepsilon)^2]^{1/2}$$

And typical values were chosen:

$\delta A = \pm 0.005$

$\delta\varepsilon = \pm 0.2 \times 10^3$

$A = 1$

$\varepsilon = 25 \times 10^3$

$b = 1$

Then,

$$\Delta\text{Conc.} = 0.04 \times 10^{-5}$$

Typical concentrations were $1/(25 \times 10^3) = 4 \times 10^{-5}$, and typical $\theta° = 0.01$. $\delta\theta°$ was taken as ± 0.0002. Then,

$$\Delta(\varepsilon_L - \varepsilon_R) = \pm 0.09$$

This was for the dimers and monomers, and thus upon monomer subtractions the error propagated to ± 0.15. Figures 2 and 3 illustrate some of the plots used to set the limits shown in Chapter 6. The limits for each dimer were thus separately determined.

IV. NMR Parameters Error Analysis

(A) Two-State Fit Parameters

Errors in the chemical shifts were estimated at ± 0.005 ppm. Thus the error in dimerization changes are $\sim\pm 0.01$ ppm. Coupling constant errors are ± 0.2 Hz, and dimerization changes $\sim\pm 0.3$ Hz. Using these values, some graphical analyses (as with the CD) of some of the better fitting data were performed. In most cases, no lower limits on K's could be achieved because of the relatively large fitting errors. Thus, in determining some of the errors listed in Chapter 6, values of P_s greater than 2.0 ppm were ruled out as highly unlikely - thus the limit was arbitrarily set. Those fits with larger fitting errors (Error $\times 10^2$, tabulated in Chapter 6) will exhibit correspondingly larger errors in the fit parameters.

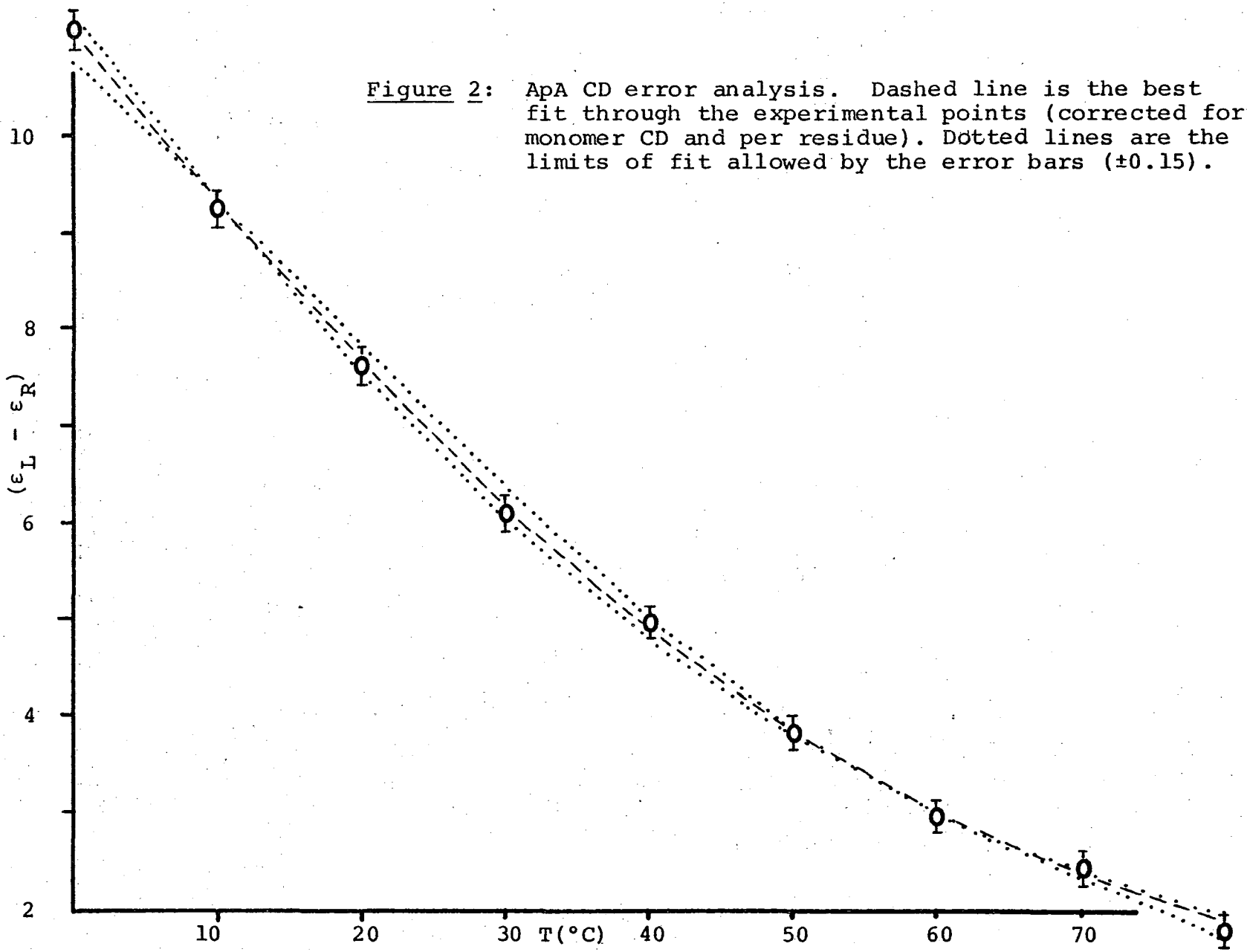

Figure 2: ApA CD error analysis. Dashed line is the best fit through the experimental points (corrected for monomer CD and per residue). Dotted lines are the limits of fit allowed by the error bars (±0.15).

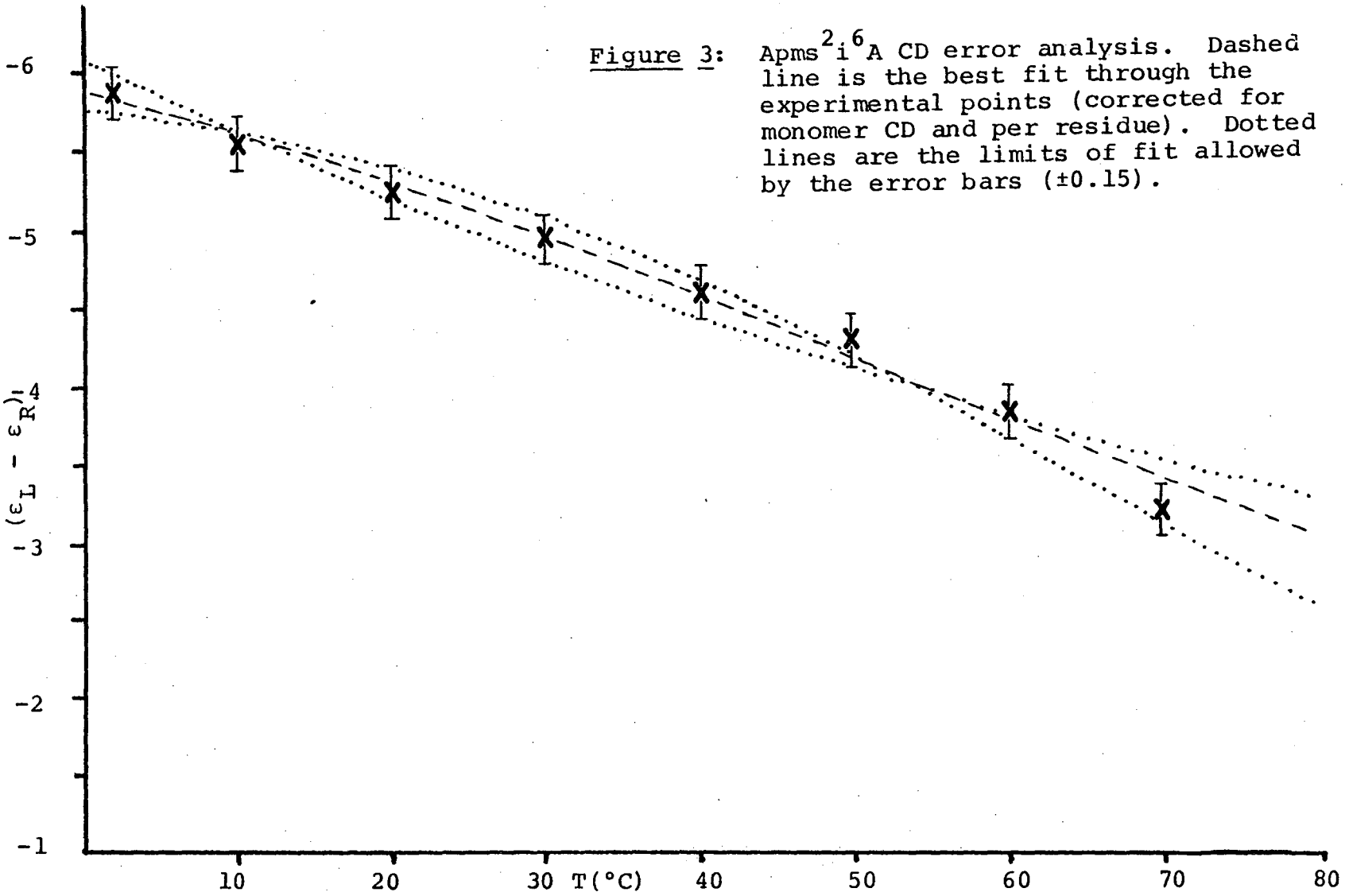

Figure 3: Apms^{2}i^{6}A CD error analysis. Dashed line is the best fit through the experimental points (corrected for monomer CD and per residue). Dotted lines are the limits of fit allowed by the error bars (±0.15).

(B) 3'-Endo Method Errors

Errors in the K's were determined as follows:

$$\Delta K = [(1/J_{1'2'dimer})^2(\delta\Delta J_{1'2'})^2 + (-\Delta J_{1'2'}/J_{1'2'dimer})^2 \cdot (\delta J_{1'2'dimer})^2]^{1/2}$$

$$\delta J_{1'2'd} = \pm 0.2 \text{ Hz}$$

$$\delta\Delta J_{1'2'} = \pm 0.3 \text{ Hz}$$

Typical values:

$$J_{1'2'd} = 4 \text{ Hz}$$

$$\Delta J_{1'2'} = 2 \text{ Hz}$$

Thus $K = \pm 0.08$

$$\Delta \ell n\ K = [(\partial \ell n\ K/\partial K)^2(\delta K)^2]^{1/2} = \pm 0.027$$

These error bars are shown in Figure 5 of Chapter 6. No estimate has been made of the resulting errors in the $\Delta H°$ or $\Delta S°$, as even the best line lay outside of the limits of the error bars. It is suspected that the error in the assumptions made in obtaining the K's will be much greater than any due to the actual measurement of the coupling constants.

Appendix 3

ABBREVIATIONS

Some commonly used abbreviations are:

A	adenosine
Ap(or any Xp)	(3'AMP) adenosine 3'-monophosphoric acid
Api^{6}A	adenylyl(3'-5')N^6-(Δ^2-isopentenyl)adenosine
Apms^{2}i^{6}A	adenylyl(3'-5')N^6-(Δ^2-isopentenyl)-2-methylthioadenosine
ApεA	adenylyl(3'-5')1-N^6-ethenoadenosine
εA	1-N^6-ethenoadenosine
A_{260}	Absorbance in 1 cm pathlength cell at wavelength = 260 nm
BAP	Bacterial alkaline phosphatase
BSP	Bovine spleen phosphodiesterase
C	cytosine
CD	circular dichroism
DCC	dicyclohexylcarbodiimide
DNA	deoxyribonucleic acid
EtOH	ethanol
G	guanosine
%H	percent hypochromism
%h	percent hypochromicity
$\Delta H°$	standard enthalpy change
i^6	isopentenyl attached to N^6 of adenosine
J	coupling constant
K	equilibrium constant
mRNA	messenger RNA
ms^2	thiomethyl attached to C^2 of adenosine
NMR	nuclear magnetic resonance
OD	optical density unit
ORD	optical rotatory dispersion

pA(or any pX)	(5'AMP) adenosine 5'-monophosphoric acid
ppm	parts per million of electromagnetic field frequency
P_s	property of the stacked state
RNA	ribonucleic acid
$\Delta S°$	standard entropy change
SVP	Snake venom phosphodiesterase
T	temperature
TEA	triethylamine
TEAB	triethylammonium bicarbonate
tRNA	transfer RNA
t^6	threonine attached via ureido bond to N^6 of adenosine
U	uracil
Upt^6A	uridylyl(3'-5')N-[9(β*D*ribofuranosyl)-purin -6-ylcarbamoyl]-threonine
UV	ultra violet
yW	the 'Y' base
ε	extinction coefficient
μ	micro, or ionic strength
λ	lambda (10^{-6} ml), or wavelength
θ	ellipticity
δ_{TSP}	chemical shift relative to sodium trimethysilylpropionate

This report was done with support from the United States Energy Research and Development Administration. Any conclusions or opinions expressed in this report represent solely those of the author(s) and not necessarily those of The Regents of the University of California, the Lawrence Berkeley Laboratory or the United States Energy Research and Development Administration.

TECHNICAL INFORMATION DIVISION
LAWRENCE BERKELEY LABORATORY
UNIVERSITY OF CALIFORNIA
BERKELEY, CALIFORNIA 94720